A Possible Link between the Electroweak Phase Transition and the Dark Matter of the Universe

Thesis submitted for the degree of
Doctor of Philosophy

Candidate:
Talal Ahmed Chowdhury

Supervisor:
Prof. Goran Senjanović

Theoretical Particle Physics
Scuola Internazionale Superiore di Studi Avanzati-SISSA
Trieste, Italy

September, 2014

Abstract

A possible connection between the dark matter and strong first order electroweak phase transition, which is an essential ingredient of the electroweak baryogenesis, has been explored in this thesis. It is shown that the extension of the Standard Model's minimal Higgs sector with an inert $SU(2)_L$ scalar doublet can provide light dark matter candidate and simultaneously induce a strong first order phase transition. There is however no symmetry reason to prevent the extension using scalars with higher $SU(2)_L$ representations. Therefore, by making random scans over the models' parameters, we show, in the light of electroweak physics constraints, strong first order electroweak phase transition and the possibility of having a sub-TeV cold dark matter candidate, that the higher representations are rather disfavored compared to the inert doublet. This is done by computing generic perturbativity behavior and impact on electroweak phase transitions of higher representations in comparison with the inert doublet model. Explicit phase transition and cold dark matter phenomenology within the context of the inert triplet and quartet representations are used for detailed illustrations.

Acknowledgements

I am deeply indebted to my supervisor Prof. Goran Senjanović for his guidance in every step of my research. My sincerest gratitude to him for his teaching and supervision since the ICTP diploma course and for the freedom he has given me to pursue and find my ways. I have greatly benefited not only from his deep insight of physics but also from his advice regarding physics and life. His words and guidance will always be one of the most valuable lessons in my life.

My sincerest gratitude to Prof. Jim Cline and Prof. Fabrizio Nesti for their careful considerations on the thesis and giving important suggestions.

I am grateful to Prof. Roberto Iengo, Prof. Serguey Petcov, Prof. Marco Serone, Prof. Matteo Bertolini, Prof. Andrea Romanino, Prof. Andrea De Simone, Prof. Piero Ullio, Prof. Stefano Liberati, Prof. Giulio Bonelli, Prof. Loriano Bonora, Prof. Guido Martinelli and Prof. Marco Fabbrichesi for teaching me advanced topics of high energy physics during my PhD coursework in SISSA.

I am also grateful to Prof. Seifallah Randjbar-Daemi, Prof. Edi Gava, Prof. Bobby Acharya, Prof. Alexei Smirnov, Prof. Kumar Narain and Prof. Paolo Creminelli for helping me build up the foundation with their teachings in ICTP's high energy physics diploma course. I am thankful to Kerim Suruliz, Mahdi Torabian, T. Enkhbat, Aseem Paranjape, Koji Tsumura and Enrico Trincherini for enjoyable tutorials during the course. I am also thankful to Prof. George Thompson and Prof. Giovanni Villadoro.

My special thanks to Prof. Arshad Momen, Prof. Kamrul Hassan, Prof, Khorshed Ahmed Kabir, Prof. Golam Mohammad Bhuiyan and Dr. Mahbub Majumder for the guidance during my undergraduate studies in University of Dhaka.

I am thankful to Prof. A. M. Harun-Ar-Rashid and late Prof. Jamal Nazrul Islam for the giving me the inspiration to pursue physics from the very early stage in my life.

I am grateful to Yue Zhang, Miha Nemevsek, Shehu S. AbdusSalam, Amine Ahriche, Salah Nasri and Rachik Soualah for the collaboration and giving me the opportunity to learn in the process.

I am indebted to Basudeb Dasgupta for his advice and suggestions on research and Xiaoyong Chu for numerous discussions on various topics of physics and life. I am also grateful to Rajesh Kumar Gupta and Gabrijela Zaharijas for many discussions. My special thanks to Ehsan Hatefi, Emiliano Sefusatti, Diana Lopez Nacir and Kate Shaw.

My heartfelt gratitude to my friends and classmates: Marko, Emanuele, Gabriele, Nouman, Alejandro, Alberto, Piermarco, David, Carlo, Marco,

Lorezo, Flavio, Eolo, Pietro and Claudia. My special thanks to Luca Di Luzio, Marco Nardecchia and Aurora Meroni. I am also thankful to my classmates from the diploma course; and my seniors, classmates and juniors from University of Dhaka. Also thanks to my friends scattered all over the world for their continuous support.

I am grateful to Prof. Rohini Godbole, Prof. Dilip Kumar Ghosh and Prof. Sunil Mukhi for the advice, encouragement and collaboration. I am thankful to Prof. Syed Twareque Ali and Prof. Jean Pierre Gazeau for the advice and collaboration. I am greatly indebted to Prof. Fernando Quevedo for his support, advice and encouragement.

I am also grateful to Riccardo, Federica, Barbara and Rosanna for helping me completing all the administrative requirements.

I am thankful to Gabriele, Lucina, Adriano, Angie, Rosie, Maria and Guendalina for giving me the warmth of a family. My thanks to Nicoletta, Natalia and Ettore for the kindness and support. Also a special thanks to the members of Manoaperta for the exciting moments.

My special thanks to Anamika.

Last but not least, I want to thank my family for everything they have done for me. This thesis is dedicated to my mother and to the memory of my father.

Contents

Chapter 1

Introduction

The discovery of an about 126 GeV Higgs boson [1, 2] is yet another important support for and completion of the Standard Model (SM). The SM with minimal Higgs sector contains one complex Higgs doublet which after electroweak symmetry breaking gives a neutral CP-even Higgs boson. But one can consider a scenario with singlets, with more than one doublet or with an N copies of $SU(2)_L$ n-tuplets where the (non standard) Higgs sector can be used to explicitly account for Baryogenesis and cold dark matter. Using these phenomena and related experimental data we set to qualitatively explore for the preferred scalar representation in the SM.

Extensive astrophysical and cosmological observations have already put dark matter (DM) as a constituent of the universe. The existence of DM has been indicated by the rotation curves for spiral galaxies [3], velocity dispersion of individual galaxies in galaxy clusters, large x-ray temperatures of clusters [4], bulk flows and the peculiar motion of our own local group [5], Moreover, inferred from the gravitational lensing of background images, the mass of galaxy clusters turn out to be consistent with the large dark-to-visible mass ratios [6]. Furthermore, one of the most compelling evidence, at a statistical significance of 8σ comes from the two colliding clusters of galaxies, known as the Bullet cluster [7] for which the spatial displacement of the center of the total mass from the center of the baryonic mass peaks cannot be explained with an alteration of gravitational force law. Also, the large scale structure formation from the initial seed perturbations from inflation requires a significant non-baryonic dark matter component [8]. Finally the observed acoustic peaks in the cosmic microwave background radiation enables us to determine most precisely the relic density of DM in the universe to be, $\Omega_{DM}h^2 = 0.1196 \pm 0.0031$ (68% CL) [9] as the DM density provides the required potential well for the observed acoustic oscillation seen in the

CMB. Still we have to determine the exact nature of the dark matter from particle physics point of view. Within many viable candidates for DM, the most popular one is considered to be the stable weakly interacting particle (WIMP) [10] for which the observed DM relic density is obtained if it's mass lies near the electroweak scale.

Apart from DM identification, one other unresolved question within the SM is the observed matter-antimatter asymmetry of the universe. Such asymmetry is described by Baryogenesis scenario first put forward by Sakharov [11] and one essential ingredient of this mechanism is 'out of equilibrium process'. Now that the study of beyond standard model (BSM) physics is being explored with the LHC, a well motivated scenario within the testable reach of LHC is Electroweak Baryogenesis [12] where out of equilibrium condition is given by strong first order phase transition. The SM has all the tools required by the Sakharov's condition for Baryogenesis, i.e. baryon number violation at high temperature through sphalerons [13–16], C and CP violation with CKM phase and strong first order phase transition [17, 18]. However, it was shown that to avoid baryon washout by sphalerons, Higgs mass has to be below 45 GeV for strong electroweak phase transition (EWPhT) [19–22], which was later confirmed by lattice studies [23–25] and eventually it was ruled out by the LEP data [26]. Now with Higgs at 126 GeV, clearly one can see the requirement of extending SM by new particles, possibly lying nearly the electroweak scale, which could not only provide strong EWPhT for explaining matter asymmetry but also the DM content of the universe.

One promising way is to extend the scalar sector of the SM. Within the literature there are numerous considerations for non minimal Higgs sector with various representations of the additional Higgs multiplet in order to account for Baryogenesis and/or dark matter. For instance, in the inert doublet case considered in [27–29], it was shown that it can enable one to achieve strong EWPhT with DM mass lying between 45 GeV and 80 GeV and predicts a lower bound on the direct detection that is consistent with XENON direct detection limit [208] (in case of sub-dominant DM, see [30]). Inert doublet is a well motivated and minimal extension of scalar sector which was first proposed as dark matter [31], was studied as a model for radiative neutrino mass generation [32], improved naturalness [33] and follows naturally [34, 35] in case of mirror families [36–39] that was to fulfill Lee and Yang's dream to restore parity [40]. The DM phenomenology regarding Inert doublet model has been studied extensively in Refs. [41–55]. Moreover, tentative 130 GeV gamma line from galactic center can be accommodated in inert doublet framework [57]. Therefore, one can extend scalar sector by in-

troducing inert scalar representations and explore the nature of phase transition, consistency of the theory at high scale and dark matter phenomenology.

Apart from the doublet, one other possibility is the scalar singlet [58–62] (and references there) which can be accounted for strong EWPhT and light DM candidate but not simultaneously (for exceptions, see [63–65]). Scalar singlet can also be a force carrier between SM and dark matter sector inducing strong EWPhT [66,67] or trigger EWPhT independent of being DM [68].

In the case of larger representations, a systematic study for DM candidate has been performed in [69] from doublet to 7-plet of $SU(2)_L$ with both fermionic and scalar DM where only allowed interactions of DM are gauge interactions. Additionally, scalar multiplet allows renormalizable quartic couplings with Higgs doublet. In [70], study of DM phenomenology for such scalar multiplet was carried out for large odd dimensional and real representation and the mass of the DM turned out to be larger than the scale relevant for strong EWPhT. Besides, fermions with large yukawa couplings to Higgs can trigger strong EWPhT by producing large entropy when they decouple and also they can be viable dark matter candidates [71] but it requires some fine tuning of Higgs potential. Another approach with vector-like fermions is explored in [72].

The work presented in the thesis focused on the comparison among various models of extended the Higgs sector using different representations in order to find the favored representation that not only provides a viable DM candidates but also trigger strong 1st order EWPhT accounting for Baryogenesis.

Outline The thesis is organized as follows. In chapter 2 we have presented the elements of finite temperature field theory. In chapter 3 we have presented a brief review of electroweak baryogenesis and showed how the requirement of baryon number violating sphaleron decoupling leads to strong first order electroweak phase transition (EWPhT) condition where results obtained in original work [137] have been partly used in 3.3.1. Chapter 4 is based on original works [27,144] where the results of the investigation regarding scalar representations: inert doublet, triplet and quartet in triggering strong first order EWPhT and providing cold dark matter in the universe, are presented in details. We conclude in chapter 5. In appendix A some mathematical formulas are collected. Appendix B collects the expressions of the Coleman

Weinberg potential in $\overline{MS}$ and cut-off schemes. Appendix C focuses on the derivation of high and low temperature limit of various thermodynamic quantities and finite temperature effective potential. In appendix D we have presented the asymptotic solutions of sphaleron profile functions and their dependence on scalar representations [137]. The explicit form of generators and vertex factors in gauge-scalar sector are given in appendix E. Appendix F has described tree unitarity condition briefly. In appendix G we have described a method to derive renormalization group (RG) equations from effective potential and collected RG equations for inert doublet and triplet cases.

Chapter 2

Elements of finite temperature field theory

Finite temperature field theory has a wide range of applications in particle physics, condensed matter physics, astrophysics and cosmology.In this chapter we have mainly focused on the background tools needed to understand the electroweak phase transition because of its importance in the evolution of the universe.

The chapter is organized as follows. In section 2.1, we have derived the thermodynamic quantities from the statistical point of view. Section 2.3 is devoted to describe briefly key ingredients of thermal field theory: Imaginary time formalism and finite temperature effective potential. In section 2.4 we have addressed the basics of phase transition in the early universe. In section 2.5 we have pointed out infrared divergences which occur in finite temperature field theory.

2.1 Thermodynamic quantities

The investigation of equilibrium thermodynamics and the determination of relevant thermodynamic quantities can be readily determined once partition function is defined. In the section, starting from the partition function of the Bosonic and fermionic oscillator we have derived finite temperature effective potential [73].

First consider the ensemble of bosonic harmonic oscillators. The creation and annihilation operators for a i-th bosonic oscillator are a_i and $a_i^\dagger$ which follow the commutation relation $[a_i, a_j^\dagger] = \delta_{ij}$, In case of non-interacting oscillators, the Hamiltonian associated with the ensemble is just the sum of individual Hamiltonians of the oscillators,

$$
\begin{aligned}
H_B &= \sum_i H_{Bi} = \sum_i \frac{\omega_i}{2}(a_i^\dagger a_i + a_i a_i^\dagger) \\
&= \sum_i \omega_i (N_i + \frac{1}{2})
\end{aligned}
$$

where the energy of the i-th oscillator is ω_i and occupation number $N_i = a_i^\dagger a_i$. Also, $H_{Bi}|n\rangle = (n + \frac{1}{2})\omega_i|n\rangle$.

On the other hand, fermionic annihilation and creation operators, b_i and $b_i^\dagger$ respectively for i-th oscillator follows anticommutation relation, $\{b_i, b_j^\dagger\} = \delta_{ij}$. Therefore the total Hamiltonian associated with the ensemble of fermionic oscillators is

$$
\begin{aligned}
H_F &= \sum_i H_{Fi} = \sum_i \frac{\omega_i}{2}(b_i^\dagger b_i + b_i b_i^\dagger) \\
&= \sum_i \omega_i (N_i - \frac{1}{2})
\end{aligned}
$$

where the number operator for fermionic oscillator is $N_i = b_i^\dagger b_i$ and $H_{Fi}|n\rangle = (n - \frac{1}{2})\omega_i|n\rangle$

In the continuum limit where V is the volume of the system, we have

$$
\begin{aligned}
\sum_i &= V \int \frac{d^3\vec{p}}{(2\pi)^3} && (2.1) \\
\omega_i &\rightarrow \omega = \sqrt{\vec{p}^2 + m^2} && (2.2) \\
H_{B(F)i} &\rightarrow H_{B(F)}(\omega) && (2.3)
\end{aligned}
$$

Therefore, the total Hamiltonian of an ensemble of particles is,

$$
H_{B(F)} = V \int \frac{d^3\vec{p}}{(2\pi)^3} H_{B(F)}(\omega) \tag{2.4}
$$

The partition function of i-th oscillator in the discrete case, is given by,

$$
Z_i = \mathrm{Tr}\, e^{-H_i/T} \tag{2.5}
$$

and in the continuum limit,

$$
Z(\omega) = \mathrm{Tr}\, e^{-H(\omega)/T} \tag{2.6}
$$

For bosonic oscillator,

$$
Z_B(\omega) = \sum_n e^{-(n+\frac{1}{2})\omega/T} = e^{-\omega/2T}(1 - e^{-\omega/T}) \tag{2.7}
$$

And for the fermionic oscillator,

$$Z_F(\omega) = \sum_n e^{-(n-\frac{1}{2})\omega/T} = e^{\omega/2T}(1 + e^{-\omega/T}) \tag{2.8}$$

Starting from $H = \sum_i H_i$ and using the fact that unitary transformation which changes basis does not change the spectrum of the Hamiltonian operator, it can be shown that $Z = \mathrm{Tr}\, e^{-H/T} = \prod_i Z_i$. So, $\ln Z = \sum_i \ln Z_i$ or in the continuum limit,

$$\ln Z_{B(F)} = V \int \frac{d^3\vec{p}}{(2\pi)^3} Z_{B(F)}(\omega) \tag{2.9}$$

The occupation number and the energy The average occupation number of the oscillator is,

$$\bar{n}_{B(F)}(\omega) = \frac{\mathrm{Tr}\, N e^{-H_{B(F)}/T}}{Z_{B(F)}} \tag{2.10}$$

Therefore the average occupation number of the system,

$$\begin{aligned} n_{B(F)} &= \int \frac{d^3\vec{p}}{(2\pi)^3} \bar{n}_{B(F)}(\omega) \\ &= \int \frac{d^3\vec{p}}{(2\pi)^3} \frac{\sum_n n e^{-(n\pm\frac{1}{2})\omega/T}}{Z_{B(F)}(\omega)} \\ &= \int \frac{d^3\vec{p}}{(2\pi)^3} \frac{1}{e^{\omega/T} \mp 1} \end{aligned} \tag{2.11}$$

On the other hand, the average energy of the oscillator is

$$\epsilon(\omega) = \frac{\mathrm{Tr}\, H_{B(F)} e^{-H_{B(F)}/T}}{Z_{B(F)}} \tag{2.12}$$

Therefore, the energy density associated with the system is

$$\begin{aligned} \rho_{B(F)} &= \int \frac{d^3\vec{p}}{(2\pi)^3} \frac{\sum_n \omega(n \pm \frac{1}{2})(e^{-(n\pm\frac{1}{2})\omega/T}}{Z_{B(F)}(\omega)} \\ &= \int \frac{d^3\vec{p}}{(2\pi)^3} \left[\pm\frac{\omega}{2} + \omega n_{B(F)}\right] \end{aligned} \tag{2.13}$$

Free energy, entropy and the pressure The probability for an oscillator to be in the state with energy E_n is

$$P_n = \frac{e^{-E_n/T}}{Z} \tag{2.14}$$

Here, $E_n = \omega(n \pm \frac{1}{2})$ for boson and fermion respectively. Therefore the entropy of the oscillator is $S(\omega) = -\sum_n P_n \ln P_n$. And the total entropy of the ensemble is

$$\begin{aligned} s_{B(F)} &= \int \frac{d^3\vec{p}}{(2\pi)^3} S_{B(F)}(\omega) && (2.15) \\ &= \int \frac{d^3\vec{p}}{(2\pi)^3} \left[\frac{\omega}{T} n_{B(F)} \mp \ln(1 \mp e^{-\omega/T})\right] && (2.16) \end{aligned}$$

The free energy is defined as $F = E - TS$ where, $E = V\rho$, $S = Vs$ and $F = Vf$. From the first law of thermodynamics,

$$dE = -pdV + TdS \tag{2.17}$$

So the relation for the Free energy is,

$$dF = -pdV - SdT \tag{2.18}$$

For free energy density, $f = F/V$,

$$f = \rho - Ts \tag{2.19}$$

So now if we plug Eq.(2.11), Eq.(2.13) and Eq.(2.15) into the relation Eq.(2.19), we have the free energy density of the ensemble,

$$f_{B(F)} = \int \frac{d^3\vec{p}}{(2\pi)^3} \left[\pm\frac{\omega}{2} \pm T \ln(1 \mp e^{-\omega/T})\right] \tag{2.20}$$

From Eq.(2.18), we have the pressure associated with the system,

$$p = -\left(\frac{\partial F}{\partial V}\right)_T = -f \tag{2.21}$$

The above set of expressions provides us the necessary tools to investigate the thermodynamic behavior of the system. At this point we will look into two limits: a. relativistic and b. non-relativistic limits of the relevant quantities.

Relativistic and non-relativistic limits The relativistic limit is considered to be $T \gg m$. The detailed derivation of the results collected in this section is given in appendix C. In this limit, the total number density n of the system containing boson and fermion is,

$$n = (g_B + \frac{3}{4} g_F) \frac{\zeta(3)}{\pi^2} T^3 \tag{2.22}$$

where g_B and g_F are the bosonic and fermionic degrees of freedom.

Again, the total energy density ρ of the system is,

$$\rho = (g_B + \frac{7}{8} g_F) \frac{\pi^2}{30} T^4 \tag{2.23}$$

Moreover, the entropy density s associated with that system is

$$s = (g_B + \frac{7}{8} g_F) \frac{2\pi^2}{45} T^3 \tag{2.24}$$

And, the free energy density f of the system, which is also negative of the pressure p

$$f = -p = (g_B - \frac{7}{8} g_F) \frac{\pi^2}{90} T^4 \tag{2.25}$$

On the other hand at the non-relativistic limit where $m \gg p, T$, the number density n is

$$n = \left(\frac{mT}{2\pi} \right)^{3/2} e^{-m/T} \tag{2.26}$$

Furthermore, the energy density is given as

$$\rho = \rho_B = \rho_F = m\, n \tag{2.27}$$

2.2 Tools of finite temperature field theory

In the previous section we have derived the essential thermodynamic quantities from statistical mechanics point of view. In this section we are going to describe how one can incorporate temperature in quantum field theory and apply the field theoretical tools to investigate thermodynamic system. Finite temperature field theoretic approach to investigate the symmetry behavior and the phase transition of the universe was first addressed in [74–79]. The following telegraphic review of finite temperature field theory is heavily leaned on [80–85] where the topics of finite temperature field theory are covered in a more detailed manner.

The statistical behavior of a quantum system, in thermal equilibrium, is normally studied using appropriate ensemble. If the density matrix for the system is

$$\rho(\beta) = e^{-\beta\mathcal{H}} \tag{2.28}$$

Here $\beta = 1/T$, the inverse of the temperature and $\mathcal{H}$ is the Hamiltonian depending on the choice of the ensemble. For example, in grand canonical ensemble, $\mathcal{H} = H - \sum_i \mu_i N_i$ where H, N_i and μ_i are the dynamical Hamiltonian, number operator and the chemical potential of the system. On the other hand, for microcanonical ensemble where the number of particles of the system remains constant, we have $\mathcal{H} = H$. We will adopt the particular ensemble based on the nature of thermodynamic system under study.

Again the partition function of the system is

$$Z_\beta = \mathrm{Tr}\,\rho(\beta) = \mathrm{Tr}\ e^{-\beta\mathcal{H}} \tag{2.29}$$

And the ensemble average of any observable A is

$$\langle A\rangle_\beta = Z_\beta^{-1}\mathrm{Tr}\,\rho(\beta)A \tag{2.30}$$

Let us also define, the Heisenberg operator $A_H(t)$ for corresponding Schroedinger operator A as

$$A_H(t) = e^{i\mathcal{H}t}Ae^{-i\mathcal{H}t} \tag{2.31}$$

So for thermal correlation between two Heisenberg operators $A_H(t)$ and $B_H(t')$ is

$$\begin{aligned}
\langle A_H(t)B_H(t')\rangle_\beta &= Z_\beta^{-1}\mathrm{Tr}\,e^{-\beta\mathcal{H}}A_H(t)B_H(t') \\
&= Z_\beta^{-1}\mathrm{Tr}\,e^{-\beta\mathcal{H}}A_H(t)e^{\beta\mathcal{H}}e^{-\beta\mathcal{H}}B_H(t') \\
&= Z_\beta^{-1}\mathrm{Tr}\,A_H(t+i\beta)e^{-\beta\mathcal{H}}B_H(t') \\
&= Z_\beta^{-1}\mathrm{Tr}\,e^{-\beta\mathcal{H}}B_H(t')A_H(t+i\beta) \\
&= \langle B_H(t')A_H(t+i\beta)\rangle_\beta
\end{aligned} \tag{2.32}$$

The above Eq.(2.32) holds independent of the grassmann parities of the operators A and B. This relation is known as Kubo-Martin-Schwinger (KMS) relation and such relation can be viewed as a general criterion for thermal equilibrium of the system.

2.2.1 Imaginary time formalism

In this section, we are going to describe one of the prescription for finite temperature field theory-Imaginary time formalism [86] which is suitable to study thermodynamic system in equilibrium or near-equilibrium state.

As the dynamical Hamiltonian H can be separated into free and an interaction part, $H = H_0 + H'$, we can write, total Hamiltonian in the density matrix as $\mathcal{H} = \mathcal{H}_0 + H'$. Then the density matrix can be written as

$$\rho(\beta) = e^{-\beta\mathcal{H}} = \rho_0(\beta)S(\beta) \tag{2.33}$$

where $\rho_0(\beta) = e^{-\beta\mathcal{H}_0}$ and $S(\beta) = e^{\beta\mathcal{H}_0}e^{-\beta\mathcal{H}} = \rho_0^{-1}(\beta)\rho(\beta)$. The density matrix satisfies the following evolution equation over the interval $0 \leq \tau \leq \beta$,

$$\begin{aligned} \frac{\partial\rho_0(\tau)}{\partial\tau} &= -\mathcal{H}_0\rho_0(\tau) \\ \frac{\partial\rho(\tau)}{\partial\tau} &= -\mathcal{H}\rho(\tau) = -(\mathcal{H}_0 + H')\rho(\tau) \end{aligned} \tag{2.34}$$

Using equations Eq.(2.34), we have the evolution equation for $S(\beta)$,

$$\begin{aligned} \frac{\partial S(\tau)}{\partial\tau} &= -\rho_0^{-1}(\tau)H'\rho_0(\tau)S(\tau) \\ &= -H'_I(\tau)S(\tau) \end{aligned} \tag{2.35}$$

Here, we have defined $H'_I = \rho_0^{-1}(\tau)H'\rho_0(\tau) = e^{\tau\mathcal{H}_0}H'e^{-\tau\mathcal{H}_0}$ which is taken in the interaction picture. These two relations resemble the evolution equation of the evolution operator as in zero temperature field theory.

Consider the transformation, $A_I(\tau) = e^{\tau\mathcal{H}_0}Ae^{-\tau\mathcal{H}_0}$ which is not necessarily unitary for real τ and therefore, $A_I^\dagger(\tau) = e^{\tau\mathcal{H}_0}A^\dagger e^{-\tau\mathcal{H}_0} \neq (A_I(\tau))^\dagger$. However, if τ were a complex variable, then for imaginary values of τ, the transformation will be unitary. For this reason, we have to identify τ on the negative imaginary time axis,

$$t = -i\tau \tag{2.36}$$

We can also see from Eq.(2.35) that we have

$$S(\beta) = P_\tau(e^{-\int_0^\beta d\tau H'_I(\tau)}) \tag{2.37}$$

where, P_τ stands for ordering in the τ variable. Eq.(2.37) resembles the usual S-matrix of the zero temperature field theory except for the fact that the time integration is over a finite interval along imaginary time axis. So as in zero temperature, we can expand the exponential and each term in the expansion would give rise to a (modified) Feynman diagram.

Let us now address the 2-point temperature Green's functions. It is defined as the following,

$$G_\beta(\tau,\tau') = \langle P_\tau(\phi_H(\tau)\phi_H^\dagger(\tau'))\rangle_\beta \tag{2.38}$$

$\phi_H(\tau)$ accounts for both bosonic and fermionic field operator and we have suppressed spatial and spinorial indices for notational simplicity. Also τ ordering is sensitive to the Grassmann parity of the field variables and it is defined as

$$P_\tau(\phi_H(\tau)\phi_H^\dagger(\tau')) = \theta(\tau-\tau')\phi_H(\tau)\phi^\dagger(\tau') \pm \theta(\tau'-\tau)\phi^\dagger(\tau')\phi_H(\tau) \quad (2.39)$$

where the minus sign in the second term is for fermionic fields. The relation between the Heisenberg and interaction picture is in the following

$$\begin{aligned} A_H(\tau) &= e^{\tau\mathcal{H}}Ae^{-\tau\mathcal{H}} \\ &= S^{-1}(\tau)A_I(\tau)S(\tau) \end{aligned} \quad (2.40)$$

Therefore the 2-point temperature green's function for τ and τ' such that $0 \le \tau, \tau' \le \beta$,

$$G_\beta(\tau,\tau') = \frac{\mathrm{Tr}\, e^{-\beta\mathcal{H}_0}P_\tau(\phi_I(\tau)\phi_I^\dagger(\tau')S(\beta)}{\mathrm{Tr}\, e^{-\beta\mathcal{H}_0}S(\beta)} \quad (2.41)$$

Matsubara frequencies The temperature Green's functions are

$$G_\beta(\tau,\tau') = \langle P_\tau(\phi_H(\tau)\phi_H^\dagger(\tau'))\rangle_\beta \quad (2.42)$$

Here we are going to show the periodic (anti-periodic) behavior of 2 point Green's function in τ variable. Consider for $\tau > 0$,

$$\begin{aligned} G_\beta(0,\tau) &= \pm\langle\phi_H^\dagger(\tau)\phi_H(0)\rangle_\beta \\ &= \pm Z_\beta^{-1}\mathrm{Tr}\, e^{-\beta\mathcal{H}}\phi_H^\dagger(\tau)\phi_H(0) \\ &= \pm Z_\beta^{-1}\mathrm{Tr}\, e^{-\beta\mathcal{H}}\phi_H(\beta)\phi_H^\dagger(\tau) \\ &= \pm G_\beta(\beta,\tau) \end{aligned} \quad (2.43)$$

where + and − signs are for bosonic and fermionic operators respectively. So we can see that the bosonic and fermionic Green's function has to satisfy periodic and anti-periodic boundary conditions.

Since the Green's functions are defined within a finite time interval, the corresponding Fourier transformation will only involve discrete frequencies. Suppressing spatial co-ordinates,

$$\tilde{G}_\beta(\omega_n) = \frac{1}{2}\int_{-\beta}^{\beta} e^{i\omega_n\tau}G_\beta(\tau) \quad (2.44)$$

where $\omega_n = \frac{n\pi}{\beta}$ with $n = 0, \pm1, \pm2, ...$ Now because of periodicity of Green's function for bosonic and fermionic operators are different, we will see that

only even integer modes contribute to bosonic Green's function while only odd integer modes contribute to the fermionic Green's function.

$$\begin{aligned}
\tilde{G}_\beta(\omega_n) &= \frac{1}{2}\int_{-\beta}^{0} e^{i\omega_n\tau}G_\beta(\tau) + \frac{1}{2}\int_{0}^{\beta} e^{i\omega_n\tau}G_\beta(\tau) \\
&= \pm\frac{1}{2}\int_{-\beta}^{0} e^{i\omega_n\tau}G_\beta(\tau+\beta) + \frac{1}{2}\int_{0}^{\beta} e^{i\omega_n\tau}G_\beta(\tau) \\
&= \frac{1}{2}(1 \pm e^{-i\omega_n\beta})\int_{0}^{\beta} e^{i\omega_n\tau}G_\beta(\tau) \\
&= \frac{1}{2}(1 \pm (-1)^n)\int_{0}^{\beta} e^{i\omega_n\tau}G_\beta(\tau) \qquad (2.45)
\end{aligned}$$

So we immediately see that for bosons $\tilde{G}_\beta(\omega_n)$ vanishes for odd n while for fermions it vanishes for n even. Therefore,

$$\omega_n = \begin{pmatrix} \frac{2\pi n}{\beta} & \text{for bosons} \\ \frac{(2n+1)\pi}{\beta} & \text{for fermions} \end{pmatrix} \qquad (2.46)$$

They are commonly referred to as the Matsubara frequencies. The spatial co-ordinates are continuous as in the case of zero temperature field theory so putting together, the Fourier transform of 2-point Green's function is,

$$G_\beta(\vec{x},\tau) = \frac{1}{\beta}\sum_n \int \frac{d^3k}{(2\pi)^3} e^{-i(\omega_n\tau - \vec{k}.\vec{x})}\tilde{G}_\beta(\vec{k},\omega_n) \qquad (2.47)$$

To find the form of bosonic propagator, we take zero temperature Klein-Gordon equation

$$(\partial^\mu\partial_\mu + m^2)G(x) = -\delta^4(x) \qquad (2.48)$$

and by making the transformation $t \to -i\tau$ or $p^0 \to ip^0$, which is the Wick rotation and using Eq.(2.47), we have

$$\tilde{G}_\beta(\vec{k},\omega_n) = \frac{1}{\omega_n^2 + \vec{k}^2 + m^2} = \frac{1}{4n^2\pi^2/\beta^2 + \vec{k}^2 + m^2} \qquad (2.49)$$

Similarly we can determine the fermionic propagator to be

$$\begin{aligned}
\tilde{S}_\beta(\vec{k},\omega_n) &= \frac{\gamma^0\omega_n + \vec{\gamma}.\vec{k} - m}{\omega_n^2 + \vec{k}^2 + m^2} \\
&= \frac{\gamma^0((2n+1)\pi/\beta) + \vec{\gamma}.\vec{k} - m}{(2n+1)^2\pi^2/\beta^2 + \vec{k}^2 + m^2} \qquad (2.50)
\end{aligned}$$

Again, after wick rotation, $k^0 \to ik^0$ we identify the loop integral as follows,

$$\int \frac{d^4k}{(2\pi)^4} \to \frac{1}{\beta}\sum_n \int \frac{d^3k}{(2\pi)^3} \tag{2.51}$$

In summary, in imaginary time formalism the Feynman rules are the zero temperature rules with temperature, $\beta = 1/T$ and the following replacements,

- Performing the wick rotation for the momenta, $k^0 \to ik^0$.
- The zero component of the momentum,

$$\begin{aligned} k^0 &= 2\pi nT \text{ for bosons} \\ k^0 &= (2n+1)\pi T \text{ for fermions} \end{aligned}$$

- Loop integral is identified as

$$\int \frac{d^4k}{(2\pi)^4} \to T\sum_{n=-\infty}^{\infty} \int \frac{d^3k}{(2\pi)^3}$$

- The propagators are the following

$$\begin{aligned} \text{Boson Propagator} &: \frac{1}{4n^2\pi^2T^2 + \vec{k}^2 + m^2} \\ \text{Fermion Propagator} &: \frac{\gamma^0((2n+1)\pi T) + \vec{\gamma}.\vec{k} - m}{(2n+1)^2\pi^2T^2 + \vec{k}^2 + m^2} \end{aligned}$$

- Vertex factor: $\frac{1}{T}(2\pi)^3\delta_{\omega_{n_1}+\omega_{n_2}+\ldots}\delta^{(3)}(\vec{k}_1 + \vec{k}_2 + \ldots)V$, where V involves couplings.

2.2.2 A toy model at finite temperature

We have considered Yukawa model as an example to demonstrate imaginary time formalism of the previous subsection. The Lagrangian is the following

$$\mathcal{L} = \frac{1}{2}\partial_\mu\phi\partial^\mu\phi + i\bar{\psi}\gamma^\mu\partial_\mu\psi - \frac{1}{2}m_\phi^2\phi^2 + m_\psi\bar{\psi}\psi - \frac{1}{4!}\lambda\phi^4 - y_\phi\bar{\psi}\psi\phi \tag{2.52}$$

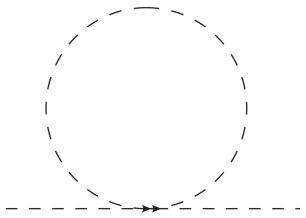

Figure 2.1: One loop correction to the scalar self energy due to its self interaction

One loop mass correction Here we are going to calculate the one loop mass correction of the scalar field due to it's self interaction and interaction with fermions at finite temperatures. We will see that how finite temperature modifies the mass of a scalar particle. This is the thermal screening of particle in the plasma. First we look into one loop correction due to scalar field itself.

From Fig. 2.1, we have

$$\begin{aligned} -i\delta^{(B)}m^2 &= -i\frac{\lambda T}{2}\sum_{n,\text{even}}\int\frac{d^3k}{(2\pi)^3}\frac{1}{n^2T^2+\vec{k}^2+m_\phi^2} \\ \text{or } \delta^{(B)}m^2 &= \frac{\lambda}{2\pi^2T}\sum_{n}\int\frac{d^3k}{(2\pi)^3}\frac{1}{n^2+(\omega_k/\pi T)^2} \end{aligned} \tag{2.53}$$

where, $\omega_k^2 = \vec{k}^2 + m_\phi^2$. Now if $y = \omega_k/\pi T$, using Eq.(A.18), we have from Eq.(2.53),

$$\delta^{(B)}m^2 = \frac{\lambda}{4}\int\frac{d^3k}{(2\pi)^3}\frac{1}{\omega_k}\coth\left(\frac{\omega}{2T}\right) \tag{2.54}$$

Furthermore, using Eq.(A.20), Eq.(2.54) reduces into

$$\delta^{(B)}m^2 = \frac{\lambda}{4}\int\frac{d^3k}{(2\pi)^3}\frac{1}{\omega_k} + \frac{\lambda}{2}\int\frac{d^3k}{(2\pi)^3}\frac{1}{\omega_k}\frac{1}{e^{\omega_k/T}-1} \tag{2.55}$$

The first part is the zero temperature part of the mass correction and contains the divergence. The temperature dependent part is free from ultraviolet divergences. Therefore it is enough to use zero temperature counter-terms to renormalize the theory. As the integral in the second part can not be evaluated in a closed form, we need to look into the high temperature limit, $m_\phi/T \ll 1$ and low temperature limit $m_\phi/T \gg 1$. But before going into high temperature expansion we look into fermionic contribution to self energy of the scalar.

From Fig. 2.2, we have,

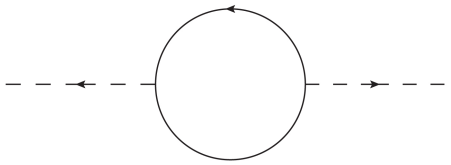

Figure 2.2: One loop correction to the scalar self energy by fermions

$$\begin{aligned}
-i\delta^{(F)}m^2 &= -y_\phi^2 \int \frac{d^4k}{(2\pi)^4} \frac{\mathrm{Tr}\left[(\not{k}+\not{p}+m_\psi)(\not{k}+m_\psi)\right]}{((k+p)^2-m_\psi^2)(k^2-m_\psi^2)} \\
&= 4iy_\phi^2 T \sum_{n,\mathrm{odd}} \int \frac{d^3k}{(2\pi)^3} \frac{n^2\pi^2T^2+\omega_k^2-2m_\psi^2}{(n^2\pi^2T^2+\omega_k^2)^2} \\
&= 4iy_\phi^2 T \sum_{n,\mathrm{odd}} \int \frac{d^3k}{(2\pi)^3} \left(\frac{1}{n^2\pi^2T^2+\omega_k^2} - \frac{2m_\psi^2}{(n^2\pi^2T^2+\omega_k^2)^2} \right) \qquad (2.56)
\end{aligned}$$

In the second step, we have taken zero external momentum. First part of Eq.(2.56) gives,

$$\begin{aligned}
\delta^{(F)}m_1^2 &= -4y_\phi^2 T \sum_{n,\mathrm{odd}} \int \frac{d^3k}{(2\pi)^3} \frac{1}{n^2\pi^2T^2+\omega_k^2} \\
&= -2y_\phi^2 \int \frac{d^3k}{(2\pi)^3} \frac{1}{\omega_k} \tanh\left(\frac{\omega_k}{2T}\right) \\
&= -2y_\phi^2 \int \frac{d^3k}{(2\pi)^3} \frac{1}{\omega_k} + 4y_\phi^2 \int \frac{d^3k}{(2\pi)^3} \frac{1}{\omega_k} \frac{1}{e^{\omega_k/T}+1} \qquad (2.57)
\end{aligned}$$

where the first term is the zero temperature quadratic divergent contribution which can be regulated by the usual counterterms introduced at zero temperature. The second term contains the finite temperature contribution of fermion to the self energy of the scalar. Also, the second integral in the finite temperature part is actually logarithmically divergent therefore it will not provide $O(T^2)$ correction which is given by quadratic divergent loop contribution as the momentum is now cut off with the temperature.

As the the scalar and fermion contribution in finite temperature part cannot be evaluated in closed form apart from some limiting cases, in the following, we present the results of the integrals in the high temperature limit.

High temperature expansion In the high temperature limit $m_i/T \ll 1$, the correction to scalar self energy due to it's self interaction[1] is,

$$\delta^{(B)} m_T^2 = \frac{\lambda T^2}{24} \tag{2.58}$$

On the other hand the correction due to fermion is

$$\delta^{(F)} m_T^2 = y_\phi^2 \frac{T^2}{6} \tag{2.59}$$

Therefore we can see that due to temperature correction, the mass of the scalar has become

$$m_\phi^2(T) = m_R^2 + \Pi(T) \tag{2.60}$$

where m_R is the renormalized mass and $\Pi(T)$ is the thermal correction which is

$$\Pi(T) = \left(\frac{\lambda}{2} + 2y_\phi^2\right) \frac{T^2}{12} \tag{2.61}$$

Eq.(2.60) expresses the thermal mass of the scalar with the Debye screening $\Pi(T)$.

2.3 Effective potential at finite temperature

In the previous sections, the main ingredients of finite temperature field theory have been introduced. In this section, we describe the steps to obtain the finite temperature effective potential which is equivalent to the free energy of the thermodynamic system and essential to investigate the nature of phase transition.

For simplicity, let us consider a theory with a real scalar field $\phi(x)$ with the Lagrangian density $\mathcal{L}$ and the action

$$S[\phi] = \int d^4x \mathcal{L} \tag{2.62}$$

The generating functional (vacuum-to-vacuum amplitude) is

$$Z[j] = \langle 0_{\text{out}} \mid 0_{\text{in}} \rangle_j \equiv \int \mathcal{D}\phi \exp[i(S[\phi] + \int d^4x \phi(x) j(x))] \tag{2.63}$$

The connected generating functional $W[j]$ is

$$Z[j] = e^{iW[j]} \tag{2.64}$$

[1]The derivations are given in the appendix C

The effective action $\Gamma[\Phi]$ is as the Legendre transform of $W[j]$,

$$\Gamma[\Phi] = W[j] - \int d^4x \frac{\delta W[j]}{\delta j(x)} j(x) \tag{2.65}$$

where Φ is the vacuum expectation value of the field operator $\hat{\phi}$ in the presence of the source j which is $\Phi(x) = \langle 0|\hat{\phi}(x)|0\rangle_j$. It is also determined from

$$\Phi(x) = \frac{\delta W[j]}{\delta j(x)} \tag{2.66}$$

In particular, from Eq.(2.65) and Eq.(2.66), we can have

$$\frac{\delta \Gamma[\Phi]}{\delta \Phi} = -j \tag{2.67}$$

In the absence of the external source, Eq.(2.67) implies that,

$$\frac{\delta \Gamma[\Phi]}{\delta \Phi}|_{j=0} = 0 \tag{2.68}$$

which defines the vacuum of the theory.

There are two ways to obtain the one loop effective potential. One method involves the summing of one particle irreducible (1PI) diagrams. Another one is directly from the path integral by shifting the field with respect to a classical background field. In the following we describe two methods in order.

2.3.1 Effective potential as the sum of 1PI digrams

The one-loop effective potential one can also obtain it as the sum of all 1PI diagrams as shown first by [87]. We can expand $Z[j]$ ($W[j]$) in a power series of j, to obtain its representation in terms of Green functions $G_{(n)}$ (connected Green functions $G^c_{(n)}$) as,

$$Z[j] = \sum_{n=0}^{\infty} \frac{i^n}{n!} \int d^4x_1 \dots d^4x_n j(x_1) \dots j(x_n) G_{(n)}(x_1, \dots, x_n) \tag{2.69}$$

and

$$iW[j] = \sum_{n=0}^{\infty} \frac{i^n}{n!} \int d^4x_1 \dots d^4x_n j(x_1) \dots j(x_n) G^c_{(n)}(x_1, \dots, x_n) \tag{2.70}$$

The effective action is also expanded in powers of Φ as

$$\Gamma[\Phi] = \sum_{n=0}^{\infty} \frac{1}{n!} \int d^4x_1 \dots d^4x_n \Phi(x_1) \dots \Phi(x_n) \Gamma^{(n)}(x_1, \dots, x_n) \tag{2.71}$$

where $\Gamma^{(n)}$ are the one-particle irreducible (1PI) Green functions.

We can make the Fourier transform of $\Gamma^{(n)}$ and $\Phi(x)$ as,

$$\Gamma^{(n)}(x_1, \dots, x_n) = \int \prod_{i=1}^{n} \left[\frac{d^4p_i}{(2\pi)^4} \exp\{ip_i x_i\} \right] (2\pi)^4 \delta^{(4)}(p_1 + \dots + p_n) \Gamma^{(n)}(p_1, \cdots, p_n) \tag{2.72}$$

$$\overline{\Phi}(p) = \int d^4x e^{-ipx} \Phi(x) \tag{2.73}$$

and by using them in Eq.(2.71) we have,

$$\Gamma[\Phi] = \sum_{n=0}^{\infty} \frac{1}{n!} \int \prod_{i=1}^{n} \left[\frac{d^4p_i}{(2\pi)^4} \overline{\Phi}(-p_i) \right] (2\pi)^4 \delta^{(4)}(p_1 + \dots + p_n) \Gamma^{(n)}(p_1, \dots, p_n) \tag{2.74}$$

The effective action can also be expanded in powers of the momentum, about the point where all external momenta vanish. In configuration space this expansion is

$$\Gamma[\Phi] = \int d^4x \left[-V_{\text{eff}}(\Phi) + \frac{1}{2} (\partial_\mu \Phi(x))^2 Z(\Phi) + \cdots \right] \tag{2.75}$$

For a translationally invariant theory $\Phi(x) = \phi_c$ where ϕ_c is a constant. So Eq.(2.75) becomes

$$\Gamma[\phi_c] = -\int d^4x V_{\text{eff}}(\phi_c) \tag{2.76}$$

where $V_{\text{eff}}(\phi_c)$ is the effective potential. Now using the definition of Dirac δ-function,

$$\delta^{(4)}(p) = \int \frac{d^4x}{(2\pi)^4} e^{-ipx} \tag{2.77}$$

we obtain,

$$\overline{\Phi}(p) = (2\pi)^4 \phi_c \delta^{(4)}(p). \tag{2.78}$$

Therefore using Eq.(2.78) in (2.74), we can write the effective action for constant field configurations as,

$$\Gamma(\phi_c) = \sum_{n=0}^{\infty} \frac{1}{n!} \phi_c^n (2\pi)^4 \delta^{(4)}(0) \Gamma^{(n)}(p_i = 0) = \sum_{n=0}^{\infty} \frac{1}{n!} \phi_c^n \Gamma^{(n)}(p_i = 0) \int d^4x \tag{2.79}$$

where $\delta^{(4)}(0)$ is the space-time volume factor $\int d^4x$. Now comparing it with (2.76) we obtain the final expression for the effective potential,

$$V_{\rm eff}(\phi_c) = -\sum_{n=0}^{\infty} \frac{1}{n!}\phi_c^n \Gamma^{(n)}(p_i = 0) \tag{2.80}$$

2.3.2 Effective potential from the path integral

Determining the effective potential by summing 1PI diagrams may become cumbersome at times. There is another procedure shown in [88] to determine the effective potential by shifting the scalar field $\phi(x)$ as follows

$$\phi(x) = \phi_c + \tilde{\phi}(x) \tag{2.81}$$

where ϕ_c is the space time independent constant field value and $\tilde{\phi}(x)$ is the small fluctuation. The exponential in the partition function Eq.(2.63) becomes

$$\begin{aligned} S[\phi_c &+ \tilde{\phi}(x)] + \int d^4x j(x)(\phi_c + \tilde{\phi}(x)) \\ &= S[\phi_c] + \int d^4x j(x)\phi_c + \int d^4x \{j(x) + \frac{\delta S}{\delta\phi}|_{\phi=\phi_c}\}\tilde{\phi} \\ &+ \frac{1}{2}\int d^4x d^4y \tilde{\phi}(x)\frac{\delta^2 S}{\delta\phi(x)\delta\phi(y)}|_{\phi=\phi_c}\tilde{\phi}(y) \end{aligned} \tag{2.82}$$

In the classical limit the path integral over the field $\phi(x)$ is dominated by the classical solution ϕ_c which extremizes the exponent in Eq.(2.63),

$$\frac{\delta S}{\delta\phi(x)}|_{\phi=\phi_c} = -j \tag{2.83}$$

Moreover, the propagator of the theory is given by,

$$iD^{-1}(x, y; \phi_c) = \frac{\delta^2 S}{\delta\phi(x)\delta\phi(y)}|_{\phi=\phi_c} \tag{2.84}$$

Therefore, Eq.(2.83) implies that the third term of second line of Eq.(2.82) is zero. So the partition function is

$$\begin{aligned} Z[j] &= \exp\{iW[j]\} \sim \exp[i\{S[\phi_c] + \int d^4x j(x)\phi_c\}] \\ &\quad \int \mathcal{D}\tilde{\phi}(x)\exp[\frac{i}{2}\int d^4x d^4y \tilde{\phi}(x)(iD^{-1}(x, y; \phi_c))\tilde{\phi}(y)] \\ &\sim \exp[i\{S[\phi_c] + \int d^4x j(x)\phi_c\}](\mathrm{Det} iD^{-1}(x, y; \phi_c))^{-1/2} \\ &\sim \exp[i\{S[\phi_c] + \int d^4x j(x)\phi_c + \frac{i}{2}\mathrm{logDet} iD^{-1}(x, y; \phi_c)\}] \end{aligned} \tag{2.85}$$

where we have used

$$\int \mathcal{D}\phi \exp[\frac{i}{2}\phi M \phi] = (\mathrm{Det} M)^{-1/2} \tag{2.86}$$

Also from Eq.(2.65) we have,

$$W[j] = \Gamma[\phi_c] + \int d^4x \phi_c j(x) \tag{2.87}$$

And,

$$\Gamma[\phi_c] = -\int d^4x V_{\text{eff}}(\phi_c) \tag{2.88}$$

So from Eq.(2.85), Eq.(2.87) and Eq.(2.88) and removing the space-time volume factor, the effective potential at 1-loop is given by,

$$V_{\text{eff}}(\phi_c) = V_0(\phi_c) - \frac{i}{2} \ln \mathrm{Det}\, iD^{-1}(x, y; \phi_c) \tag{2.89}$$

Here, $V_0(\phi_c)$ is the tree-level potential. Using $\ln \mathrm{Det}\, M = \mathrm{Tr} \ln M$ and going to the momentum space, from Eq.(2.89),

$$V_{\text{eff}}(\phi_c) = V_0(\phi_c) - \frac{i}{2} \mathrm{Tr} \int \frac{d^4k}{(2\pi)^4} \ln iD^{-1}(k; \phi_c) \tag{2.90}$$

In case of determining the fermionic contribution to the effective potential we follow the same procedure of shifting the fermion fields $\psi(x) = \psi_b + \tilde{\psi}(x)$ where ψ_b is the classical background field and $\tilde{\psi}(x)$ is the quantum fluctuation. The Lagrangian describing the fermion fields is

$$\mathcal{L} = i\bar{\psi}\partial\!\!\!/\psi - m\bar{\psi}\psi - y\bar{\psi}\psi\phi \tag{2.91}$$

By shifting both scalar and fermion fields we extract the part of Lagrangian quadratic in the fermion fields,

$$\hat{\mathcal{L}}(\phi_c, \tilde{\psi}(x)) = i\bar{\tilde{\psi}}\partial\!\!\!/\tilde{\psi} - \bar{\tilde{\psi}} M(\phi_c) \tilde{\psi} \tag{2.92}$$

So the partition function for fermion fields is

$$Z_F = \int \mathcal{D}\bar{\psi}\mathcal{D}\psi \exp[i \int d^4x \mathcal{L}] \tag{2.93}$$

Keeping up to the quadratic fluctuations, we have

$$\begin{aligned} Z_F &= \exp[iW] \sim \int \mathcal{D}\bar{\psi}\mathcal{D}\psi \exp[i \int d^4x d^4y \bar{\tilde{\psi}}(x)(iD_F^{-1}(x, y; \phi_c))\tilde{\psi}(y)] \\ &\sim \exp[i\{-i \ln \mathrm{Det}(iD_F^{-1}(x, y; \phi_c)\} \end{aligned} \tag{2.94}$$

Therefore from Eq.(2.76), we can have,

$$V_{\text{eff}}(\phi_c) = i\ln \text{ Det}\, iD_F^{-1}(x,y;\phi_c) \tag{2.95}$$

$$= i\text{Tr}\int \frac{d^4k}{(2\pi)^4}\ln iD_F^{-1}(k;\phi_c) \tag{2.96}$$

where

$$iD_F^{-1}(k;\phi_c) = \not{k} - M(\phi_c) \;\; ; M(\phi_c) = m + y\phi_c \tag{2.97}$$

2.3.3 Effective potential for scalar, fermion and vector fields

In the following sections, because of its simplicity and straightforward features, we will use the second procedure to determine the effective potential for scalar, fermion and gauge fields respectively.

Scalar fields Consider a model of self interacting real scalar field described by the Lagrangian,

$$\mathcal{L} = \frac{1}{2}\partial_\mu\phi\partial^\mu\phi - \frac{1}{2}m^2\phi^2 - \frac{\lambda}{4!}\phi^4 \tag{2.98}$$

Now we shift the field, $\phi(x) = \phi_c + \tilde{\phi}(x)$ and the inverse of the propagator in momentum space, $iD^{-1}(k;\phi_c)$ is given by

$$iD^{-1}(k;\phi_c) = k^2 - m^2(\phi_c) \tag{2.99}$$

where the field dependent mass $m^2(\phi_c)$ is

$$m^2(\phi_c) = m^2 + \frac{1}{2}\lambda\phi_c^2 \tag{2.100}$$

Therefore the effective potential at one-loop is

$$V_{\text{eff}}(\phi_c) = V_0(\phi_c) - \frac{i}{2}\text{Tr}\int \frac{d^4k}{(2\pi)^4}\ln\left[k^2 - m^2(\phi_c)\right] \tag{2.101}$$

After the Wick rotation, $k^0 \to ik^0$, we have

$$V_{\text{eff}}(\phi_c) = V_0(\phi_c) + \frac{1}{2}\text{Tr}\int \frac{d^4k}{(2\pi)^4}\ln\left[k^2 + m^2(\phi_c)\right] \tag{2.102}$$

The result can be generalized for the case of N_s complex scalar fields described by the Lagrangian

$$\mathcal{L} = \partial_\mu\phi_a^\dagger\partial^\mu\phi^a - V_0(\phi_a^\dagger,\phi^a) \tag{2.103}$$

Therefore the effective potential at one loop is given by

$$V_{\rm eff}(\phi_c) = V_0(\phi_c) + \frac{1}{2}{\rm Tr}\int \frac{d^4k}{(2\pi)^4}\ln\left[k^2 + M_s^2(\phi_c)\right] \tag{2.104}$$

where

$$(M_s^2)^a_b = \frac{\partial^2 V_0}{\partial\phi^\dagger_a \partial\phi^b}|_{\phi=\phi_c} \tag{2.105}$$

Fermion fields The Lagrangian describing the fermion field is

$$\mathcal{L} = i\bar{\psi}\partial\!\!\!/\psi - m\bar{\psi}\psi - y\bar{\psi}\psi\phi \tag{2.106}$$

By shifting the fields, we have,

$$iD_F^{-1}(k;\phi_c) = k\!\!\!/ - M(\phi_c)\ \ ; M(\phi_c) = m + y\phi_c \tag{2.107}$$

Therefore from Eq.(2.95), the fermionic contribution to the effective potential at one loop is

$$V^1_{\rm eff}(\phi_c) = i\int \frac{d^4k}{(2\pi)^4}\ln\ {\rm Det}(k\!\!\!/ - M(\phi_c)) \tag{2.108}$$

As the determinant of an operator remains invariant under transposition, we can have

$$\begin{aligned}\ln\ {\rm Det}(k\!\!\!/ - M(\phi_c)) &= \ln\ {\rm Det}(k\!\!\!/ - M(\phi_c))^T \\ &= \ln\ {\rm Det}(-C^{-1}\gamma^\mu C k_\mu - M(\phi_c))\ , C\gamma^\mu C^{-1} = -\gamma^{\mu T} \\ &= \ln\ {\rm Det}(-k\!\!\!/ - M(\phi_c))\end{aligned} \tag{2.109}$$

Therefore we can write Eq.(2.108) as

$$V^1_{\rm eff}(\phi_c) = 2i{\rm Tr}\int \frac{d^4k}{(2\pi)^4}\ln(k^2 - M^2(\phi_c)) \tag{2.110}$$

where trace is taken over the internal indices. Now again doing the Wick rotation $k^0 \to ik^0$, we have from Eq.(2.110),

$$V^1_{\rm eff}(\phi_c) = -2{\rm Tr}\int \frac{d^4k}{(2\pi)^4}\ln(k^2 + M^2(\phi_c)) \tag{2.111}$$

If there are N_F fermion fields with the Lagrangian

$$\mathcal{L} = i\bar{\psi}_i\partial\!\!\!/\psi_i - \bar{\psi}_i M_{ij}\psi_j - i\bar{\psi}_i Y^a_{ij}\psi_j\phi_a \tag{2.112}$$

After shifting the fields, the mass matrix for the fermion is $(M_f)_{ij} = M_{ij} + Y^a_{ij}\phi^a_c$. Therefore the effective potential will be,

$$V^1_{\rm eff}(\phi_c) = -2g_f\frac{1}{2}{\rm Tr}\int \frac{d^4k}{(2\pi)^4}\ln(k^2 + M_f^2(\phi_c)) \tag{2.113}$$

where $g_f = 1$ for Weyl fermions and $g_f = 2$ for the Dirac fermions.

Gauge fields Consider the gauge fields described by the Lagrangian,

$$\mathcal{L} = -\frac{1}{4}Tr(F_{\mu\nu}F^{\mu\nu}) + (D_\mu\phi)^\dagger D^\mu\phi - V_0(\phi_i) \tag{2.114}$$

For physical results, we need to fix the gauge. A convenient choice is the Landau gauge which preserves the renormalizability of the theory. In this gauge the propagator for the gauge field is purely transverse,

$$\Delta^{ab}_{\mu\nu}(k) = \frac{-i\delta^{ab}}{k^2 + i\epsilon}[\eta_{\mu\nu} - \frac{k_\mu k_\nu}{k^2}] \tag{2.115}$$

One calculational advantage of this gauge is that in theories with scalars which acquire vevs, the Faddeev-Popov ghost fields decouple from these scalar fields in this gauge.

After shifting the scalar fields, the mass term for the gauge bosons is

$$\mathcal{L}_m = \frac{1}{2}(M_{gb})^2_{ab}A^a_\mu A^{\mu b} \tag{2.116}$$

where

$$(M_{gb})^2_{ab}(\phi_c) = g^2\phi_c^\dagger T^a T^b \phi_c \tag{2.117}$$

Following the procedure of determining the effective potential for the scalar fields, we have the vector boson contribution to the effective potential at one loop

$$V^1_{gb}(\phi_c) = g_v\frac{1}{2}\mathrm{Tr}\int\frac{d^4k}{(2\pi)^4}\ln[k^2 + M^2_{gb}(\phi_c)] \tag{2.118}$$

where $g_v = 3$ is the degrees of freedom of a massive gauge boson.

Therefore for a gauge theory with N_s scalar fields and N_F fermion fields, we have from Eq.(2.105), Eq.(2.113) and Eq.(2.118),

$$\begin{aligned} V_{\text{eff}}(\phi_c) &= V_0(\phi_c) + \frac{1}{2}\mathrm{Tr}\int\frac{d^4k}{(2\pi)^4}\ln[k^2 + M^2_s(\phi_c)] \\ &- 2g_f\frac{1}{2}\mathrm{Tr}\int\frac{d^4k}{(2\pi)^4}\ln(k^2 + M^2_f(\phi_c)) \\ &+ g_v\frac{1}{2}\mathrm{Tr}\int\frac{d^4k}{(2\pi)^4}\ln[k^2 + M^2_{gb}(\phi_c)] \end{aligned} \tag{2.119}$$

2.3.4 Finite temperature effective potential

In the previous sections we have presented the effective potential for scalar, fermion and vector fields. Now, by using the Feynman rules for the imaginary

time formalism, we can derive the finite temperature effective potential and compare the results with those of section 2.1.

Let us first concentrate on scalar effective potential. Using the Feynman rules for finite temperature, one loop contribution of Eq.(2.102) can be expressed as

$$\begin{aligned} V_{\rm eff}^{T}(\phi_c) &= T\sum_{n=-\infty}^{\infty}\int\frac{d^3k}{(2\pi)^3}\ln(4\pi^2n^2T^2+\vec{k}^2+m(\phi_c)^2) \\ &= T\sum_{n=-\infty}^{\infty}\int\frac{d^3k}{(2\pi)^3}\ln(4\pi^2n^2T^2+\omega^2) \end{aligned} \tag{2.120}$$

where $\omega^2=\vec{k}^2+m(\phi_c)^2$. Let us define,

$$v(\omega)=\sum_{n=-\infty}^{\infty}\ln(4\pi^2n^2T^2+\omega^2) \tag{2.121}$$

therefore

$$\begin{aligned} \frac{\partial v}{\partial\omega} &= \sum_{n=-\infty}^{\infty}\frac{2\omega}{4\pi^2n^2T^2+\omega^2} \\ &= \frac{\omega}{2\pi^2T^2}\sum_{n=-\infty}^{\infty}\frac{1}{n^2+(\omega/2\pi T)^2} \\ &= \frac{1}{T}\coth\left(\frac{\omega}{2T}\right) \end{aligned} \tag{2.122}$$

So we have

$$\frac{\partial v}{\partial\omega}=\frac{1}{T}(1+\frac{2}{e^{\omega/T}-1}) \tag{2.123}$$

By integrating Eq.(2.123),

$$v(\omega)=\frac{\omega}{T}+2\ln(1-e^{-\omega/T}) \tag{2.124}$$

So we have from Eq.(2.120),

$$V_{\rm eff}^{T}=\int\frac{d^3k}{(2\pi)^3}\left[\frac{\omega}{2}+T\ln(1-e^{-\omega/T})\right] \tag{2.125}$$

In the following we show that the first term of Eq.(2.125) is zero temperature Coleman-Weinberg (CW) one loop effective potential. Details of

renormalization of of the CW potential is presented in appendix B. We again start from Eq.(2.102) where Wick rotation is already performed.

$$V_{\rm eff}^{(1)} = \frac{1}{2}\int \frac{dk^0}{2\pi}\frac{d^3k}{(2\pi)^3}\ln(k^{0^2}+\vec{k}^2+m^2) \tag{2.126}$$

Let us again define

$$f(\omega) = \int_{-\infty}^{\infty}\frac{dk^0}{2\pi}\ln(k^{0^2}+\omega^2) \tag{2.127}$$

Therefore

$$\frac{\partial f}{\partial \omega} = \int_{-\infty}^{\infty}\frac{dk^0}{2\pi}\frac{2\omega}{k^{0^2}+\omega^2} \tag{2.128}$$

The poles for the integrand in Eq.(2.128) are $k^0 = \pm i\omega$. Now defining the contour from $-\infty$ to ∞ covering the upper half plane of complex k^0 plane, we pick up the pole at $k^0 = i\omega$. Therefore the contour integration in Eq.(2.128) gives

$$\frac{\partial f}{\partial \omega} = \int_{C}\frac{dk^0}{2\pi}\frac{2\omega}{k^{0^2}+\omega^2} = 1 \tag{2.129}$$

So by integrating Eq.(2.129) we have

$$f(\omega) = \omega \tag{2.130}$$

So from Eq.(2.126) we have

$$V_{\rm eff}^{(1)} = \int \frac{d^3k}{(2\pi)^3}\frac{\omega}{2} \tag{2.131}$$

Therefore decomposing zero temperature and finite temperature part of Eq.(2.125),

$$\begin{aligned} V_{\rm eff}^{T} &= V_{\rm CW}^{(1)} + V_{T}^{(1)} \\ V_{\rm CW}^{(1)} &= \int \frac{d^3k}{(2\pi)^3}\frac{\omega}{2} \qquad (2.132) \\ V_{T}^{(1)} &= T\int \frac{d^3k}{(2\pi)^3}\ln(1-e^{-\omega/T}) \qquad (2.133) \end{aligned}$$

We can see that finite temperature scalar effective potential, Eq.(2.133) is exactly the temperature-dependent part of the bosonic free energy density given in Eq.(2.20). By changing variable $x = k/T$ we have from Eq.(2.133),

$$V_{T}^{(1)} = \frac{T^4}{2\pi^2}\int_0^{\infty} dx x^2 \ln(1-e^{-\sqrt{x^2+m^2(\phi_c)/T^2}}) \tag{2.134}$$

Fermionic finite temperature effective potential To determine the finite temperature effective potential for fermions we start from Eq.(2.113) and using again Feynman rules for finite temperature, we have

$$V_{F\text{eff}}^{T} = -2g_f \frac{1}{2} T \sum_{n,\text{odd}} \int \frac{d^3k}{(2\pi)^3} \ln(n^2\pi^2T^2 + \vec{k}^2 + m_f^2) \tag{2.135}$$

Again we define

$$v_F(\omega) = \sum_{n,\text{odd}} \ln(n^2\pi^2T^2 + \omega^2) \tag{2.136}$$

where $\omega^2 = \vec{k}^2 + m_f^2$.

$$\frac{\partial v_F}{\partial \omega} = \sum_{n,\text{odd}} \frac{2\omega}{n^2\pi^2T^2 + \omega^2} \tag{2.137}$$

The sum over odd integer can be recasted as follows. If we denote,

$$S(y) = \sum_{n=-\infty}^{\infty} \frac{1}{n^2 + y^2} = \frac{\pi}{y} \coth(\pi y) \tag{2.138}$$

then,

$$\begin{aligned} \sum_{n,\text{odd}} \frac{1}{n^2 + y^2} &= S(y) - \frac{1}{4} S(y/2) \\ &= \frac{\pi}{y} \coth(\pi y) - \frac{\pi}{2y} \coth\left(\frac{\pi y}{2}\right) \end{aligned} \tag{2.139}$$

Using Eq.(2.139), from Eq.(2.137), we have

$$\begin{aligned} \frac{\partial v_F}{\partial \omega} &= \frac{2\omega}{\pi^2T^2} \sum_{n,\text{odd}} \frac{1}{n^2 + (\omega/\pi T)^2} \\ &= \frac{1}{T}(2\coth(\omega/T) - \coth(\omega/2T)) \\ &= \frac{1}{T}(1 - \frac{2}{e^{\omega/T} + 1}) \end{aligned} \tag{2.140}$$

Therefore by integrating Eq.(2.140) we have

$$v_F(\omega) = \frac{\omega}{T} + 2\ln(1 + e^{-\omega/T}) \tag{2.141}$$

Inserting Eq.(2.141) back in Eq.(2.111), we have

$$V_{F\text{eff}}^{T} = -2g_f \int \frac{d^3k}{(2\pi)^3} \left[\frac{\omega}{2} + T\ln(1 + e^{-\omega/T})\right] \tag{2.142}$$

Like in the case of scalar effective potential, we can decompose the zero and finite temperature contribution for fermion effective potential.

$$\begin{aligned} V^{T}_{F\text{eff}} &= V^{(1)}_{F\text{CW}} + V^{(1)}_{FT} \\ V^{(1)}_{F\text{CW}} &= -2g_f \int \frac{d^3k}{(2\pi)^3}\frac{\omega}{2} \qquad (2.143) \\ V^{(1)}_{FT} &= -2g_f T \int \frac{d^3k}{(2\pi)^3}\ln(1+e^{-\omega/T}) \qquad (2.144) \end{aligned}$$

where again, Eq.(2.144) is exactly the temperature-dependent part of fermionic free energy density given by Eq.(2.20). Now by changing the variable $x = k/T$ we have from Eq.(2.144),

$$V^{(1)}_{F\,T} = \frac{T^4}{2\pi^2}\int_0^\infty dx x^2 \ln(1+e^{-\sqrt{x^2+m_f^2(\phi_c)/T^2}}) \qquad (2.145)$$

Finite temperature effective potential for gauge fields The determination of finite temperature effective potential for gauge boson is similar to the case of scalar effective potential. In the Landau gauge, after shifting the scalar field, $\phi = \phi_c + \tilde{\phi}$, the gauge boson acquires the mass $m_{gb}(\phi_c)$. Therefore the finite temperature effective potential is

$$\begin{aligned} V^{\beta}_{gb\text{eff}} &= V^{(1)}_{gb\text{CW}} + V^{(1)}_{gbT} \\ V^{(1)}_{gb\text{CW}} &= 3\int \frac{d^3k}{(2\pi)^3}\frac{\omega}{2} \qquad (2.146) \\ V^{(1)}_{gbT} &= 3T\int \frac{d^3k}{(2\pi)^3}\ln(1-e^{-\omega/T}) \qquad (2.147) \end{aligned}$$

where $\omega^2 = \vec{k}^2 + m^2_{gb}(\phi_c)$ and 3 enters because of degrees of freedom for massive gauge boson. Again the finite temperature part can be recasted by changing the variable as follows,

$$V^{(1)}_{gbT} = 3\frac{T^4}{2\pi^2}\int_0^\infty dx x^2 \ln(1-e^{-\sqrt{x^2+m^2_{gb}(\phi_c)/T^2}}) \qquad (2.148)$$

Therefore we can write the finite temperature effective potential as

$$\begin{aligned} V_{\text{eff}}(\phi_c) &= V_0(\phi_c) + \sum_B g_B \frac{m_B^4(\phi_c)}{64\pi^2}\left[\ln\frac{m_B^2(\phi_c)}{\mu^2} - c_B\right] \\ &+ g_B\frac{T^4}{2\pi^2}\int_0^\infty dx x^2 \ln(1 - e^{-\sqrt{x^2+m_B^2(\phi_c)/T^2}}) \\ &- \sum_F g_F \frac{m_F^4(\phi_c)}{64\pi^2}\left[\ln\frac{m_F^2(\phi_c)}{\mu^2} - c_F\right] \\ &+ g_F\frac{T^4}{2\pi^2}\int_0^\infty dx x^2 \ln(1 + e^{-\sqrt{x^2+m_F^2(\phi_c)/T^2}}) \end{aligned} \tag{2.149}$$

where $\overline{MS}$ renormalization is used for CW potential. Here, $c_B = 3/2$ for scalar particles and $c_B = 5/6$ for the gauge bosons. On the other hand for fermions $c_F = 3/2$.

High temperature effective potential

The high temperature expansion[2] of thermal effective potential Eq.(2.149) is

$$\begin{aligned} V_T(\phi_c) &= \sum_B g_B\left[\frac{m_B^2(\phi_c)T^2}{12} - \frac{m_B^3(\phi_c)T}{12\pi} - \frac{m_B^4(\phi_c)}{64\pi^2}\left(\ln\frac{m_B^2(\phi_c)}{a_b T^2} - \frac{3}{2}\right)\right] \\ &+ \sum_F g_F\left[\frac{m_F^2(\phi_c)T^2}{48} + \frac{m_F^4(\phi_c)}{64\pi^2}\left(\ln\frac{m_F^2(\phi_c)}{a_f T^2} - \frac{3}{2}\right)\right] \end{aligned} \tag{2.150}$$

where, $a_b = 16\pi^2 e^{-2\gamma_E}$ and $a_f = \pi^2 e^{-2\gamma_E}$.

Scalar thermal masses

As the main focus of the presented work is the EWPhT in the SM with extended scalar sector, we have listed here the general formula for scalar thermal mass at the high temperature limit following [75, 78, 79].

Consider a gauge theory with group G where the scalar Q is in representation R and the fermion Ψ is in representation F of G. The scalar potential can be written as,

$$V = M_\Phi^2 \Phi^\dagger\Phi + \lambda_1(\Phi^\dagger\Phi)^2 + \lambda_2(\Phi^\dagger T^a \Phi)^2 \tag{2.151}$$

where T^a is the generator of G in Φ's representation. Also the yukawa term is

$$L_Y = \bar{\Psi}\Gamma\Psi\Phi + \Phi^\dagger\bar{\Psi}\bar{\Gamma}\Psi \tag{2.152}$$

[2]The derivation is given in appendix C.3

where Γ is the gauge covariant Yukawa matrix and $\bar{\Gamma} = \gamma^0\Gamma\gamma^0$. Furthermore, the scalar gauge boson interaction term contributing to the thermal mass is

$$L_g = g^2\Phi^\dagger T^a T^b \Phi V_\mu^a V^{\mu b} \tag{2.153}$$

Now at finite temperature with, $T \gg m$ we have for non-zero scalar condensate $\langle\Phi\rangle = \phi_c$, the thermal mass term, $(m^2)_i^j(\phi_c, T)\phi^{\dagger i}\phi_j$ where,

$$(m^2)_i^j(\phi_c, T) = (m^2)_i^j(\phi_c) + \frac{T^2}{12}\left[2\lambda_1(N+1)\delta_i^j + 2\lambda_2(T^aT^a)_i^j + 3g^2(T^aT^a)_i^j + \mathrm{Tr}\left(\bar{\Gamma}_i\Gamma^j\right)\right] \tag{2.154}$$

Here N is the dimension of the representation R and trace is taken over spinor and representation indices of F.

2.4 Phase transition in the early universe

To study the phases of a general thermodynamic system, we basically deal with the free energy associated with the system (for detailed review [89]). The system will involve, in general sense, coupling constants $\{K_n\}$ and the combinations of dynamical degrees of freedom, $\{\Theta_n\}$. $\{K_n\}$ can be external parameters like temperature, field values and $\{\Theta_n\}$ will be local operators. Therefore if the partition function of the system is $Z[\{K_n\}]$ then the free energy is

$$F[\{K_n\}] = -T\ln Z[\{K_n\}] \tag{2.155}$$

For notational simplicity we denote $[K] = \{K_n\}$. The phases of the system is characterized by the region of analyticity of $F[K]$ in the phase diagram. If there are D number of external parameters K_1,...,K_D, then phase diagram is a D-dimensional space. The possible non-analyticities are points, lines, planes, hyperplanes etc in the phase diagram. Therefore the phase transition is signaled by a singularity in the thermodynamic potential such as free energy. There are two types of phase transitions:

- If either one or more of $\frac{\partial F}{\partial K_i}$ is discontinuous across the phase boundary the transition is said to be first order phase transition.
- If $\frac{\partial F}{\partial K_i}$ is continuous across the phase boundary then it is called continuous phase transition. One subset of this class is second order phase transition where first derivatives are continuous but second order derivatives $\frac{\partial^2 F}{\partial K_i \partial K_j}$ across the phase boundary are discontinuous.

Order parameters The phenomenological approach to the phase transition is the Landau theory where the thermodynamic potential, for example, the free energy, is written as the function of order parameter η. The order parameter is the quantity which distinguishes the phase of the system, i.e. when $\eta = 0$ for the temperature $T > T_c$, where T_c is critical temperature, the system is in disordered phase. On the other hand, at temperature $T < T_c$, $\eta \neq 0$ and the system is in ordered phase. For example the Gibbs free energy, $G(P, T)$ will be function of order parameter η too. But as the free energy is uniquely determined by P and T, $\eta = \eta(P, T)$ and it is determined from the condition,

$$\frac{\partial G}{\partial \eta} = 0 \; ; \; \frac{\partial^2 G}{\partial \eta^2} > 0 \tag{2.156}$$

which is the condition for minima of the free energy. Moreover, the free energy can be expanded in the following,

$$G(P, T, \eta) = G_0(P, T) + A\eta^2 + B\eta^3 + C\eta^4 + ... \tag{2.157}$$

The order parameter can be a scalar, vector, tensor, pseudoscalar or a group element of a symmetry group. Also the order parameter is not uniquely defined for a given system because any thermodynamic variable which becomes zero in the disordered phase and non-zero in an ordered phase can be a possible choice of the order parameter.

To address the cosmological phase transition, we have chosen the order parameter to be vacuum expectation value of the scalar field: $\phi_c(T)$. In the standard hot big bang scenario, the universe is initially at the very high temperature and it can be in the symmetric phase, $\phi_c = 0$ which is the absolute minimum of the free energy or equivalently that of the finite temperature effective potential, $V^T_{\text{eff}}(\phi_c)$. At some critical temperature T_c the minimum at $\phi_c = 0$ becomes metastable and the phase transition will take place. The phase transition may be first or second order in nature depending on the parameters of the theory.

2.4.1 First and second order phase transitions

In the section we are going to illustrate the difference between the first and second order phase transitions by using a simplified example [17, 18].

$$V(\phi, T) = D(T^2 - T_o^2)\phi^2 + \frac{\lambda_T}{4}\phi^4 \tag{2.158}$$

where D and T_o^2 are the constant terms and λ_T is a coupling constant which can have temperature dependence. At zero temperature, the potential has

a negative mass-squared term $-DT_0^2$, which indicates that the state $\phi = 0$ is unstable, and the energetically favored state corresponds to the minimum at $\phi = \pm\sqrt{\frac{2D}{\lambda_T}}T_o$, where the symmetry $\phi \leftrightarrow -\phi$ of the original theory is spontaneously broken.

From finite temperature potential Eq.(2.158) we have T-dependent mass,

$$m^2(\phi, T) = 3\lambda_T\phi^2 + 2D(T^2 - T_o^2) \tag{2.159}$$

and its stationary points, i.e. solutions to $dV(\phi, T)/d\phi = 0$, are given by,

$$\begin{aligned} \phi(T) &= 0 \\ &\text{and} \\ \phi(T) &= \sqrt{\frac{2D(T_o^2 - T^2)}{\lambda_T}} \end{aligned} \tag{2.160}$$

Therefore the critical temperature is given by T_o. At $T > T_o$, $m^2(0, T) > 0$ and the origin $\phi = 0$ is a minimum. At the same time only the solution $\phi = 0$ in Eq.(2.160) does exist. At $T = T_o$, $m^2(0, T_o) = 0$ and both solutions in Eq.(2.160) collapse at $\phi = 0$. The potential Eq.(2.158) becomes,

$$V(\phi, T_o) = \frac{\lambda_T}{4}\phi^4 \tag{2.161}$$

At $T < T_o$, $m^2(0, T) < 0$ and the origin becomes a maximum. Simultaneously, the solution $\phi(T) \neq 0$ does appear in Eq.(2.160). This phase transition is a second order transition, because there is no barrier between the symmetric and broken phases. Actually, when the broken phase is formed, the origin (symmetric phase) becomes a maximum and the phase transition may be achieved by a thermal fluctuation for a field located at the origin.

However, a barrier can develop between the symmetric and broken phases during phase transition. This is the characteristic of first order phase transitions. A typical example is provided by the following potential,

$$V(\phi, T) = D(T^2 - T_o^2)\phi^2 - ET\phi^3 + \frac{\lambda_T}{4}\phi^4 \tag{2.162}$$

where, as before, D, T_0 and E are T independent coefficients, and λ_T is a slowly varying T-dependent function. The difference between Eq.(2.162) and Eq.(2.158) is in the cubic term with coefficient E. This term is provided by the zero mode contribution in bosonic effective thermal potential Eq.(C.39). At $T > T_1$ the only minimum is at $\phi = 0$. At $T = T_1$

$$T_1^2 = \frac{8\lambda_T D T_o^2}{8\lambda_T D - 9E^2} \tag{2.163}$$

a local minimum at $\phi \neq 0$ appears as an inflection point. The value of the field ϕ at $T = T_1$ is,

$$\phi_* = \frac{3ET_1}{2\lambda_T} \tag{2.164}$$

At $T < T_1$, ϕ_* splits into a barrier ϕ_- and a local minimum, ϕ_+.

$$\phi_\pm(T) = \frac{3ET}{2\lambda_T} \pm \frac{1}{2\lambda_T}\sqrt{9E^2T^2 - 8\lambda_T D(T^2 - T_o^2)} \tag{2.165}$$

At the temperature $T = T_c$, $V(\phi(T_c), 0) = V(0, T_c)$, so we have,

$$T_c^2 = \frac{\lambda_T D T_o^2}{\lambda_T D - E^2} \tag{2.166}$$

$$\phi_+(T_c) = \frac{2ET_c}{\lambda_T} \tag{2.167}$$

and

$$\phi_-(T_c) = \frac{ET_c}{\lambda_T} \tag{2.168}$$

For $T < T_c$ the minimum at $\phi = 0$ becomes metastable and the minimum at ϕ_+ becomes the global one. At $T = T_o$ the barrier disappears, the origin becomes a maximum and

$$\phi_-(T_o) = 0 \tag{2.169}$$

and the second minimum becomes equal to

$$\phi_+(T_o) = \frac{3ET_o}{\lambda_T} \tag{2.170}$$

2.4.2 Electroweak phase transition in the Standard Model

For the zero temperature CW part of the finite temperature effective potential for the standard model, we have taken

$$V(\phi) = V_0(\phi) + \frac{1}{64\pi^2}\sum_{i=W^\pm,Z,t}\left\{m_i^4(\phi)\left(\log\frac{m_i^2(\phi)}{m_i^2(v)} - \frac{3}{2}\right) + 2m_i^2(v)m_i^2(\phi)\right\} \tag{2.171}$$

where the radiative corrections due to the W, Z bosons and the top quark are considered. For the thermal part, we have taken the high temperature approximation, Eq.(2.150).

To address the nature of transition in the SM, though the mass of the Higgs is greater than the W boson, we have taken as an illustration, the same approximation of the Higgs mass being much smaller than W boson

mass, considered in the previous works on the electroweak phase transition. In section 2.5.2 we will see that such approximation was essential to ensure the validity of the perturbation theory in the SM at finite temperature. The finite temperature effective potential of the SM is

$$V_{\rm SM}(\phi, T) = D(T^2 - T_0^2)\phi^2 - ET\phi^3 + \frac{\lambda_T}{4}\phi^4 \tag{2.172}$$

where the coefficients are given by

$$D = \frac{2m_W^2 + m_Z^2 + 2m_t^2}{8v^2} \tag{2.173}$$

$$E = \frac{2m_W^3 + m_Z^3}{4\pi v^3} \tag{2.174}$$

$$T_o^2 = \frac{m_h^2 - 8Bv^2}{4D} \tag{2.175}$$

$$B = \frac{3}{64\pi^2 v^4}\left(2m_W^4 + m_Z^4 - 4m_t^4\right) \tag{2.176}$$

$$\lambda_T = \lambda - \frac{3}{16\pi^2 v^4}\left(2m_W^4 \log\frac{m_W^2}{a_b T^2} + m_Z^4 \log\frac{m_Z^2}{a_b T^2} - 4m_t^4 \log\frac{m_t^2}{a_f T^2}\right) \tag{2.177}$$

where $a_b = 16\pi^2 e^{-2\gamma_E}$ and $a_f = \pi^2 e^{-2\gamma_E}$

Denoting $\phi_+(T_c) = \phi_c$, from Eq.(2.167) and Eq.(2.172) we have

$$\frac{\phi_c}{T_c} = \frac{2E}{\lambda_T} = \frac{4Ev^2}{m_h^2} \tag{2.178}$$

where,

$$E = \frac{2m_W^3 + m_Z^3}{4\pi v^3} = 9.6 \times 10^{-3}$$

The criterion for the strong first order phase transition in the SM (which is shown in details in section 3.3.3) is given by

$$\frac{\phi_c}{T_c} \geq 1.0 - 1.3 \tag{2.179}$$

which puts a bound on the Higgs mass from Eq.(2.178),

$$m_h \leq \sqrt{4Ev^2/1.3} \sim 42\,\text{GeV} \tag{2.180}$$

This bound was already excluded by higgs searches at LEP [26]. Moreover, now Higgs with $m_h = 125.5$ GeV discovered in ATLAS [1] and CMS [2] clearly indicates that standard model cannot provide strong first order phase transition for keeping any previously generated baryon asymmetry. For this reason, one explores beyond SM scenario which can satisfy the bound, Eq.(2.179) for physical Higgs mass.

2.5 Infrared problems and resummation

In this section we are going to address the appearance of infrared divergences in high temperature field theory.

It was pointed out in [75] that symmetry restoration implies that ordinary perturbation theory must break down at the onset of phase transition. Otherwise perturbation theory should hold and, since the tree level potential is temperature independent, radiative corrections (which are temperature dependent) should be unable to restore the symmetry. Moreover it mentioned that the appearance of infrared divergences for the zero Matsubara modes of bosonic degrees of freedom leads to failure of perturbative expansion. This just means that the usual perturbative expansion in powers of the coupling constant fails at temperatures beyond the critical temperature. It has to be replaced by an improved perturbative expansion where an infinite number of diagrams are resummed at each order in the new expansion. Consider a diagram which has superficial divergence D. By rescaling all internal momenta by T, we have

$$T^D f(p_{ext}/T, \omega_{ext}/T, m_{int}/T) \tag{2.181}$$

where p_{ext} and ω_{ext} represent the various external momenta and energies and m_{int} represents various internal masses. Thus at $T \to \infty$, the graph behaves like T^D unless there are infrared divergences when the arguments of the function f vanish.

Bosonic zero mode sets the form of the expansion parameter in finite temperature field theory. The zero mode contribution $n = 0$ to the propagator in the loop integral is of the form

$$T \sum_n \int \frac{d^3k}{(2\pi)^3} \frac{1}{4\pi^2 n^2 T^2 + \omega^2}|_{n=0} \sim T \int d^3k \frac{1}{\omega^2} \tag{2.182}$$

On the other hand, for fermionic propagator there is no zero mode contribution. Therefore in that case, at high temperature, for $n = \pm 1$,

$$T \sum_{n,\text{odd}} \int \frac{d^3k}{(2\pi)^3} \frac{1}{n^2\pi^2 T^2 + \omega^2}|_{n=\pm 1} \sim_{\frac{T}{(\pi T)^2}} \sim \frac{1}{\pi^2 T} \tag{2.183}$$

Based on the above estimates, let us construct a dimensionless expansion parameter relevant for high temperature. Apart from additional propagator, each loop order also brings in an additional vertex whose coupling is denoted by g^2. As the summation involves factor of T, the expansion parameter will contain $g^2 T$. Now we have to use other scales of the theory to transform it into a dimensionless quantity. For zero modes from Eq.(2.182), we can

see that the inverse of ω or after carrying out the spatial momentum integration, inverse power of m enters. Therefore we can assume that for large temperature $\pi T \gg m$ we have the expansion parameter for bosonic case as

$$\epsilon_b \sim \frac{g^2 T}{\pi m} \tag{2.184}$$

In case of fermions, Eq.(2.183) tells that after integration over spatial momenta, the inverse power of m does not appear in $\pi T \gg m$ limit. So we are lead to estimate

$$\epsilon_f \sim \frac{g^2 T}{\pi^2 T} \sim \frac{g^2}{\pi^2} \tag{2.185}$$

We are going to address the perturbative and non-perturbative regime of both theories shortly.

Now that we have estimated the expansion parameter for bosonic and fermionic high temperature field theory, we again consider real scalar field theory as a simple example.

$$\mathcal{L} = \frac{1}{2}(\partial_\mu \phi)^2 - \frac{1}{2}\phi^2 - \frac{\lambda}{4!}\phi^4 \tag{2.186}$$

Shifting the field will give $\phi = \phi_c + \tilde{\phi}(x)$ and the mass of scalar is $m^2(\phi_c) = m^2 + \frac{1}{2}\lambda\phi_c^2$. Now the one loop contribution to the self-energy of Fig. 2.3 is quadratically divergent ($D = 2$), and so from Eq.(2.181), it will behave

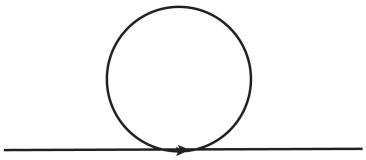

Figure 2.3: One-loop contribution to the scalar self-energy.

like λT^2. In the case of $D \leq 0$, i.e. logarithmically divergent or convergent loop contributes a factor of T only. For instance Fig. 2.4 contains two loga-

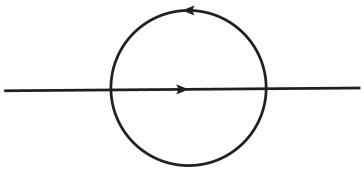

Figure 2.4: Two-loop contribution to the scalar self-energy.

rithmically divergent loops and so behaves like, $\lambda^2 T^2 = \lambda(\lambda T^2)$. It is clear

that to a fixed order in the loop expansion the largest graphs are those with the maximum number of quadratically divergent loops. These diagrams are obtained from the diagram in Fig. 2.3 by adding N quadratically divergent loops on top of it, as shown in Fig. 2.5. They behave as,

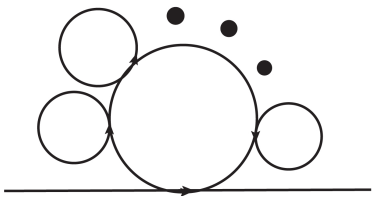

Figure 2.5: Daisy (N+1)-loop contribution to the scalar self-energy diagram.

$$\lambda^{N+1}\frac{T^{2N+1}}{M^{2N-1}} = \lambda^2\frac{T^3}{M}\left(\frac{\lambda T^2}{M^2}\right)^{N-1} \tag{2.187}$$

where M is the mass scale of the theory and as seen from Eq.(2.182), the zero mode contribution implies that inverse power of M will enter in the expansion parameter. Also from Eq. (2.187), we can see that adding a quadratically divergent bubble to a propagator which is part of a logarithmically divergent or finite loop amounts to multiplying the diagram by

$$\alpha \equiv \lambda\frac{T^2}{M^2} \tag{2.188}$$

This means that for the one-loop approximation to be valid it is required that

$$\lambda\frac{T^2}{M^2} \ll 1$$

along with the usual requirement for the ordinary perturbation expansion

$$\lambda \ll 1$$

If the mass of the scalar at high temperature is

$$M(\phi, T) = M + c\lambda T^2 \tag{2.189}$$

where c is O(1) numerical factor then at critical temperature we have $T_c \sim M/\sqrt{\lambda}$. Therefore we can see that the expansion parameter, Eq.(2.188) becomes O(1) at T_c and so the perturbation theory breaks down at critical temperature. For this reason, higher loop diagrams where multiple quadratically divergent bubbles are inserted, cannot be neglected. By using daisy

resummation technique [90, 91], one can consistently resum all powers of α and provides a theory where mass of the theory becomes $m^2(\phi_c) \to m^2_{\rm eff} \equiv m^2(\phi_c) + \Pi(T)$, where $\Pi(T)$ is the self-energy corresponding to the one-loop resummed diagram of order $O(T^2)$.

Now let us consider two-loop diagram of Fig. 2.4 which is suppressed by λ with respect to the diagram of Fig. 2.3 as follows.

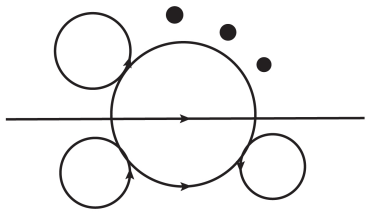

Figure 2.6: Non-daisy (n+2)-loop contribution to the self-energy for the scalar theory.

$$\lambda^{N+2}\frac{T^{2N+2}}{M^{2N}} = \lambda^{N+1}\frac{T^{2N+1}}{M^{2N-1}}\left(\lambda\frac{T}{M}\right) \tag{2.190}$$

and it is suppressed with respect to the multiple loop diagram of Eq. (2.187) by $\lambda T/M$. Therefore the validity of the improved expansion is guaranteed provided that,

$$\begin{aligned} \lambda &\ll 1 \\ \beta \equiv \lambda\frac{T}{M} &\ll 1 \end{aligned} \tag{2.191}$$

2.5.1 The scalar theory

In the following we have shown the contribution to the effective potential due the the daisy diagrams where the zero modes dominate. Therefore for $n = 0$ we have [92]

$$V_{\rm daisy} = -\frac{1}{2}T\int\frac{d^3k}{(2\pi)^3}\sum_{N=1}^{\infty}\frac{(-1)^N\Pi(T)^N}{(k^2+m^2(\phi_c))^2} \tag{2.192}$$

where $\Pi(T)$ are the one loop bubble diagrams which are independent of the loop momentum k. Using Eq.(A.12) we have

$$\begin{aligned} V_{\rm daisy} &= -\frac{1}{2}T\sum_{N=1}^{\infty}\frac{1}{N}(-\Pi(T))^N\frac{\pi^{\frac{3}{2}}}{\Gamma(\frac{3}{2})(2\pi)^3}(m^2(\phi_c))^{\frac{3}{2}-N}\frac{\Gamma(\frac{3}{2})\Gamma(N-\frac{3}{2})}{\Gamma(N)} \\ &= -\frac{T}{16\pi^{\frac{3}{2}}}\sum_{N=1}^{\infty}\frac{1}{N}(-1)^N\left(\frac{\Pi(T)}{m^2(\phi_c)}\right)^N m^3(\phi_c)\frac{\Gamma(N-\frac{3}{2})}{\Gamma(N)} \\ &= -\frac{m^3(\phi_c)T}{12\pi}\sum_{N=1}^{\infty}(-1)^N\frac{3}{4\sqrt{\pi}}\left(\frac{\Pi(T)}{m^2(\phi_c)}\right)^N\frac{\Gamma(N-\frac{3}{2})}{\Gamma(N+1)} \\ &= -\frac{T}{12\pi}[(m^2(\phi_c)+\Pi(T))^{\frac{3}{2}}-m^3(\phi_c)] \end{aligned} \tag{2.193}$$

Therefore the effective potential is

$$V_{\rm eff}(\phi_c) = V_0(\phi_c) + V_{\rm CW}(\phi_c) + V_T^{(1)}(\phi_c,T) + V_{\rm daisy}(\phi_c,T) \tag{2.194}$$

And taking the high temperature expansion of thermal effective potential $V_T^{(1)}(\phi_c,T)$ and recollecting terms which are relevant for present case, we have,

$$V(\phi_c,T) = \frac{1}{2}(m^2+\frac{\lambda}{12}T^2)\phi_c^2 - \frac{T}{12\pi}(m^2(\phi_c)+\Pi(T))^{\frac{3}{2}} + \frac{\lambda}{4}\phi_c^4 + \cdots \tag{2.195}$$

In the limit, $m^2+\Pi(T) \ll \lambda\phi_c^2$, the potential (2.195) yields a first order phase transition. At $T \sim T_c$, we have the mimimum,

$$\phi_c \sim \sqrt{\lambda}T_c \tag{2.196}$$

Then from Eq.(2.191), with $M \sim m^2(\phi_c,T)$ and considering the limit $m^2+\Pi(T) \ll \lambda\phi_c^2$ again we have,

$$\beta \sim \lambda\frac{T_c}{\lambda T_c} = \mathcal{O}(1) \tag{2.197}$$

which indicates that the expansion parameter is of O(1) and therefore perturbation theory is invalidated for first order phase transition shown by the scalar theory. On the other hand if $m^2+\Pi(T)$ is significantly larger, it will reduce the order parameter and the transition will cease to be first order.

2.5.2 The Standard Model

For the Standard Model, where there are gauge and Yukawa interactions, the case is different from the previous example of the scalar theory. From the simplified effective potential of the SM, Eq.(2.162) and Eq.(2.167) we have

$$\phi_c \sim \frac{g^3}{\lambda} T_c \tag{2.198}$$

Here we have only considered the contribution of transverse gauge bosons to the phase transition strength, and neglected that of the (screened) longitudinal gauge bosons.

The expansion parameter β associated with the Standard Model is,

$$\beta_{\mathrm{SM}} \sim g^2 \frac{T}{m_W(\phi)} \tag{2.199}$$

Therefore at the vicinity of the symmetry breaking mimimum,

$$\beta_{\mathrm{SM}} \sim g \frac{T_c}{\phi_c} \sim \frac{\lambda}{g^2} \sim \frac{m_H^2}{m_W^2} \tag{2.200}$$

For this reason, in the Standard Model, the validity of the perturbation theory implies that $m_H \ll m_W$ and as this requirement is already invalidated by the experimental results, we have to extend the SM to accommodate strong first order electroweak phase transition within the validity of the perturbation theory.

Chapter 3

Electroweak Baryogenesis: the need for strong phase transition

The observed baryon asymmetry of the universe still does not have any satisfactory explanation and it requires us to explore possible beyond the standard model scenarios. In this chapter we have presented a telegraphic review of the electroweak baryogenesis and the requirement of strong first order electroweak phase transition in this scenario. Section 3.1 has described the key ingredients for successful baryogenesis. In section 3.2, we have described the features of electroweak baryogenesis briefly. In section 3.3, we have constructed the sphaleron solution for $SU(2)$ scalar multiplets, described the baryon number violating rate at above and below the critical temperature and showed how the sphaleron decoupling condition leads to strong first order electroweak phase transition. More detailed account on Baryogenesis can be found in [93–99].

The baryon asymmetry of the universe is evident from

- The null observation of abundance of the antimatter in the universe. Naturally it is only found in the cosmic ray. The antiproton in the cosmic ray is produced as secondaries in collisions ($pp \to 3p + \overline{p}$). The ratio of the number density of anti-proton to proton is bounded by $\frac{n_{\overline{p}}}{n_p} \sim 3 \times 10^{-4}$ [100–104]. Also, the flux ratio of antihelium to helium in the cosmic ray has the upper bound of 1.1×10^{-6} [105].

- The baryon to photon ratio is,

$$\eta = \frac{n_B - n_{\bar{B}}}{n_\gamma} \tag{3.1}$$

  where n_B, $n_{\bar{B}}$ and n_γ are the number density of baryon, antibaryon and photon respectively. This parameter is essential for big bang nu-

cleosynthesis (BBN) because abundances of ^3He, ^4He, D, ^6Li and ^7Li are sensitive to the value of η. From one measured value of deuterium abundance (D/H), η is given as [106]

$$\eta = 6.28 \pm 0.35 \times 10^{-10} \tag{3.2}$$

- The Cosmic Microwave Background (CMB) radiation facilitates an independent measurement of the baryon asymmetry of the universe because the observed Doppler peaks of the temperature anisotropy in CMB are sensitive to the value of η [107] and the accuracy is better than the BBN measurement [108]. With measured value $\Omega_B h^2 = 0.02207 \pm 0.00033$ (68% limit) by Planck collaboration [9], η is

$$\eta = 6.1 \pm 0.1 \times 10^{-10} \tag{3.3}$$

$\eta = n_B/n_\gamma$ (as $n_{\bar{B}} \sim 0$) is a good measurement of baryon asymmetry at late time because n_B and n_γ stay constant but at the early time, when the temperature of the universe was low enough to decouple baryon violating processes but still high enough to keep various heavy particles in thermal equilibrium, η is not suitable because the annihilation or decay of those heavy particles afterwards, would create photons. So, it is convenient to consider entropy instead of number density of photons for expressing baryon to photon ratio.

$$s = \frac{\pi^4}{45\zeta(3)} 3.91\ n_\gamma = 7.04\ n_\gamma \ \text{ and } \ \frac{n_B - n_{\bar{B}}}{n_\gamma} = \frac{1}{7.04}\eta \tag{3.4}$$

3.1 Sakharov's conditions for baryogenesis

Although the universe was initially baryon symmetric ($n_B \simeq n_{\overline{B}}$) one needs to explain the matter-antimatter asymmetry observed today in the universe. Either one has to put it as an initial condition or there are some dynamical mechanism which would lead to the observed asymmetry. It was first suggested by Sakharov [11] that it is possible to produce a small baryon asymmetry in the early universe dynamically. The three ingredients necessary for baryogenesis are:

1. Baryon number nonconservation This condition is obvious since we want to start with a baryon symmetric universe ($\Delta B = 0$) and evolve it to a universe where $\Delta B \neq 0$. Although still lacking positive results from experiments searching for B non-conservation, the baryon asymmetry of the universe is a unique observational evidence in favour of it.

2. C and CP violation If C and CP were conserved, the rate of reactions with particles would be the same as the rate with antiparticles. If the initial state of the universe was C and CP symmetric, no charge asymmetry could develop from it. Consider the initial density matrix that commutes with C and CP operations, $\rho_0 = U_{C,CP}\rho_0 U_{C,CP}^\dagger$ and the Hamiltonian, H of the system is C and CP invariant. If the time evolution operator is $U(t) = \exp(iHt)$, the density matrix at time t, $\rho(t) = U(t)\rho_0 U(t)^\dagger$ will also be C and CP invariant. In such cases, the average of any C or CP odd operator, for example B and L, is zero.

Here we elaborate more on the role of this second condition in baryon asymmetry. Consider a process $A \to B + C$ that produces baryon B. Charge conjugation of this process is $\bar{A} \to \bar{B} + \bar{C}$. So the net production rate of baryon is

$$\frac{dB}{dt} \sim \Gamma(\bar{A} \to \bar{B} + \bar{C}) - \Gamma(A \to B + C) \tag{3.5}$$

When charge conjugation is a symmetry, we have

$$\Gamma(A \to B + C) = \Gamma(\bar{A} \to \bar{B} + \bar{C}) \tag{3.6}$$

Therefore, Eq.(3.5) yields zero net production of baryon. But C violation alone is not enough for baryon asymmetry. One also requires CP violation in conjunction with C violation. Let us first denote the how left and right handed fermions transform under P, C and CP:

$$\begin{aligned} P &: \psi_L \longrightarrow \psi_R, \quad \psi_R \longrightarrow \psi_L \\ C &: \psi_L \longrightarrow \psi_L^C \equiv i\sigma_2\psi_R^*, \quad \psi_R \longrightarrow \psi_R^C \equiv -i\sigma_2\psi_L^* \\ CP &: \psi_L \longrightarrow \psi_R^C, \quad \psi_R \longrightarrow \psi_L^C \end{aligned} \tag{3.7}$$

Consider A decays into two left handed and two right handed quarks

$$A \to q_L\ q_L\ , \quad A \to q_R\ q_R \tag{3.8}$$

Now the C violation implies

$$\begin{aligned} \Gamma(A \to q_L\ q_L) &\neq \Gamma(\bar{A} \to q_L^C\ q_L^C) \\ \Gamma(A \to q_R\ q_R) &\neq \Gamma(\bar{A} \to q_R^C\ q_R^C) \end{aligned} \tag{3.9}$$

But CP invariance will imply that

$$\begin{aligned} \Gamma(A \to q_L\ q_L) &= \Gamma(\bar{A} \to q_R^C\ q_R^C) \\ \Gamma(A \to q_R\ q_R) &= \Gamma(\bar{A} \to q_L^C\ q_L^C) \end{aligned} \tag{3.10}$$

When one adds up two decay channels,

$$\Gamma(A \to q_L\ q_L) + \Gamma(A \to q_R\ q_R) = \Gamma(\bar{A} \to q_R^C\ q_R^C) + \Gamma(\bar{A} \to q_L^C\ q_L^C) \quad (3.11)$$

For this reason, as long as we have equal number density for A and $\bar{A}$, we will not obtain any net quark asymmetry. The only asymmetry that will be generated because of C violation is the asymmetry between number density of left and right handed quarks.

3. Departure from thermal equilibrium As the consequence of CPT invariance, if B violating process are in thermal equilibrium, the inverse process will wash out any the pre-existing asymmetry. For this reason a departure from thermal equilibrium is needed to retain the baryon asymmetry of the universe. There are several ways to achieve departure from equilibrium.

1. Out-of-equilibrium decay or scattering: In this case, the rate of interaction must be smaller than the expansion rate of the universe, $\Gamma < H$.

2. Phase transition: First order phase transition proceeds through bubble nucleation which creates a temporary departure from equilibrium. Second order transition can't provide such non-equilibrium condition as it doesn't have any barrier between symmetric and broken phase and the transition is continuous.

3. Non-adiabatic motion of a scalar field: A coherent scalar field can be trapped in a local minimum of the potential but if the shape of the potential changes to become a maximum in such a way that the field may not have enough time to re-adjust with the potential, it will onset a completely non-adiabatic motion of the field. This is similar to a second order phase transition but it is the non-adiabatic classical motion which prevails over the quantum fluctuations, and therefore, departure from equilibrium can be achieved. If such field condensate carries a global charge such as the baryon number, the motion can charge up the condensate. Such mechanism has been used in the Affleck-Dine baryogenesis [109] and its variants (for review, [110, 111]).

3.2 Electroweak baryogenesis

Electroweak Baryogenesis involves a first order phase transition which proceeds through the nucleation of bubbles of broken phase within the surrounding electroweak plasma in the symmetric phase. These bubbles expand, col-

lide and coalesce until the broken phase remains. Steps involving electroweak baryogenesis are [99]:

- Particles in the electroweak plasma scatter at the bubble wall. If the theory contains CP violation, this scattering can generate C and CP asymmetries in particle number densities in front of bubble wall.
- These asymmetries diffuse into symmetric phase ahead of bubble wall, where they will bias electroweak sphaleron transition to produce more baryons than antibaryons.
- Some of the net baryon charge created outside the bubble wall is swept up by the expanding wall into the broken phase. In the broken phase, the rate of sphaleron transition is strongly suppressed and can be small enough to avoid washing away the baryons created in first two steps.

From the above steps of EWBG, we can see that Sakharov's three conditions are satisfied manifestly. First, departure from thermal equilibrium is achieved by the rapidly expanding bubble walls through electroweak plasma. Second, violation of baryon number is provided by the rapid sphaleron transition in the symmetric phase. And third, both C and CP violating scattering processes of the particles at phase boundary create particle number asymmetries over those of antiparticles and this excess biases sphaleron transition to create more baryons over antibaryons.

Anomalous nonconservation of fermion quantum numbers

Consider a theory with left handed ψ_L and right handed ψ_R fermions belonging to different representations of the gauge group. The partition function is given as

$$Z = \int \mathcal{D}A_\mu \mathcal{D}\psi \mathcal{D}\bar{\psi} e^{iS} \tag{3.12}$$

The following transformations

$$\psi'_L = e^{i(Q_V - Q_A)\alpha(x)}\psi_L \tag{3.13}$$
$$\psi'_R = e^{i(Q_V + Q_A)\alpha(x)}\psi_R \tag{3.14}$$

will induce additional terms in the action given by,

$$\delta S = \int d^4x \bar{\psi}_{L(R)} \gamma^\mu (Q_V \mp Q_A) \psi_{L(R)} \partial_\mu \alpha(x) \tag{3.15}$$

The transformations also give rise to non-trivial Jacobian due to the non-invariance of the measure $\mathcal{D}\psi\mathcal{D}\bar{\psi}$. This anomaly can be expressed as the additional contribution to the action as [112, 113],

$$\delta S_{\text{anomaly}} = \int d^4x\alpha(x)[g_L^2\frac{Q_V - Q_A}{16\pi^2}\text{Tr}\, F^{(L)\mu\nu}\tilde{F}_{(L)\mu\nu} - g_R^2\frac{Q_V + Q_A}{16\pi^2}\text{Tr}\, F^{(R)\mu\nu}\tilde{F}_{(R)\mu\nu}] \tag{3.16}$$

where $F^{(L)\mu\nu}$ and $F^{(R)\mu\nu}$ are the field strengths with coupling constants g_L and g_R and they are coupled to left handed and right handed fermionic current respectively. Here, $\tilde{F}_{\mu\nu} = \frac{1}{2}\epsilon_{\mu\nu\rho\sigma}F^{\rho\sigma}$. First consider the transformation related to baryon number which is $Q_V = \frac{1}{3}$ and $Q_A = 0$. Now integrating by parts Eq.(3.15) and requiring that the partition function is invariant under baryonic number transformation, we have the baryon current in the standard model,

$$J_B^\mu = \sum_q \frac{1}{3}\bar{q}\gamma^\mu q \tag{3.17}$$

to be anomalous,

$$\partial_\mu J_B^\mu = \frac{N_F}{32\pi^2}(-g^2F^{a\mu\nu}\tilde{F}^a_{\mu\nu} + g'^2 f^{\mu\nu}\tilde{f}_{\mu\nu}) \tag{3.18}$$

where N_F is the number of fermion generation, $F^a_{\mu\nu}$ is the field strength of $SU(2)_L$ and $f_{\mu\nu}$ is that of $U(1)_Y$ with coupling constants g and g' respectively. Also here $Tr(T^aT^b) = \frac{1}{2}\delta^{ab}$ is used for $SU(2)_L$ generators and in the case of $U(1)_Y$, we have used $Y = 1/6, 2/3, -1/3$ for $Q_L = (u_L, d_L)$, u_R and d_R respectively.

Similarly for lepton number transformation we have $Q_V = 1$ and $Q_A = 0$. Therefore, following the same steps for Eq.(3.18), we have the lepton current,

$$J_L^\mu = \sum_l (\bar{l}\gamma^\mu l + \bar{\nu}_l\gamma^\mu\nu_l) \tag{3.19}$$

with it's non vanishing divergence,

$$\partial_\mu J_L^\mu = \frac{N_F}{32\pi^2}(-g^2F^{a\mu\nu}\tilde{F}^a_{\mu\nu} + g'^2 f^{\mu\nu}\tilde{f}_{\mu\nu}) \tag{3.20}$$

where $Y = -1/2, -1$ are used for $l_L = (\nu_L, e_L)$ and e_R respectively in the case of $U(1)_Y$. Therefore we have

$$\partial_\mu J_B^\mu = \partial_\mu J_L^\mu \tag{3.21}$$

which shows that the current associated with $B - L$ is conserved. Moreover, since each quark and lepton family gives same contribution to the anomaly

and as lepton flavor is conserved in the SM (because of neutrino mass being zero in the SM at the renormlizable level), there are three conserved charges in the SM

$$l_i = \frac{1}{3}B - L_i \tag{3.22}$$

where $L_i\,(i = e, \mu, \tau)$ are the leptonic flavors and $\sum_i L_i = L$.

Baryon number violation

The RHS of Eq.(3.18) can be re-expressed in the following way,

$$\partial_\mu J^\mu_B = \frac{N_F}{32\pi^2}(-g^2\partial_\mu K^\mu + g'^2\partial_\mu k^\mu) \tag{3.23}$$

where

$$K^\mu = \epsilon^{\mu\nu\rho\sigma}(\partial_\nu W^a_\rho W^a_\sigma - \frac{1}{3}g\epsilon_{abc}W^a_\nu W^b_\rho W^c_\sigma) \tag{3.24}$$

$$k^\mu = \epsilon^{\mu\nu\rho\sigma}(\partial_\nu B_\rho B_\sigma) \tag{3.25}$$

Here, W^a_μ and B_μ are the $SU(2)$ and $U(1)$ gauge field respectively.

The variation of the baryon number $B = \int d^3x J^0_B$ over time interval Δt is ΔB. It is proportional to the variation of the Chern-Simons number over the same time interval. The Chern-Simons numbers are defined as follows,

$$N_{CS} = -\frac{g^2}{16\pi^2}\int d^3x\epsilon^{ijk}Tr[\partial_i W_j W_k + \frac{2i}{3}gW_iW_jW_k] \tag{3.26}$$

$$n_{CS} = -\frac{g'^2}{16\pi^2}\int d^3x\epsilon^{ijk}\partial_i B_j B_k \tag{3.27}$$

where N_{CS} and n_{CS} are associated with $SU(2)$ and $U(1)$ respectively. The variation of Chern-Simons number is related to the nonzero winding number associated with non-abelian gauge transformation.

Consider an element of $SU(2)$, $U = exp(i\alpha^a\tau^a)$ which can also be written as $U(x) = x^0 + ix^a\tau^a$ where $(x^0, x^a) \in R^4$. Because of $UU^\dagger = U^\dagger U = 1$, x^0 and x^a satisfies, $x^{02} + x^a x^a = 1$ which describes S^3. As $SU(2)$ is isomorphic to S^3, $U(x)$ can be associated with the mapping $S^3 \to S^3$. The mappings $\vec{x} \to U_1(\vec{x})$ and $\vec{x} \to U_2(\vec{x})$ will belong to the same equivalence class if there exists a continuous deformation from $U_1(\vec{x})$ to $U_2(\vec{x})$. The equivalence class is characterized by positive or negative integer which is called winding number. This topological winding number n associated with $U(x_0, \vec{x})$ is

$$n = -\frac{1}{24\pi^2}\int d^3x\epsilon^{ijk}\mathrm{Tr}\,(A_iA_jA_k) \tag{3.28}$$

with $A_i = \partial_i U(x_0, \vec{x}) U^{-1}(x_0, \vec{x})$.

Now first consider the transformation of $SU(2)$, $U^{(0)} = \mathbf{1}$ and it's continuous deformation

$$\tilde{U}(x) = (\mathbf{1} + i\epsilon^a(x)\tau^a)U^{(0)} \tag{3.29}$$

For $U^{(0)}$ and any $\tilde{U}(x)$, the winding number $n[U]$ is zero. On the other hand, for transformation

$$U^{(1)} = \frac{x_0 + i\vec{x}.\vec{\tau}}{r} \ , r = \sqrt{x_0^2 + |\vec{x}|^2} \tag{3.30}$$

we have $n[U^{(1)}] = 1$. This result also holds for any continuous deformation of $U^{(1)}$. Furthermore, if $U^{(n)} = [U^{(1)}]^n$, we have $n[U^{(n)}] = n$. So the $SU(2)$ gauge transformation is divided into two classes: those which have zero winding numbers and those which have non-zero winding numbers.

Now under the $U(1)$ gauge transformation $B_i \to B_i + \frac{i}{g'}\partial_i U U^{-1}$ where $U = e^{i\alpha(x)}$, n_{CS} remains unchanged. On the other hand, $SU(2)$ gauge transformation for which one has non-zero winding number Eq.(3.28), will induce non-vanishing variation of N_{CS},

$$\delta N_{CS} = -\frac{1}{24\pi^2}\int \ d^3x \ \epsilon^{ijk}\mathrm{Tr}(U\partial_i U^{-1} \cdot U\partial_j U^{-1} \cdot U\partial_k U^{-1}). \tag{3.31}$$

Classically the ground state of the gauge theory should be time independent field configuration with vanishing energy density. Therefore we have $F^a_{\mu\nu} = 0$ which implies that the gound state will be pure gauge state $\vec{W}_{vac} = \frac{i}{g}\nabla U U^{-1}$. Furthermore, the transformation U is required to satisfy $U \to \mathbf{1}$ as $|\vec{x}| \to \infty$. For $SU(2)_L$ gauge theory with Higgs field Φ, in the temporal gauge, $W_0 = 0$, we have the vacuum defined as

$$\begin{aligned} W_i^{(0)} &= \frac{i}{g}\partial_i U^{(0)} U^{(0)-1} \\ \Phi^{(0)} &= (0, v/\sqrt{2}) \\ N_{CS} &= 0 \end{aligned}$$

Using the gauge transformation $U^{(n)}$, we can have classically degenerate vacua with different Chern-Simons numbers as follows

$$\begin{aligned} W_i^{(n)} &= \frac{i}{g}\partial_i U^{(n)} U^{(n)-1} \\ \Phi^{(n)} &= U^{(n)}\Phi^{(0)} \\ N_{CS} &= n \end{aligned}$$

As ΔB is proportional to the change of the Chern-Simons number, n_{CS} associated with $U(1)$, will not contribute to ΔB. So, when the system makes a transition from n-th vacuum to $n+1$-th vacuum, the Chern-Simons number changes by one unit and therefore the variations in B, L and $B+L$ are,

$$\Delta B = \Delta L = N_f \ \ , \Delta(B+L) = 2N_f \tag{3.32}$$

For the SM, number of generation is $N_f = 3$. When $\Delta N_{CS} = 1$, the vacuum to vacuum transition, because of fermion number nonconservation, will lead to the production of 9 left handed quarks (3 color states for each generations) and 3 left handed leptons so that $\Delta B = \Delta L = 3$. Moreover, in the SM $\Delta(B+L) = 6$ whereas proton decay, $p \to e^+\pi^0$ requires $\Delta(B+L) = 2$. Therefore, despite having B violation due to the anomaly, proton decay is forbidden in the SM. The probability amplitude for tunneling from n-th vacuum to $n + \Delta N_{CS}$ was estimated by WKB method [114, 115],

$$P(\Delta N_{CS}) \sim \exp(-\frac{4\pi\Delta N_{CS}}{\alpha_W}) \sim 10^{-162\Delta N_{CS}} \tag{3.33}$$

which implies that baryon number violation in the SM is completely negligible at zero temperature.

3.3 Baryon number violation at finite temperature by the sphaleron

As already pointed out in Section 3.2, in the Standard Model (SM), the anomalous baryonic and leptonic currents lead to fermion number non-conservation because of the instanton induced transitions between topologically distinct vacua of $SU(2)$ gauge fields [114, 115] and at zero temperature, the rate is of the order, $e^{-2\pi/\alpha_w}$, $\alpha_w \sim 1/30$, which is irrelevant for any physical phenomena. However, there exists static unstable solution of the field equations, known as sphaleron [13, 14, 116, 117], that represents the top of the energy barrier between two distinct vacua and at finite temperature, because of thermal fluctuations of fields, fermion number violating vacuum to vacuums transition can occur which is only suppressed by a Boltzmann factor which contains the height of the barrier at the given temperature, i.e. the energy of the sphaleron [12]. Such baryon number violation induced by the sphaleron is one of the essential ingredients of Electroweak Baryogenesis [15, 16, 19, 21, 118, 119] and therefore, it has been extensively studied not only in the SM [120–124, 126–131] and but also in extended SM variants such

as, SM with a singlet [59, 132], two higgs doublet model [133], Minimal Supersymmetric Standard Model [134], the next-to-Minimal Supersymmetric Standard Model [135] and 5 dimensional model [136].

3.3.1 Sphaleron in $SU(2)_L$ scalar representation

The standard way to find sphaleron solution in the Yang-Mills-Higgs theory is to construct the non-contractible loops in the field space [14]. As the sphaleron is a saddle point solution of the configuration space, it is really hard to find them by solving the full set of equations of motion. Instead one starts from an ansatz depending on a parameter μ that characterizes the non-contractible loop in the configuration space and corresponds to the vacuum for $\mu = 0$ and π while $\mu = \frac{\pi}{2}$ corresponds the highest energy configuration, in other words, the sphaleron. In the following, we have focused on determining the energy functional and profile functions for the sphaleron in the SM for general scalar multiplet [137].

Consider the scalar multiplet Q, charged under $SU(2)_L \times U(1)_Y$ group, is in J representation and has $U(1)$ charge Y. The generators in this representation are denoted as J^a such that, $Tr[J^a J^b] = D(R)\delta^{ab}$ where $D(R)$ is the Dynkin index for the representation. We define the charge operator, $Q = J_3 + Y$ and require the neutral component ($J_3 = -Y$) of the multiplet to have the vacuum expectation value. The gauge-scalar sector of the Lagrangian is

$$\mathcal{L} = -\frac{1}{4}F^{a\mu\nu}F^a_{\mu\nu} - \frac{1}{4}f^{\mu\nu}f_{\mu\nu} + (D_\mu Q)^\dagger D^\mu Q - V(Q), \tag{3.34}$$

with scalar potential

$$V(Q) = -\mu^2 Q^\dagger Q + \lambda_1 (Q^\dagger Q)^2 + \lambda_2 (Q^\dagger J^a Q)^2. \tag{3.35}$$

It was shown in [59] that the kinetic term of the scalar field makes larger contribution to the sphaleron energy than the potential term. Therefore, for simplicity, we have considered CP-invariant scalar potential involving single scalar representation to determine the sphaleron solution. It is straightforward to generalize the calculation for the potential with multiple scalar fields[1].

[1] In fact, in the SM, one needs large couplings between Higgs and extra scalars to trigger a strong first order phase transition.

Also for convenience we elaborate,

$$\begin{aligned} F^a_{\mu\nu} &= \partial_\mu W^a_\nu - \partial_\nu W^a_\mu + g\epsilon^{abc} W^b_\mu W^c_\nu, \\ f_{\mu\nu} &= \partial_\mu B_\nu - \partial_\nu B_\mu, \\ D_\mu Q &= \partial_\mu Q - igW^a_\mu J^a Q - ig' B_\mu Y Q, \end{aligned} \tag{3.36}$$

where, g and g' are the $SU(2)$ and $U(1)$ gauge couplings. The mixing angle θ_W is $\tan\theta_W = g'/g$.

The energy functional and variational equations

In the following, we have addressed the energy functional and the variational equations of the sphaleron. The classical finite energy configuration are considered in a gauge where the time component of the gauge fields are set to zero. Therefore the classical energy functional over the configuration is

$$E(W^a_i, B_i, Q) = \int d^3x [\frac{1}{4} F^a_{ij} F^a_{ij} + \frac{1}{4} f_{ij} f_{ij} + (D_i Q)^\dagger (D_i Q) + V(Q)]. \tag{3.37}$$

The non-contractible loop (NCL) in the configuration space is defined as map, $S^1 \times S^2 \sim S^3$ into $SU(2) \sim S^3$ using the following matrix $U^\infty \in SU(2)$ [126],

$$\begin{aligned} U^\infty(\mu,\theta,\phi) = (\cos^2\mu + \sin^2\mu\cos\theta) I_2 + i\sin 2\mu(1-\cos\theta)\tau^3 \\ + 2i\sin\mu\sin\theta(\sin\phi\tau^1 + \cos\phi\tau^2), \end{aligned} \tag{3.38}$$

where μ is the parameter of the NCL and θ, ϕ are the coordinates of the sphere at infinity. Also, τ^a are the $SU(2)$ generators in the fundamental representation. We also define the 1-form in the following,

$$iU^{\infty -1} dU^\infty = \sum_a F_a \tau^a, \tag{3.39}$$

which gives

$$\begin{aligned} F_1 &= -[2\sin^2\mu\cos(\mu-\phi) - \sin 2\mu\cos\theta\sin(\mu-\phi)] d\theta \\ &\quad - [\sin 2\mu\cos(\mu-\phi)\sin\theta + \sin^2\mu\sin 2\theta\sin(\mu-\phi)] d\phi, \\ F_2 &= -[2\sin^2\mu\sin(\mu-\phi) + \sin 2\mu\cos\theta\cos(\mu-\phi)] d\theta \\ &\quad + [\sin^2\mu\sin 2\theta\cos(\mu-\phi) - \sin 2\mu\sin\theta\sin(\mu-\phi)] d\phi, \\ F_3 &= -\sin 2\mu\sin\theta d\theta + 2\sin^2\theta\sin^2\mu d\phi. \end{aligned} \tag{3.40}$$

As shown in [126] the NCL starts and ends at the vacuum and consists of three phases such that in first phase $\mu \in [-\frac{\pi}{2}, 0]$ it excites the scalar

configuration, in the second phase $\mu \in [0, \pi]$ it builds up and destroys the gauge configuration and in the third phase $\mu \in [\pi, \frac{3\pi}{2}]$ it destroys the scalar configuration.

The field configurations in the first and third phases, $\mu \in [-\frac{\pi}{2}, 0]$ and $\mu \in [\pi, \frac{3\pi}{2}]$ are

$$gW_i^a \tau^a dx^i = g' B_i dx^i = 0, \tag{3.41}$$

and

$$Q = \frac{v(\sin^2\mu + h(\xi)\cos^2\mu)}{\sqrt{2}} \begin{pmatrix} 0 & .. & 1 & .. & 0 \end{pmatrix}^T, \tag{3.42}$$

with $\xi = g\Omega r$ is radial dimensionless coordinate and Ω is the mass parameter used to scale r^{-1}, which we choose in what follows as $\Omega = m_W/g$. In the second phase $\mu \in [0, \pi]$, the field configurations are

$$\begin{aligned} gW_i^a \tau^a dx^i &= (1 - f(\xi))(F_1\tau^1 + F_2\tau^2) + (1 - f_3(\xi))F_3\tau^3, \\ g' B_i dx^i &= (1 - f_0(\xi))F_3, \end{aligned} \tag{3.43}$$

and

$$Q = \frac{vh(\xi)}{\sqrt{2}} \begin{pmatrix} 0 & .. & 1 & .. & 0 \end{pmatrix}^T. \tag{3.44}$$

Here, $f(\xi)$, $f_3(\xi)$, $f_0(\xi)$ and $h(\xi)$ are the radial profile functions. From Eq.(3.43), one can see that, in the spherical coordinate system, for the chosen ansatz, the gauge fixing has led to, $W_r^a = B_r = B_\theta = 0$. Moreover, similar to Eq.(3.43), the gauge fields acting on the scalar field Q can be written as

$$gW_i^a J^a dx^i = (1 - f)(F_1 J^1 + F_2 J^2) + (1 - f_3)F_3 J^3. \tag{3.45}$$

Finally the energy over the NCL for first and third phases is,

$$E(h, \mu) = \frac{4\pi\Omega}{g} \int_0^\infty d\xi [\cos^2\mu \frac{v^2}{\Omega^2} \frac{1}{2} \xi^2 h'^2 + \xi^2 \frac{V(h, \mu)}{g^2\Omega^2}], \tag{3.46}$$

and for second phase,

$$\begin{aligned} E(\mu, f, f_3, f_0, h, \mu) = \frac{4\pi\Omega}{g} \int_0^\infty d\xi [&\sin^2\mu (\frac{8}{3} f'^2 + \frac{4}{3} f_3'^2) + \frac{8}{\xi^2} \sin^4\mu \{\frac{2}{3} f_3^2 (1 - f)^2 \\ &+ \frac{1}{3}\{f(2 - f) - f_3\}^2\} + \frac{4}{3}(\frac{g}{g'})^2 \{\sin^2\mu f_0'^2 + \frac{2}{\xi^2} \sin^4\mu (1 - f_0)^2\} \\ &+ \frac{v^2}{\Omega^2} \{\frac{1}{2}\xi^2 h'^2 + \frac{4}{3} \sin^2\mu h^2 \{(J(J+1) - J_3^2)(1 - f)^2 + J_3^2 (f_0 - f_3)^2\}\} \\ &+ \frac{\xi^2}{g^2\Omega^4} V(h)]. \end{aligned} \tag{3.47}$$

From Eq.(3.47), the maximal energy is attained at $\mu = \frac{\pi}{2}$ which corresponds to the sphaleron configuration.

If there are multiple representations $J^{(i)}$ with non-zero neutral components $J_3^{(i)}$,
$Q^{(i)} = \frac{v_i h_i(\xi)}{\sqrt{2}}(0, .., 1.., 0)^T$, we have the energy of the sphaleron can be parameterized as

$$E_{sph} = E(\mu = \frac{\pi}{2}) = \frac{4\pi\Omega}{g}\int_0^\infty d\xi[\frac{8}{3}f'^2 + \frac{4}{3}f_3'^2 + \frac{8}{3\xi^2}\{2f_3^2(1-f)^2 + (f(2-f)-f_3)^2\} + \frac{4}{3}(\frac{g}{g'})^2\{f_0'^2 + \frac{2}{\xi^2}(1-f_0)^2\} + \sum_i\{\frac{1}{2}\frac{v_i^2}{\Omega^2}\xi^2 h_i'^2 + \frac{4}{3}h_i^2[2\alpha_i(1-f)^2 + \beta_i(f_0-f_3)^2]\} + \xi^2\frac{V(v_i h_i)}{g^2\Omega^4}], \tag{3.48}$$

where the parameters

$$\alpha_i = \frac{(J^{(i)}(J^{(i)}+1) - J_3^{(i)2})v_i^2}{2\Omega^2},\ \beta_i = \frac{J_3^{(i)2}v_i^2}{\Omega^2}, \tag{3.49}$$

refer to the scalar field couplings to the charged and neutral gauge fields. respectively.

The energy functional, Eq.(3.48) will be minimized by the solutions of the following variational equations

$$f'' + \frac{2}{\xi^2}(1-f)[f(f-2) + f_3(1+f_3)] + \sum_i \alpha_i h_i^2(1-f) = 0,$$
$$f_3'' - \frac{2}{\xi^2}[3f_3 + f(f-2)(1+2f_3)] + \sum_i \beta_i h_i^2(f_0 - f_3) = 0,$$
$$f_0'' + \frac{2}{\xi^2}(1-f_0) - \frac{g'^2}{g^2}\sum_i \beta_i h_i^2(f_0 - f_3) = 0,$$
$$h_i'' + \frac{2}{\xi}h_i' - \frac{8\Omega^2}{3v_i^2\xi^2}h_i[2\alpha_i(1-f)^2 + \beta_i(f_0-f_3)^2] - \frac{1}{g^2 v_i\Omega^2}\frac{\partial}{\partial\phi_i}V(\phi)\Big|_{\phi_k = v_k h_k} = 0, \tag{3.50}$$

with the boundary conditions for (3.50) are given by: $f(0) = f_3(0) = h(0) = 0$, $f_0(0) = 1$ and $f(\infty) = f_3(\infty) = f_0(\infty) = h_i(\infty) = 1$. For $g' \to 0$, we have, $f_0(\xi) \to 1$. The behavior of the field profiles Eq.(3.50) at the limits $\xi \to 0$ and $\xi \to \infty$ are given in appendix D. According to the last term in both first and second lines in Eq.(3.50), it seems that the couplings of the scalar to gauge components, i.e (3.49), will play the most important role on the shape of the field profiles as well the sphaleron energy.

Estimating the energy of the sphaleron

The sphaleron is therefore the solution which interpolates between the vacuum at $N_{CS} = 0$ (for $\xi \to 0$) and the vacuum with $N_{CS} = 1$ (for $\xi \to \infty$). The energy and the typical dimension of the sphaleron configuration are basically the result of the competition between the energy of the gauge configuration and the energy of the Higgs field. The latter introduces the weak scale into the problem.

For the doublet case, we can set $(J, Y) = (1/2, 1/2)$ in Eq.(3.48) and Eq.(3.50) to determine the energy of the sphaleron and field profiles numerically. In fact, this investigation has been carried out in [137] for scalar multiplets, $(J, Y) = (1/2, 1/2), (1, 0), (1, 1), (3/2, 1/2), (3/2, 3/2), (2, 0), (2, 1)$ and $(2, 2)$. But as our main focus is on the Higgs doublet of the SM, the results regarding larger representations are not presented here. The quantitative numerical results for Higgs doublet case is already presented in [14]. Still qualitative estimate can give a more physical intuitive picture of the sphaleron. As we pointed out before, the potential energy of the Higgs field is less important so for the sphaleron configuration of dimension l, we have

$$\begin{aligned} W_i &\sim \frac{1}{gl}, \\ E(W_i) &\sim \frac{4\pi}{g^2 l}, \end{aligned} \tag{3.51}$$

while the energy of the Higgs field is

$$E(\phi) \sim 4\pi v^2 l. \tag{3.52}$$

Minimizing the sum $E(W_i) + E(\phi)$, we obtain that the typical dimension of the sphaleron is

$$l_{\rm sp} \sim \frac{1}{gv} \sim 10^{-16}\ \text{cm}, \tag{3.53}$$

and

$$E_{\rm sp} \sim \frac{8\pi v}{g} \sim 10\ \text{TeV}. \tag{3.54}$$

The energy of the sphaleron in the case for doublet can be recast into the following form,

$$E_{\rm sp} = \frac{4\pi v}{g} B(\frac{\lambda}{g^2}) \tag{3.55}$$

where B is a function which depends very weakly on λ/g^2: $B(0) \simeq 1.52$ and $B(\infty) \simeq 2.72$. Inclusion of the mixing angle θ_W changes the energy of the sphaleron at most of 0.2%. The calculation done so far for the sphaleron

energy is when the temperature is zero. However, it was shown that at finite temperature, its energy follows approximately the scaling law

$$E_{\rm sp}(T) = E_{\rm sp}\frac{\phi(T)}{v}, \tag{3.56}$$

where $\phi(T)$ is the VEV of the Higgs field at finite temperature in the broken phase. This energy can be re-written as

$$E_{\rm sp}(T) = \frac{2m_W(T)}{\alpha_W} B\left(\frac{\lambda}{g^2}\right), \tag{3.57}$$

where $m_W(T) = \frac{1}{2}g\phi(T)$ is the mass of W boson at finite temperature.

Moreover, the Chern-Simons number of the sphaleron can be computed in a straightforward manner by using Eq.(3.43) into Eq.(3.26) for $\mu = \frac{\pi}{2}$ and one can obtain

$$N_{\rm CS}^{\rm sp} = \frac{1}{2}. \tag{3.58}$$

3.3.2 Baryon number violation at $T > T_c$ and $T < T_c$

The rate at $T > T_c$: At temperatures above the electroweak phase transition, the vacuum expectation value of the Higgs field is zero, $\phi(T) = 0$, the Higgs field decouples and the sphaleron configuration ceases to exist.

Let us estimate the rate $\Gamma_{\rm sp}$ on dimensional grounds. As we mentioned, at high temperature T the Higgs field decouples from the dynamics and it suffices to consider a pure $SU(2)$ gauge theory. Topological transitions take place through the creation of non-perturbative, nearly static, magnetic field configurations that generate a change in the Chern-Simons number, $\Delta N_{\rm CS}$ with a corresponding baryon number generation, $\Delta B = N_f \Delta N_{\rm CS}$.

If the field configuration responsible for the transition has a typical scale l, a change $\Delta N_{\rm CS} \simeq 1$ requires

$$\Delta N_{\rm CS} \sim g^2\, l^3\, \partial A_i A_i \sim g^2 l^3\, \frac{A_i}{l} A_i \sim 1 \Rightarrow A_i \sim \frac{1}{gl} \tag{3.59}$$

This means that the typical energy of the configuration is

$$E_{\rm sp} \sim l^3\, (\partial A_i)^2 \sim \frac{1}{g^2 l}. \tag{3.60}$$

To evade the Boltzmann suppression factor this energy should not be larger than the temperature T, which requires

$$l \gtrsim \frac{1}{g^2 T}. \tag{3.61}$$

Such a length scale corresponds to the one of the dynamically generated magnetic mass of order g^2T which behaves as a cut off for the maximum coherence length of the system. The rate of one unsuppressed transition per volume l^3 and time $t \sim l$ is therefore

$$\Gamma_{\rm sp} \sim \frac{1}{l^3 t} \sim (\alpha_W\, T)^4. \tag{3.62}$$

But it was pointed out in [138] that due to the damping effects in the plasma, the rate is suppressed by an extra power of α_W to give $\Gamma_{\rm sp} \sim \alpha_W^5 T^4$. The rate however is modified further as [139–141]

$$\Gamma_{\rm sym} \sim \alpha_w^5 T^4 \ln(1/\alpha_w), \tag{3.63}$$

From now on, we will parametrize the sphaleron rate in symmetric phase as

$$\Gamma_{\rm sp} = \kappa(\alpha_W\, T)^4. \tag{3.64}$$

Therefore, it can be seen that in the symmetric phase, $T > T_c$, the baryon number violating processes are unsuppressed.

The Rate at $T < T_c$: Once the temperature drops off the critical one $T < T_c$, bubbles of true vacuum ($\phi_c \neq 0$) start to nucleate where the sphaleron processes rate is suppressed as [124]

$$\Gamma_{sp} \sim \kappa\, 2.8 \times 10^5 T^4 \left(\frac{\alpha_W}{4\pi}\right)^4 \left(\frac{\xi(T)}{B(\lambda/g^2)}\right)^7 e^{-\xi(T)} \tag{3.65}$$

where, $\xi(T) = E_{sp}(T)/T$ and $B(\lambda/g^2)$ is the function entering in Eq.(3.55). The factor κ is the functional determinant associated with fluctuations around the sphaleron [16]. It has been estimated to be in the range: $10^{-4} \lesssim \kappa \lesssim 10^{-1}$ [124, 143].

B+L Washout

Considering the simplified case where all the conserved charges in the plasma (Q, L_i, $B-L$, $\ell_i = B/3 - L_i$, $\cdots$) are zero. If we introduce a chemical potential for the charge $B+L$, μ_{B+L}, the free energy density of the system (fermions) is given by

$$F = T \int \frac{d^3k}{(2\pi)^3} \left[\log\, \left(1 + e^{-(E_k - \mu_{B+L})/T}\right) + (\mu_{B+L} \to -\mu_{B+L})\right]. \tag{3.66}$$

The charge density of $B + L$ may be expressed in terms of the chemical potential by

$$n_{B+L} \sim \mu_{B+L} T^2 \tag{3.67}$$

and therefore we may relate the free energy with n_{B+L}

$$F \sim \mu_{B+L}^2 T^2 + \mathcal{O}(T^4) \sim \frac{n_{B+L}^2}{T^2} + \mathcal{O}(T^4). \tag{3.68}$$

The free energy increases quadratically with the fermion number density and the transitions which increase n_{B+L} are energetically disfavored with respect to the ones that decrease the fermion number. If these transitions are active for a long enough period of time, the system relaxes to the state of minimum energy, i.e. $n_{B+L} = 0$. Therefore any initial asymmetry in $B + L$ relaxes to zero.

To address this issue more quantitatively, one has to consider the ratio between the transition rate with $\Delta N_{\rm CS} = +1$, Γ_+ and the one with $\Delta N_{\rm CS} = -1$, Γ_-,

$$\frac{\Gamma_+}{\Gamma_-} = e^{-\Delta F/T}, \tag{3.69}$$

where ΔF is the free energy difference between the two vacua that arises due to the presence of chemical potential μ_{B+L}. If we define $\Gamma_{\rm sp}$ to be the average between Γ_+ and Γ_-, we may compute the rate at which the baryon number is being washed out [20]

$$\frac{dn_{B+L}}{dt} = \Gamma_+ - \Gamma_- \simeq -\frac{13}{2}\, N_F\, \frac{\Gamma_{\rm sp}}{T^3}\, n_{B+L}. \tag{3.70}$$

Let us now consider temperatures much above the electroweak phase transition, $T \gg m_W$. The exponential depletion of the n_{B+L} due to the sphaleron transition remains active as long as

$$\frac{\Gamma_{\rm sp}}{T^3} \gtrsim H \Rightarrow T \lesssim \alpha_W^4\, \frac{M_{pl}}{g_*^{1/2}} \sim 10^{12}\ \text{GeV}. \tag{3.71}$$

where the Hubble rate is $H(T) = 1.66\sqrt{g_*}T^2/M_{pl}$. Therefore, at any temperature below $T = 10^{12}$ GeV, the sphaleron transition will wash out any pre-existing $B + L$ asymmetry with the time scale $\tau \sim 2T^3/(13\Gamma_{\rm sp} N_F)$.

3.3.3 Sphaleron decoupling and the strong EWPhT condition

In the previous section, we can see that if the conserved charges in the plasma are taken to be zero, the asymmetry generated in B, L or $B + L$ will be

washed out by the sphaleron transitions if the system is kept in equilibrium for sufficiently long period of time because these transitions do not conserve these charges. Therefore we require the B violating sphaleron transition to get out of equilibrium after the electroweak phase transition.

The dilution $S = B_{final}/B_{initial}$ of the baryon asymmetry due to the sphaleron transition is

$$\frac{dS}{dt} =\simeq -\frac{13}{2}\, N_F\, \frac{\Gamma_{\rm sp}}{T^3} S \tag{3.72}$$

Assuming T is constant during the phase transition the integration of Eq.(3.72) yields $S = e^{-X}$ with $X = \frac{13}{2} N_f \frac{\Gamma_{\rm sp}}{T^3} t$. Using $t = 3 \times 10^{-2} \frac{M_{pl}}{T^2}$ and Eq.(3.65), the exponent X is written as $X \sim 10^{10} \kappa \xi^7 e^{-\xi}$, where we have taken the values of the parameters, $B = 1.87$, $\alpha_W = 0.0336$, $N_f = 3$, $T_c \sim 100$ GeV. Now the final baryon asymmetry seen from the observation, is, $B_{final} \sim 10^{-8} - 10^{-10}$ and largest initial asymmetry in the SM can be $B_{initial} \sim 10^{-5} - 10^{-6}$ [20,142]. Therefore, $S \gtrsim 10^{-5}$ or we have $X \lesssim 10$. This bound is translated into,

$$\xi(T_c) \gtrsim 7 \log \xi(T_c) + 9 \log 10 + \log \kappa \tag{3.73}$$

By considering first the upper bound of κ, $\kappa = 10^{-1}$, we obtain from Eq.(3.73),

$$\frac{E_{\rm sph}(T_c)}{T_c} \gtrsim 45, \tag{3.74}$$

and using the lower bound, $\kappa = 10^{-4}$ we obtain,

$$\frac{E_{\rm sph}(T_c)}{T_c} \gtrsim 37, \tag{3.75}$$

The bounds Eq.(3.74) and Eq.(3.75) put a condition on the ratio, $\phi(T_c)/T_c$. From Eq.(3.57), at critical temperature T_c, we have

$$\frac{\phi(T_c)}{T_c} = \frac{g}{4\pi B} \frac{E_{\rm sph}(T_c)}{T_c} \sim \frac{1}{36} \frac{E_{\rm sph}(T_c)}{T_c} \tag{3.76}$$

where we have used the previous values of the parameters. The bound Eq.(3.74) translates into

$$\frac{\phi(T_c)}{T_c} \gtrsim 1.3 \tag{3.77}$$

while the bound Eq.(3.75) translates into,

$$\frac{\phi(T_c)}{T_c} \gtrsim 1.0 \tag{3.78}$$

For a second order phase transition, $\phi(T_c) \simeq 0$. So, the above bounds, Eq.(3.77) and (3.78), imply that the electroweak phase transition has to be a strong first order transition so that the sphaleron transitions do not wash way the baryon asymmetry produced during the transition. However, it is already shown in section (2.4.2) that Higgs mass has to be below 45 GeV to have strong electroweak phase transition (EWPhT). Furthermore, lattice studies [23–25] pointed out that for $m_h > 75$ GeV, the transition actually become a cross-over. Therefore, now with Higgs at 126 GeV, clearly one can see the requirement of extending SM by new particles, possibly lying nearly the electroweak scale, which could provide strong EWPhT for successful electroweak baryogenesis.

Chapter 4

Scalar representations in the light of electroweak phase transition and cold dark matter phenomenology

From chapter 2 and 3, we have seen that strong first order electroweak phase transition required by the electroweak baryogenesis is not possible to obtain in the Standard Model because for this to happen, the Higgs mass has to be much smaller than the experimentally confirmed value. Also from chapter 1, we have seen that, the observed dark matter of the universe lacks a satisfactory explanation with the SM. Therefore, we explore a class of models with extended scalar sector of the SM, generally known as the inert multiplet model where we can achieve a strong first order phase transition and have a dark matter candidate.

In this chapter we have focused on the correlation between the EWPhT and DM properties for various inert scalar representations and identified the most favorable candidate from this class of models [27,144]. In section 4.1, we have presented the scalar potential and mass spectrum of the inert doublet, triplet and quartet model; an upper bound on the size of the multiplet and the electroweak precision observables. In section 4.2 we have identified the region of parameter space where strong EWPhT occurs for the inert doublet, complex tripet and quartet and also showed the impact of the size of the multiplet on the strength of the transition by calculating latent heat release. In section 4.3 we have presented the correlation between strong EWPhT and dark matter properties for the inert doublet case. Section 4.4 has featured the relic density analysis, direct detection limit for light DM in the quartet and finally the correlation between the strong EWPhT and DM properties which

has indicated that the smaller representation is favorable than the larger one in providing a light DM and simultaneously trigger strong EWPhT.

4.1 Scalar representations beyond the Standard Model

4.1.1 Scalar multiplets with cold dark matter candidates

The scalar multiplet charged under $SU(2)_L \times U(1)_Y$ gauge group is characterized by (J, Y). The electric charge for components of the multiplet is given by, $Q = T_3 + Y$. For half integer representation $J = n/2$, T_3 ranges from $-\frac{n}{2}$ to $\frac{n}{2}$. So the hypercharge of the multiplet needs to be, $Y = \pm T_3$ for one of the components to have neutral charge and can be considered as the DM. For integer representation n, similar condition holds for hypercharge.

When one considers the lightest component of the scalar multiplet as a good dark matter candidate [161], its lifetime has to be longer than about 10^{26} sec which is set by the current experimental limits on the fluxes of cosmic positrons, antiprotons and γ radiation [162, 163]. Such limits on the lifetime of the DM requires new couplings to be extremely small.[1] Therefore, it is natural to adopt a Z_2 symmetry under which all the SM particles are Z_2 even and the extra scalars are Z_2 odd such a way that the new couplings don't arise in the Lagrangian which will lead to the decay of the dark matter. Also this Z_2 symmetry becomes accidental for representations $J \geq 2$ if we only allow renormalizable terms in the Lagrangian. Moreover, our study is performed in a region of parameter space where inert scalar multiplets do not develop any vev both in zero and finite temperature.[2]

Denoting scalar multiplet as Q, and the SM Higgs as Φ, the most general Higgs-scalar multiplet potential , symmetric under Z_2, can be written in the following form,

$$\begin{aligned} V_0(\Phi, Q) &= -\mu^2 \Phi^\dagger \Phi + M_Q^2 Q^\dagger Q + \lambda_1 (\Phi^\dagger \Phi)^2 + \lambda_2 (Q^\dagger Q)^2 + \lambda_3 |Q^\dagger T^a Q|^2 \\ &+ \alpha \Phi^\dagger \Phi Q^\dagger Q + \beta \Phi^\dagger \tau^a \Phi Q^\dagger T^a Q + \gamma [(\Phi^T \epsilon \tau^a \Phi)(Q^T C T^a Q)^\dagger + \text{h.c.}] \end{aligned} \tag{4.1}$$

[1] For example, inert doublet can have yukawa coupling to fermions, $y_S \bar{f} f$, that can lead into its decay. But for $m_{DM} \sim 100$ GeV (illustrating WIMP scale), the bound on DM lifetime, $\tau_{DM} \sim 10^{25} - 10^{27}$ sec sets $y_S \sim 10^{-25} - 10^{-27}$. Also five dimensional operator, $\frac{\epsilon}{\Lambda} S F^{\mu\nu} F_{\mu\nu}$ can induce DM decay into monochromatic gamma rays. But for $m_{DM} \sim 100$ GeV and cut-off at EW scale, $\Lambda \sim v$, the DM lifetime again sets $\epsilon \sim 10^{-25} - 10^{-27}$.

[2] One can consider a scenario where inert multiplet can have non-zero vacuum expectation value at some finite temperature but it relaxes to zero as the temperature lowers down. Such scenario has been explored for doublet [56] and real triplet [193].

Here, τ^a and T^a are the $SU(2)$ generators in fundamental and Q's representation respectively. C is an antisymmetric matrix analogous to charge conjugation matrix defined as,

$$CT^aC^{-1} = -T^{aT} \tag{4.2}$$

C, being antisymmetric matrix, can only be defined for even dimensional space, i.e only for half integer representation. If the isospin of the reps. is j then C is a $(2j+1) \times (2j+1)$ dimensional matrix. The generators are normalized in such a way that they satisfy, for fundamental representation, $Tr[\tau^a\tau^b] = \frac{1}{2}\delta^{ab}$ and for other representations, $Tr(T^aT^b) = D_2(Q)\delta^{ab}$. Also $T^aT^a = C_2(Q)$. Here, $D_2(Q)$ and $C_2(Q)$ are Dynkin index and second Casimir invariant for Q's representation. The explicit form of generators, ϵ and C matrix are given in section E.1. Notice that, γ term is only allowed for representation with $(J, Y) = (\frac{n}{2}, \frac{1}{2})$.

For the doublet, real triplet, complex triplet, and the quartet, the scalar multiplet Q is respectively

$$\begin{pmatrix} C^+ \\ D^0 \equiv \frac{1}{\sqrt{2}}(S + iA) \end{pmatrix}, \begin{pmatrix} \Delta^+ \\ \Delta^0 \\ \Delta^- \end{pmatrix}_{(Y=0)}, \begin{pmatrix} \Delta^{++} \\ \Delta^+ \\ \Delta^0 \equiv \frac{1}{\sqrt{2}}(S + iA) \end{pmatrix}_{(Y=1)}, \text{ and } \begin{pmatrix} Q^{++} \\ Q^+ \\ Q^0 \equiv \frac{1}{\sqrt{2}}(S + iA) \\ Q'^- \end{pmatrix}. \tag{4.3}$$

In general, for the half-integer representation with $(J, Y) = (\frac{n}{2}, \frac{1}{2})$ and the Integer representation with $(J, Y) = (n, Y = 0 \text{ or } \pm T_3)$, the scalar multiplets with component fields denoted as $\Delta^{(Q)}$, where Q is the electric charge, are respectively

$$\mathbf{Q_{\frac{n}{2}}} = \begin{pmatrix} \Delta^{(\frac{n+1}{2})} \\ \cdots \\ \Delta^{(0)} \equiv \frac{1}{\sqrt{2}}(S + i\,A) \\ \cdots \\ \Delta^{(-\frac{n-1}{2})} \end{pmatrix} \text{ and } \mathbf{Q_n} = \begin{pmatrix} \Delta^{(n)} \\ \cdots \\ \Delta^{(0)} \\ \cdots \\ \Delta^{(-n)} \end{pmatrix}_{\mathbf{Y=0}}. \tag{4.4}$$

For the former representation every component represents a unique field while for the latter there is a redundancy $\Delta^{(-n)} = (\Delta^{(n)})^*$ except the $Y \neq 0$ case for which the component are also unique.

4.1.2 Inert Doublet, Triplet and Quartet mass spectra

Mass spectra: half integer representation with $Y = 1/2$ We now sketch the general form of mass spectrum for the multiplet. As $Y = 1/2$, T_3

value of the neutral component of the multiplet has to have $T_3 = -\frac{1}{2}$. Now for the Higgs vacuum expectation value, $\langle\Phi\rangle = (0, \frac{v}{\sqrt{2}})^T$, the term $\langle\Phi^\dagger\rangle\tau^3\langle\Phi\rangle$ gives $-\frac{v^2}{4}$. So masses for the neutral components, S and A are respectively

$$m_S^2 = M_Q^2 + \frac{1}{2}(\alpha + \frac{1}{4}\beta + p(-1)^{p+1}\gamma)v^2 \text{ and } m_A^2 = M_Q^2 + \frac{1}{2}(\alpha + \frac{1}{4}\beta - p(-1)^{p+1}\gamma)v^2. \tag{4.5}$$

Here, $p = \frac{1}{2}\text{Dim}(\frac{n}{2}) = 1, 2, ...$ comes from $2p \times 2p$ C matrix. For the charged component, with $T_3 = j$, we have,

$$m_{(j)}^2 = M_Q^2 + \frac{1}{2}\left(\alpha - \frac{1}{2}j\beta\right)v^2. \tag{4.6}$$

Now because of the γ term, there will be mixing between components carrying the same amount of charge. So to write down the mixing matrix, we have considered the ordering as follows. A component of the multiplet is denoted as $|J, T_3\rangle$. Components below the neutral component $|\frac{n}{2}, -\frac{1}{2}\rangle$ are denoted with $|\frac{n}{2}, -\frac{1}{2} - m\rangle$ where, $m = 1, 2, ..., \frac{n-1}{2}$ and corresponding charge is $Q = -m$. The piece $\langle\Phi\rangle^T\epsilon\tau^a\langle\Phi\rangle$ gives $\frac{v^2}{2\sqrt{2}}$. Therefore, the mixing term between between components with charge $|Q| = m$ is,

$$(-1)^{m+1}\frac{\gamma v^2}{4}\sqrt{(n+2m+1)(n-2m+1)}$$

In the ordering, $(\Delta^+_{(\frac{1}{2})}, \Delta^+_{(-\frac{3}{2})})$, with $m = 1$, the mass matrix becomes,

$$M_+^2 = \begin{pmatrix} m^2_{(\frac{1}{2})} & \frac{\gamma v^2}{4}\sqrt{(n+3)(n-1)} \\ \frac{\gamma v^2}{4}\sqrt{(n+3)(n-1)} & m^2_{(-\frac{3}{2})} \end{pmatrix} \tag{4.7}$$

And with $m = 2$ and $(\Delta^{++}_{(\frac{3}{2})}, \Delta^{++}_{(-\frac{5}{2})})$ we have,

$$M_{++}^2 = \begin{pmatrix} m^2_{(\frac{3}{2})} & -\frac{\gamma v^2}{4}\sqrt{(n+5)(n-3)} \\ -\frac{\gamma v^2}{4}\sqrt{(n+5)(n-3)} & m^2_{(-\frac{5}{2})} \end{pmatrix} \tag{4.8}$$

and so on, for charges with $m = 3, 4, \ldots$.

Doublet model If we consider S of the inert doublet to be the DM candidate, then following our parameterization Eq.(4.1) and Eq.(4.3), the mass spectrum, is in the following

$$\begin{aligned} m_S^2 &= M_Q^2 + \frac{1}{2}\left(\alpha + \frac{1}{4}\beta + \gamma\right) v^2 \\ m_A^2 &= m_S^2 - \gamma v^2 \\ m_C^2 &= m_S^2 - \frac{1}{2}\left(\gamma + \frac{1}{2}\beta\right) v^2 \end{aligned} \tag{4.9}$$

m_S is the smallest mass in the spectrum when $\gamma < 0$ and $\gamma + \frac{1}{2}\beta < 0$.

The couplings α, β and γ used in our parameterization is connected to λ_3, λ_4 and λ_5 used in the literature, as follows,

$$\lambda_3 = \alpha - \frac{1}{4}\beta \ , \ \lambda_4 = \frac{\beta}{2} \ , \ \lambda_5 = \gamma \tag{4.10}$$

Also, for convenience, we define,

$$\lambda_S = \alpha + \frac{1}{4}\beta + \gamma \ , \ \lambda_A = \alpha + \frac{1}{4}\beta - \gamma \ , \ \lambda_C = \alpha - \frac{1}{4}\beta \tag{4.11}$$

which are the couplings of S, A and C^+ to the higgs.

The conditions which ensure boundedness of the potential at large field values for the doublet are

$$\begin{aligned} \lambda_1 > 0 \quad &, \quad \lambda_2 > 0 \\ \alpha + \frac{1}{4}\beta \ &> \ -2\sqrt{\lambda_1 \lambda_2} \ \text{ in } (h, C^+, 0, ..) \text{ surface} \\ \alpha + \frac{1}{4}\beta + \gamma \ &> \ -2\sqrt{\lambda_1 \lambda_2} \ \text{ in } (h, S, 0, ..) \text{ surface} \end{aligned}$$

Quartet model The immediate generalization of doublet case is the $J = 3/2$ quartet case. Apart from splitting between S and A, γ term also mixes two single charged components of the quartet. According to Eq.(4.7), the mass matrix for the single charged fields in (Q^+, Q'^+) basis is

$$M_+^2 = \begin{pmatrix} M_Q^2 + \frac{1}{2}\left(\alpha - \frac{1}{4}\beta\right) v^2 & \frac{\sqrt{3}}{2}\gamma v^2 \\ \frac{\sqrt{3}}{2}\gamma v^2 & M_Q^2 + \frac{1}{2}\left(\alpha + \frac{3}{4}\beta\right) v^2 \end{pmatrix} \tag{4.12}$$

Diagonalizing the mass matrix, we have mass eigenstates for single charged fields, $Q_1^+ = Q^+ \cos\theta + Q'^+ \sin\theta$, $Q_2^+ = -Q^+ \sin\theta + Q'^+ \cos\theta$ with $\tan 2\theta = -\frac{2\sqrt{3}\gamma}{\beta}$.

Again we consider S to be the dark matter. So masses of the components of the multiplet are as follows,

$$\begin{aligned} m_S^2 &= M_Q^2 + \frac{1}{2}\left(\alpha + \frac{1}{4}\beta - 2\gamma\right)v^2 \\ m_A^2 &= m_S^2 + 2\gamma v^2 \\ m_{Q^{++}}^2 &= m_S^2 - \frac{1}{2}(\beta - 2\gamma)v^2 \\ m_{Q_1^+(Q_2^+)}^2 &= m_S^2 + \left(\gamma \mp \frac{1}{4}\sqrt{\beta^2 + 12\gamma^2}\right)v^2 \end{aligned} \tag{4.13}$$

Because of the mixing between two single charged states, the mass relation is

$$m_S^2 + m_A^2 = m_{Q_1^+}^2 + m_{Q_2^+}^2 \tag{4.14}$$

The full stability analysis for the quartet potential is an involved task so for time being, we can give a partial set of necessary stability conditions by taking Higgs-scalar two dimensional complex surface $(h, \xi^i, 0, 0, ...)$ in field space.[3].

$$\begin{aligned} \lambda_1 > 0 \quad &, \quad \lambda_2, \lambda_3 > 0 \\ \alpha + \frac{1}{4}\beta - 2\gamma &> -2\sqrt{\lambda_1(\lambda_2 + \frac{1}{4}\lambda_3)} \text{ in } (h, S, 0, ..) \text{ surface} \\ \alpha + \frac{1}{4}\beta + 2\gamma &> -2\sqrt{\lambda_1(\lambda_2 + \frac{1}{4}\lambda_3)} \text{ in } (h, A, 0, ..) \text{ surface} \\ \alpha - \frac{3}{4}\beta &> -2\sqrt{\lambda_1(\lambda_2 + \frac{3}{4}\lambda_3)} \text{ in } (h, Q^{++}, 0, ..) \text{ surface} \\ \alpha - \frac{1}{4}\beta &> -2\sqrt{\lambda_1(\lambda_2 + \frac{1}{4}\lambda_3)} \text{ in } (h, Q^{+}, 0, ..) \text{ surface} \\ \alpha + \frac{3}{4}\beta &> -2\sqrt{\lambda_1(\lambda_2 + \frac{9}{4}\lambda_3)} \text{ in } (h, Q'^{-}, 0, ..) \text{ surface} \end{aligned} \tag{4.15}$$

The last two conditions, when expressed in terms of mass eigenstates Q_1^+, Q_2^+ becomes

$$\alpha \mp \frac{1}{4}\beta(1 \mp 2\cos 2\theta) \pm \sqrt{3}\gamma \sin 2\theta > -\sqrt{\lambda_1\lambda_2 + \frac{1}{4}\lambda_1\lambda_3(3 \mp 4\cos 2\theta + 2\cos 4\theta)} \tag{4.16}$$

in $(h, Q_{1,2}^+)$ surface.

[3]For general treatment see [164]

Mass spectra: integer representation with $Y = 0$ and $Y \neq 0$ For integer representation, γ term is not allowed. Therefore, there will not be any mass splitting between real and imaginary part of the neutral component. Moreover, for $Y = 0$ or real representation, the term $Q^\dagger T^3 Q$ is zero. So tree level mass spectrum is degenerate and is given by,

$$m_\Delta^2 = M_Q^2 + \frac{1}{2}\alpha v^2. \tag{4.17}$$

On the other hand, if $Y \neq 0$, there will be mass splitting due to β term. Also one can choose Y as, from $-n$ to n, to set one component to be neutral. If $T_3 = j$, the mass is given by,

$$m_{(j)}^2 = M_Q^2 + \frac{1}{2}\left(\alpha - \frac{1}{2}\beta j\right) v^2 \tag{4.18}$$

Triplet model Two representatives from this class are the real triplet ($T = 1, Y = 0$) and the complex triplet ($T = 1, Y = 1$). For real triplet, the term, $\Delta^\dagger T_T^3 \Delta$ is zero, so the mass spectrum will be degenerate and given as,

$$m_{\Delta^+}^2 = m_{\Delta^0}^2 = M_\Delta^2 + \frac{1}{2}\alpha v^2. \tag{4.19}$$

On the other hand, for the complex case the mass spectrum is,

$$m_S^2 = m_A^2 = M_\Delta^2 + \frac{1}{2}\left(\alpha + \frac{1}{2}\beta\right) v^2 \tag{4.20}$$

$$m_{\Delta^+}^2 = M_\Delta^2 + \frac{1}{2}\alpha v^2 \tag{4.21}$$

$$m_{\Delta^{++}}^2 = M_\Delta^2 + \frac{1}{2}\left(\alpha - \frac{1}{2}\beta\right) v^2 \tag{4.22}$$

There is a relation between masses:

$$m_{\Delta^{++}}^2 - m_{\Delta^+}^2 = m_{\Delta^+}^2 - m_{\Delta^0}^2 = -\frac{1}{4}\beta v^2 \tag{4.23}$$

And the stability conditions are,

$$\begin{aligned}
\lambda_1 > 0 \quad &, \quad \lambda_2, \lambda_3 > 0 \\
2\alpha + \beta \;&>\; -2\sqrt{\lambda_1(\lambda_2 + \lambda_3)} \text{ in } (h, \Delta^0, 0, ..) \text{ surface} \\
\alpha \;&>\; -2\sqrt{\lambda_1 \lambda_2} \text{ in } (h, \Delta^+, 0, ..) \text{ surface} \qquad (4.24) \\
2\alpha - \beta \;&>\; -2\sqrt{\lambda_1(\lambda_2 + \lambda_3)} \text{ in } (h, \Delta^{++}, 0, ..) \text{ surface} \qquad (4.25)
\end{aligned}$$

When we don't consider the Z_2 symmetry and allow the new yukawa couplings with the complex triplet in the lagrangian, it will enable the neutrino to acquire mass through the Type-II seesaw mechanism [165]. But in that case, the triplet will not able to provide any no viable DM candidate.

Because of the absence of γ term as in half integer representation, there is no mass splitting between S and A of the neutral component Δ^0. S and A have vector interaction with Z boson that produces spin-independent elastic cross section which is already $8-9$ orders of magnitude above the CDMS direct detection bound [166] and for this reason, complex triplet or any larger integer multiplet with non zero hypercharge is not going to satisfy direct detection bound as one will require a non-zero splitting between S and A larger than the kinetic energy of DM in our galactic halo to make $Z-S-A$ process kinematically forbidden. Therefore, only neutral component of the real triplet can be a plausible DM candidate. In fact, real triplet DM has been already studied in [69, 70, 167, 168]. In [69, 167] it was shown that observed relic density can be accounted for the DM if the mass of the DM lies about 2.5 TeV. Being degenerate, one can easily see that, such particle would decouple from electroweak plasma and had no significant effect on EWPhT. But the question of having a strong first order EWPhT in complex triplet is relevant for cosmic evolution of the universe. Therefore we only focused on EWPhT in the complex triplet case in a later section.

4.1.3 Perturbativity and EW physics constraints on the size of the multiplets

Perturbativity: Landau pole of the gauge coupling, g

What is the largest possible inert multiplet allowed to be added to the standard model? One possible bound comes from the beta function of $SU(2)$ gauge coupling in presence of large scalar multiplets because the addition of such large multiplet not only halts the asymptotic freedom of non-Abelian gauge couplings but also lowers the scale of landau pole with its size.

Consider non-abelian gauge theory with gauge group G and coupling g. If there are N_F different fermion fields in different representations R_i^F and N_S scalar fields in different representations R_i^S, the 1-loop beta function is

$$\beta(g) = \mu\frac{dg}{d\mu} = -\frac{g^3}{16\pi^2}\left[\frac{11}{3}T(A) - \frac{2\eta}{3}\sum_{i=1}^{N_F}T(R_i^F) - \frac{1}{3}\sum_{i=1}^{N_S}T(R_i^S)\right] = -\frac{g^3}{16\pi^2}\tilde{\beta} \tag{4.26}$$

Here, $\eta = 1\,(2)$ for Weyl (Dirac) fermions and $\tilde{\beta}$ is the group theoretic factor.

Again, the Dynkin index of representation R, $T(R)$ is define as

$$\mathrm{Tr}\,(T_R^a T_R^b) = T(R)\delta^{ab} \tag{4.27}$$

$T(R)$ is determined from the following formula,

$$T(R) = \frac{\dim R}{\dim G} C_2(R) \tag{4.28}$$

where the quadratic Casimir of representation R is

$$T_R^a T_R^a = C_2(R)\mathbf{I}_{dimR} \tag{4.29}$$

Now by integrating Eq.(4.26) from μ_0, where $g(\mu_0) = g_0$, to μ where $g(\mu) = g$, we have,

$$g^2 = \frac{1}{1 + \frac{\tilde{\beta} g_0^2}{8\pi^2} \ln \frac{\mu}{\mu_0}} \tag{4.30}$$

Now if the matter contribution becomes larger than the gauge contribution in the beta function, $\tilde{\beta} < 0$. So the asymptotic freedom of non-abelian gauge theory is lost and the landau pole will occur as follows,

$$\Lambda_{\text{landau}} = \mu_0 \exp\left(\frac{8\pi^2}{|\tilde{\beta}| g_0^2}\right) \tag{4.31}$$

where we can see that, the presence of larger representation of fermion and scalar fields increase $|\tilde{\beta}|$ and therefore, the scale of landau pole, Λ_{landau} becomes smaller.

The one-loop beta function of $SU(2)$ gauge coupling for Standard Model solely augmented by a scalar multiplet of isospin J is

$$\beta(g) = \frac{g^3}{16\pi^2}\left(-\frac{19}{6} + \frac{1}{9}J(J+1)(2J+1)\right) \tag{4.32}$$

It can be seen that, $\beta(g)$ remains negative only for $J \leq \frac{3}{2}$. For, $J \geq 2$, it becomes positive and hits the landau pole as shown in Fig.(4.1). For instance adding a scalar multiplet with isospin $J \geq 5$ will bring the Landau pole of $SU(2)$ gauge coupling at $\Lambda \leq 10$ TeV and for $J \geq 10$, its even smaller, $\Lambda \leq 180$ GeV. Therefore, perturbativity of gauge coupling at the TeV scale sets a upper bound on the size of the multiplet to be $J \leq 5$.

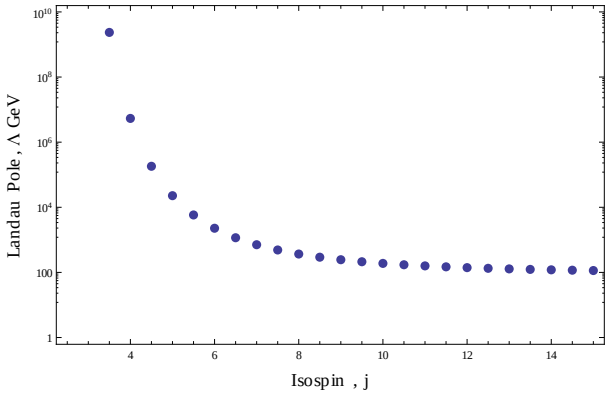

Figure 4.1: Landau pole with different scalar multiplet.

Bound from tree-unitarity

The tree-unitarity condition played an important role in development of the Standard model. The bad high energy behavior and inconsistency with the unitarity of Born-scattering in weak interaction theory mediated by intermediate massive vector bosons was first pointed out in [145] and later showed in [146] that such behavior does not occur in the case for the standard model. Subsequently the tree unitarity condition was generalized in [147–152] and was used to put the upper bound on the Higgs mass [153, 154].

Here, we are focusing on scattering of the scalar particles so from appendix F, we have for spinless particles,

$$T_{fi}(s, \cos\theta) = 16\pi \sum_J (2J+1) a_J(s) P_J(\cos\theta) \tag{4.33}$$

where s is the center of mass (CM) energy and θ is the angle between incoming and outgoing particles in CM frame. The coefficient a_J is,

$$a_J(s) = \frac{1}{32\pi} \int_{-1}^{1} d(\cos\theta) P_J(\cos\theta) T_{fi}(s, \cos\theta) \tag{4.34}$$

Since a_0 is real in the Born approximation, we can have the following bound,

$$\mathrm{Re}\, a_0 \leq \frac{1}{2} \tag{4.35}$$

In [169,170], the $2 \to 2$ scattering amplitudes for scalar pair annihilations into electroweak gauge bosons have been computed and by requiring zeroth partial wave amplitude satisfying the unitarity bound Eq.(4.35), it was shown that maximum allowed complex $SU(2)_L$ multiplet would have isospin $J \leq 7/2$ and real multiplet would have $J \leq 4$.

One-loop renormalization group equations

The presence of a larger representation of the scalar field enables the scalar quartic couplings to grow much faster than that of a lower dimension. In the case of fermions, the yukawa coupling will drive the scalar couplings to negative value at high energy and destabilizes the scalar potential.

Here, we have compared the running of Standard model and additional scalar couplings in the presence of a doublet and triplet charged under the SM group and showed that, if the scalar couplings are positive and large at EW scale m_Z, then in triplet case, the scalar quartic couplings grow much faster and will reach 4π compared to the doublet case. In the appendix G, we have presented an algebraic method to determine the one-loop beta functions for doublet scalar quartic couplings from the effective potential which matched the results of [33].

Now if we compare the triplet [171] to the doublet [33], we obtain Fig. (4.2) which shows that on increasing the size of the multiplet, the scalar couplings will run faster compared to the smaller representation and will become non-perturbative much faster if one starts with large scalar coupling at EW scale.

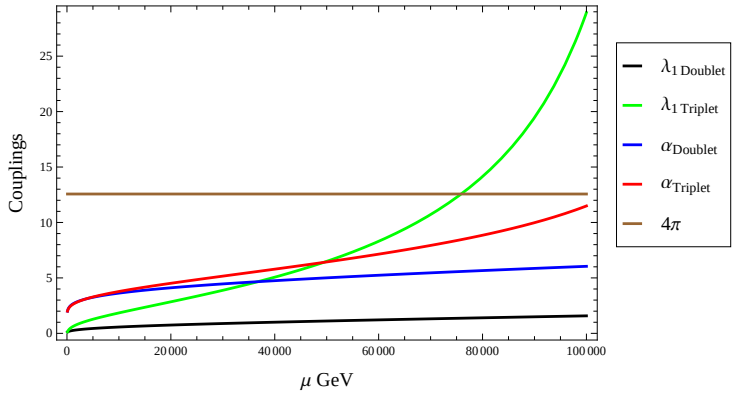

Figure 4.2: The running of Higgs quartic coupling λ_1 and coupling α. The initial values of the couplings at energy $\mu = 100$ GeV are $(\lambda_1, \lambda_2, \lambda_3, \alpha, \beta, \gamma) = (0.13, 0.1, 0.1, 2, 0.1, 0.1)$ for both cases. Here we can see that large values of α which also drives strong EWPhT, as we will see later, drives Higgs coupling to run much faster in triplet than the doublet case.

Electroweak precision observable

A straightforward way to observe the indirect effect of new physics is in the modification of vacuum polarization graph of $W^{\pm}$ and Z^0 boson and

one convenient way to parameterize these 'Oblique correction' is through S, T and U parameters [172, 173] (analysis of one-loop correction in SM was first done in [174]); plus V, W and X parameters [175] if new physics is at scale comparable to the EW scale. Oblique corrections are dominant over other 'non-oblique' corrections (vertex diagram and box diagram with SM fermions as external states) because all the particles charged under SM group will couple to gauge bosons but usually only one or two particles in a theory will couple to specific fermion species.

Because of the absence of coupling between inert scalar fields and SM fermions, the only dominant effects will come from oblique corrections. T parameter, measuring the shift of $\rho = \frac{M_W}{M_Z \cos\theta_w}$ from SM value due to the radiative correction by new particles, is

$$\alpha T = \frac{\Pi_{WW}(0)}{m_W^2} - \frac{\Pi_{ZZ}(0)}{m_Z^2} \tag{4.36}$$

where, $\Pi_{WW}(0)$ and $\Pi_{ZZ}(0)$ vacuum polarization graph of W and Z bosons evaluated at external momentum, $p^2 = 0$.

EWPO in the Inert Doublet The contribution of the inert doublet to T parameter is [33]

$$T \approx \frac{1}{24\pi^2 \alpha v^2}(m_C - m_A)(m_C - m_S) \ . \tag{4.37}$$

If the mass of the Higgs were heavier than the present value, one would then require substantial T or a non-degenerate spectrum of the inert doublet states. On the other hand, we are motivated by the first-order phase transition, which favors as light SM Higgs, which is also confirmed experimentally. This in turn implies $T \approx 0$. There are two possibilities to achieve this: a) $m_S < m_C \approx m_A$ or b) $m_S \approx m_C < m_A$. It will turn out that S, as the DM, has to be lighter than about 80 GeV. It is not completely clear whether the possibility b) is in accord with the experiment [176]. For this reason, we pursued possibility a), where A and C are quite degenerate [44] or equivalently $\gamma \approx \beta/2$ ($\lambda_4 \approx \lambda_5$).

As the scalar contribution to the S parameter is small compared to T parameter, we have from [33],

$$S = \frac{1}{2\pi}\int_0^1 dx x(1-x)\ln\frac{x\, m_S^2 + (1-x)m_A^2}{m_C^2} \tag{4.38}$$

EWPO for the Quartet The gauge-scalar-scalar vertices required for calculating S and T parameters for the quartet are given in section E.2. The quartet contribution to T parameter,

$$\begin{aligned}\frac{16\pi^2\alpha}{g^2}T &= \frac{1}{M_W^2}(\frac{3}{2}\cos^2\theta\, F(m_{Q^{++}}, m_{Q_1^+}) + \frac{3}{2}\sin^2\theta\, F(m_{Q^{++}}, m_{Q_2^+}) \\ &+ \frac{1}{4}(\sqrt{3}\sin\theta + 2\cos\theta)^2\, F(m_{Q_1^+}, m_S) + \frac{1}{4}(\sqrt{3}\sin\theta - 2\cos\theta)^2\, F(m_{Q_1^+}, m_A) \\ &+ \frac{1}{4}(\sqrt{3}\cos\theta - 2\sin\theta)^2\, F(m_{Q_2^+}, m_S) + \frac{1}{4}(\sqrt{3}\cos\theta + 2\sin\theta)^2\, F(m_{Q_2^+}, m_A)) \\ &- \frac{1}{4c_w^2 M_Z^2}(F(m_S, m_A) + \sin^2 2\theta\, F(m_{Q_1^+}, m_{Q_2^+})) \end{aligned} \tag{4.39}$$

here,

$$F(m_1, m_2) = \frac{m_1^2 + m_2^2}{2} - \frac{m_1^2 m_2^2}{m_1^2 - m_2^2}\ln\frac{m_1^2}{m_2^2} \tag{4.40}$$

In addition, S parameter for quartet multiplet is,

$$\begin{aligned} S &= \frac{s_w^2}{8\pi}\int_0^1 dx\, x(x-1)[\ln\frac{m_{Q_1^+}^2 m_{Q_2^+}^2}{m_{Q^{++}}^4} + 2\cos 2\theta \ln\frac{m_{Q_2^+}^2}{m_{Q_1^+}^2} \\ &+ \ln\frac{(1-x)m_S^2 + x m_A^2}{m_{Q^{++}}^2} + \sin^2 2\theta \ln\frac{[(1-x)m_{Q_1^+}^2 + x m_{Q_2^+}^2]^2}{m_{Q_1^+}^2 m_{Q_2^+}^2}] \end{aligned} \tag{4.41}$$

Best fit values of S and T The best fit values of S and T parameter with $(U = 0)$[4] is [178]

$$S = 0.04 \pm 0.09 \text{ and } T = 0.07 \pm 0.08 \tag{4.42}$$

Therefore, one can put constraints on S and T parameter by comparing the theoretical predictions with well measured experimental values of observables.

4.2 Electroweak phase transition (EWPhT)

4.2.1 Finite temperature effective potential

In chapter 2, we have described the finite temperature effective potential in details. Here we recapitulate the main points. If there are multiple classical

[4]The contribution to U parameter by scalar multiplet with only gauge interactions considered in our case, will be smaller compared to T parameter by a factor $(M_W/M_S)^2$, where M_S is the leading scalar mass of theory [177]

background fields ϕ_i , which act as order parameters of the thermodynamic system, the total one-loop effective potential at finite temperature is,

$$V_{eff}(\phi_i, T) = V_0(\phi_i) + V_{CW}(\phi_i) + V_T(\phi_i, T) \tag{4.43}$$

Here, V_0, V_{CW} and V_T are tree-level, 1-loop Coleman-Weinberg and finite temperature potential respectively. The daisy resummed finite temperature potential is,

$$V_T = \sum_{B(F)} (\pm) g_{B(F)} \frac{T^4}{2\pi^2} \int_0^\infty dx x^2 \ln(1 \mp e^{-\sqrt{x^2 + m^2_{B(F)}(\phi_i, T)/T^2}}) \tag{4.44}$$

Here, g_B and g_F are bosonic and fermionic degrees of freedom and $\pm$ correspond to boson and fermion respectively. Thermal mass correction determined with respect to background fields ϕ_j is,

$$m_i^2(\phi_j) \to m_i^2(\phi_j, T) = m_i^2(\phi_j) + \Pi_i(T) \tag{4.45}$$

where $\Pi_i(T)$ is the thermal self energy correction (Debye correction) and at the high temperature limit, it is of the form T^2 times coupling constants. $\Pi_i(T)$ measures how much particles are screened by thermal plasma from the classical background field ϕ (just like the Debye screening) and large screening reduces the strength of phase transition. In other words, it is the amplitude for the external particle (sourced by classical field) to forward scatter off from a real physical particle present in the thermal bath [179].

For numerical convenience, in subsequent studies, we have used the following form of the effective potential in high temperature approximation,

$$\begin{aligned} V_{eff} &= V_0 + V_{CW} + \sum_B g_B [\frac{m_B^2(\phi, T) T^2}{24} - \frac{T}{12\pi} [m_B^2(\phi, T)]^{\frac{3}{2}} \\ &+ \frac{m_B^4(\phi, T)}{64\pi^2} \ln \frac{m_B^2(\phi, T)}{A_b T^2}] + \sum_F g_F \left[\frac{m_F^2(\phi) T^2}{48} - \frac{m_F^2(\phi)}{64\pi^2} \ln \frac{m_F^2(\phi)}{A_f T^2} \right] \end{aligned} \tag{4.46}$$

It was shown in [17] that high T approximation agrees with exact potential better than 5% for $m/T < 1.6(2.2)$ for fermions (bosons). So unless great accuracy is required, one can use Eq.(4.46) to explore the thermodynamic properties of system.

Issue of imaginary effective potential and gauge dependence There will be some region of parameter space, for example, the Goldstone modes, where the effective potential will become imaginary due to the non-analytic

cubic terms $(m^2(\phi,T))^{\frac{3}{2}}$ and the log terms. It doesn't signal the breakdown of perturbative calculation, instead, as it was shown in [180, 184] that the imaginary part signals the instability of the homogeneous zero modes. Moreover, as mentioned in [181] that the imaginary part vanishes when effective potential is calculated to all orders but at any finite order, it can be present. Therefore, in calculation we are only concerned with the real part of the potential. To ameliorate the gauge dependence of finite temperature effective potential, gauge invariant prescriptions have been developed [182–185]. Moreover, in [184], it was shown that landau gauge ($\xi = 0$) is better in capturing the thermodynamic properties by comparing them with those determined with gauge invariant Hamiltonian formalism. So in this work we have chosen to follow the landau gauge to carry out our numerical calculation. The main motivation for us is to explore the phase transition qualitatively and it's already apparent from the above discussion that perturbative techniques can at best capture the approximate nature of the finite temperature phenomena. For quantitative accuracy one eventually has to use lattice methods.

4.2.2 EWPhT with the Inert Doublet, Triplet and Quartet representations

The nature of electroweak phase transition is a cross over for Higgs boson with mass about 125.5 GeV (for a recent lattice study, [186]). Therefore to achieve strong first order phase transition, one must extend the scalar sector of the theory. Consider an inert multiplet Q with isospin, j and hypercharge $Y = 0$ and the parameter space is chosen in such a way that inert multiplet does not obtain any VEV at all temperatures. So, $\langle\Phi\rangle = (0, \frac{\phi}{\sqrt{2}})^T$ and $\langle Q\rangle = 0$. Because of zero VEV at all temperatures, the only classical background field is that of Higgs doublet and therefore the sphaleron configuration is exactly like that of the Standard Model. For this reason, in this case, first order phase transition is determined by the condition $\phi_c/T_c \geq 1$ as seen in section 3.3.3.

The thermal masses for the component fields of the Higgs doublet Φ and real multiplet Q are

$$\begin{aligned} m_h^2(\phi,T) &= -\mu^2 + 3\lambda_1\phi^2 + a(j)\frac{T^2}{12} \qquad (4.47)\\ m_{G^\pm}^2(\phi,T) = m_{G^0}^2(\phi,T) &= -\mu^2 + \lambda_1\phi^2 + a(j)\frac{T^2}{12} \end{aligned}$$

and due to degenerate mass spectrum,

$$m_i^2(\phi,T) = M^2 + \frac{1}{2}\alpha\phi^2 + b(j)\frac{T^2}{12} \qquad (4.48)$$

Temperature coefficients are,

$$a(j) = 6\lambda_1 + \frac{1}{2}(2j+1)\alpha + \frac{9}{4}g^2 + \frac{3}{4}g'^2 + 3y_t^2 \quad (4.49)$$

$$b(j) = (2j+3)\lambda_2 + 2\alpha + 3j(j+1)g^2 \quad (4.50)$$

Here one can see that from 1st and 3rd term of $b(j)$ that larger representation receives relatively large thermal corrections due to the scalar loops and gauge boson loops. These coefficients capture how much particles are screened by the plasma from the classical field which determines the strength of the transition. The larger the coefficients are, the weaker the transition will become because those particles are effectively decoupled from the plasma. This plasma screening effect on the nature of phase transition for complex singlet was already studied in [187]. In the following, we showed similar effect for real multiplet as it captures the essential features that depend on size of the multiplet. Generalization to complex odd dimensional or even dimensional scalar multiplet is straightforward.

Using Eq.(4.46) and neglecting the terms coming from CW-corrections and log terms we have,

$$V_T(\phi, T) = A(T)\phi^2 + B(T)\phi^4 + C(T)[\phi^2 + K^2(T)]^{\frac{3}{2}} \quad (4.51)$$

where,

$$\begin{aligned} A(T) &= -\frac{1}{2}\mu^2 + a(j)\frac{T^2}{12} \quad (4.52)\\ B(T) &= \frac{1}{4}\lambda_1 \\ C(T) &= -(2j+1)\frac{T}{12\pi}(\frac{\alpha}{2})^{\frac{3}{2}} \\ K^2(T) &= \frac{2}{\alpha}\left(M^2 + b(j)\frac{T^2}{12}\right) \end{aligned}$$

When the universe is at very high temperature, it is in the symmetric vacuum $\phi = 0$ but when the universe cools down, there can be two characteristic temperatures: T_1 and T_2. For temperature, $T < T_2$, the origin is the maximum and there is only one global minimum at $\phi \neq 0$ that evolves towards zero temperature minimum. For $T > T_2$, the origin is a minimum and there is also a maximum at $\phi_-(T)$ and another minimum at $\phi_+(T)$ given by,

$$\phi_\pm^2(T) = \frac{1}{32B^2}[9C^2 - 16AB \pm 3|C|\sqrt{9C^2 + 32(2B^2K^2 - AB}] \quad (4.53)$$

The second order transition temperature T_2 is determined by the condition,

$$4A^2 - 9C^2K^2 = 0 \tag{4.54}$$

And the first order transition temperature, T_1 where $V_T(\phi_c(T_1), T_1) = V_T(0, T_1)$ and $\phi_+(T_1) = \phi_-(T_1)$ sets the condition,

$$9C^2 + 32(2B^2K^2 - AB) = 0 \tag{4.55}$$

From two conditions, T_1 and T_2 are determined as,

$$T_1^2 = \frac{4\lambda_1\mu^2 + \frac{8M^2+\lambda_1^2}{\alpha}}{\frac{1}{3}a(j)\lambda_1 - \frac{2b(j)\lambda_1^2}{3\alpha} - (2j+1)^2\frac{\alpha^3}{128\pi^2}} \tag{4.56}$$

and

$$T_2^2 = \frac{1}{2D}(E + \sqrt{E^2 - 4D\mu^4}) \tag{4.57}$$

with

$$\begin{aligned} D &= \frac{a(j)^2}{144} - (2j+1)^2\frac{b(j)\alpha^2}{768\pi^2} \\ E &= \frac{1}{6}a(j)\mu^2 + (2j+1)^2\frac{M^2\alpha^2}{64\pi^2} \end{aligned} \tag{4.58}$$

The nature of the transition depends on the relation between T_1 and T_2. If $T_1 > T_2$, the transition is first order and plasma screening is not so effective. When $T_1 < T_2$, the transition is actually second order due to dominant plasma screening. Actually, $T_1 = T_2$ gives the turn over condition from first to second order transition and from (4.56) and (4.57), we can have a condition on the parameter space $(\lambda_2, \alpha, M, j)$.

$$\frac{3}{256\pi^2}(2j+1)^2\alpha^4 - b(j)\lambda_1^2 \geq (a(j)\lambda_1 - \frac{3}{64\pi^2}(2j+1)^2\alpha^3)\left(\frac{M}{v}\right)^2 \tag{4.59}$$

Here, the strict inequality implies the region of parameter space where first order transition persists and equality corresponds to the turn-over. Here one can see that, this inequality saturates if M and $b(j)$ becomes large as these two terms control the plasma screening for the particle. For small values of α, we can easily see from LHS of (4.59) that the second term increases faster than the first term due to the quadratic Casimir for gauge boson contribution and self interacting quartic term in $b(j)$ (Eq.(4.49)). Also if invariant mass term M is large, the RHS will saturates the inequality much faster. So one can infer that although large representation will favor the first order

transition up to certain value of j because of more degrees of freedom in the plasma coupling to the background field, at one point, due to large thermal mass coming from gauge interaction, plasma screening will be large enough to cease the first order transition and make it as a second order.

Electroweak phase transition with scalar singlet, two higgs doublet model[5] [142,188–192] (and references therein) and real triplet [193] have been studied extensively. Therefore, in the following sections, we have focused on the inert doublet, complex triplet and the quartet to study the nature of phase transition.

Inert Doublet

The thermal mass for the Higgs and Goldstone fields are

$$m_h^2(\phi, T) = -\mu^2 + 3\lambda_1\phi^2 + a\frac{T^2}{12} \tag{4.60}$$

$$m_{G^\pm}^2 = m_{G^0}^2 = -\mu^2 + \lambda_1\phi^2 + a\frac{T^2}{12} \tag{4.61}$$

And thermal masses for the component fields of the inert doublet are

$$m_S^2(\phi, T) = M_D^2 + \frac{1}{2}(\alpha + \frac{1}{4}\beta + \gamma)\phi^2 + b\frac{T^2}{12} \tag{4.62}$$

$$m_A^2(\phi, T) = M_D^2 + \frac{1}{2}(\alpha + \frac{1}{4}\beta - \gamma)\phi^2 + b\frac{T^2}{12} \tag{4.63}$$

$$m_C^2(\phi, T) = M_D^2 + \frac{1}{2}(\alpha - \frac{1}{4}\beta)\phi^2 + b\frac{T^2}{12} \tag{4.64}$$

Here the thermal coefficients a and b are,

$$a = 6\lambda_1 + 2\alpha + \frac{9}{4}g^2 + \frac{3}{4}g'^2 + 3y_t^2 \tag{4.65}$$

$$b = 6\lambda_D + 2\alpha + \frac{9}{4}g^2 + \frac{3}{4}g'^2 \tag{4.66}$$

M_D and λ_D are denoting common mass term and self quartic coupling of the inert doublet respectively.

[5]Inert doublet can be considered as a special case of two Higgs doublet model

The thermal effective potential is

$$\begin{aligned} V_{eff}(\phi,T) &= \frac{1}{2}(-\mu^2+a\frac{T^2}{12})\phi^2+\frac{\lambda_1}{4}\phi^4+\sum_i(\pm)g_i\frac{m_i(\phi)^4}{64\pi^2}\left[\ln\frac{m_i^2(\phi)}{Q^2}-c_i\right] \\ &- \frac{T}{12\pi}\sum_B g_B[m_B^2(\phi,T)]^{3/2}-\sum_B\frac{m_B^4(\phi,T)}{64\pi^2}\ln\frac{m_B^2(\phi,T)}{A_bT^2} \\ &+ 12\frac{m_t^4(\phi)}{64\pi^2}\ln\frac{m_t^2(\phi)}{A_fT^2} \end{aligned} \tag{4.67}$$

where the bosonic sum is taken over, h, $G^\pm$, G^0, S, A, $C^\pm$, $W^\pm$ and Z with corresponding degrees of freedom, g_i are $\{h, G^\pm, G^0, S, A, C^\pm, W^\pm, Z, t\} = \{1,2,1,1,1,2,6,3,12\}$. Also Q is the renormalization scale and in $\overline{MS}$ scheme, $\{c_S, c_F, c_{GB}\} = \{3/2, 3/2, 5/6\}$.

The criterion for having a strong first-order electroweak phase transition is $\phi_c/T_c \gtrsim 1$ at the critical point, which calls for a large cubic thermal potential $\phi^3 T$. In the inert doublet model the new scalars play this crucial role with a sufficiently large coupling to the SM Higgs boson, $\lambda_i \sim \mathcal{O}(1)$ where $\lambda_C = \alpha - \frac{\beta}{4}$ and $\lambda_A = \alpha + \frac{1}{4}\beta - \gamma$. In the subsequent section, we will show that direct detection implies $\lambda_S \lesssim 0.1$. Therefore, only large λ_A and λ_C can trigger strong EWPhT, which implies that the corresponding pseudoscalar and charged components are heavy at zero temperature.

We also showed in Fig.(4.3), the dependence of the critical temperature and the Higgs VEV on the DM self coupling λ_D and the SM Higgs mass. We found that both the increase of DM self-interaction and the SM Higgs mass reduced ϕ_c and increased T_c, and thus weakened the strength of the phase transition. In particular, T_c increased very quickly with the Higgs mass and we found an upper bound on the Higgs boson mass which is now compatible with the observation.

$$m_h \lesssim 130\,\text{GeV}\ . \tag{4.68}$$

In short, the scalar doublet DM can trigger the strong electroweak phase transition, as long as it is light, below 80 GeV or so, and its partners end up being heavier.

Complex Triplet

The thermal mass for the Higgs and Goldstone fields are

$$m_h^2(\phi,T) = -\mu^2+3\lambda_1\phi^2+a\frac{T^2}{12} \tag{4.69}$$

$$m_{G^\pm}^2 = m_{G^0}^2 = -\mu^2+\lambda_1\phi^2+a\frac{T^2}{12} \tag{4.70}$$

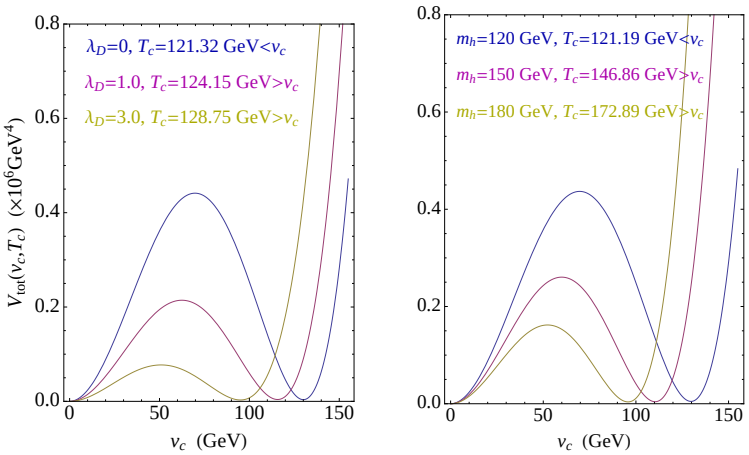

Figure 4.3: Shape of the Higgs potential at the critical temperature and its dependence on different choices of parameters: DM self-interaction λ_D (left panel) and SM Higgs boson mass m_h (right panel). While varying λ_D, we have fixed $m_h = 120\,\text{GeV}$, $m_S = 60\,\text{GeV}$, $m_A = m_C = 300\,\text{GeV}$ and while varying m_h, we have fixed $\lambda_D = 0$, $m_S = 76\,\text{GeV}$, $m_A = m_C = 300\,\text{GeV}$, respectively. Taken from [27].

And thermal masses for the component fields of the triplet are

$$m_S^2(\phi,T) = m_A^2(\phi,T) = M_\Delta^2 + \frac{1}{2}(\alpha + \frac{1}{2}\beta)\phi^2 + b\frac{T^2}{12} \tag{4.71}$$

$$m_{\Delta^+}^2(\phi,T) = M_\Delta^2 + \frac{1}{2}\alpha\phi^2 + b\frac{T^2}{12} \tag{4.72}$$

$$m_{\Delta^{++}}^2(\phi,T) = M_\Delta^2 + \frac{1}{2}(\alpha - \frac{1}{2}\beta)\phi^2 + b\frac{T^2}{12} \tag{4.73}$$

Here the thermal coefficients a and b are,

$$a = 6\lambda_1 + 3\alpha + \frac{9}{4}g^2 + \frac{3}{4}g'^2 + 3y_t^2 \tag{4.74}$$

$$b = 8\lambda_2 + 6\lambda_3 + 2\alpha + 6g^2 + 3g'^2 \tag{4.75}$$

Also, M_Δ and λ_2 are denoting common mass term and self quartic coupling of the inert complex triplet respectively. So the effective potential is

$$\begin{aligned} V_{eff}(\phi,T) &= \frac{1}{2}(-\mu^2+a\frac{T^2}{12})\phi^2+\frac{\lambda_1}{4}\phi^4+\sum_i(\pm)g_i\frac{m_i(\phi)^4}{64\pi^2}\left[\ln\frac{m_i^2(\phi)}{Q^2}-c_i\right] \\ &- \frac{T}{12\pi}\sum_B g_B[m_B^2(\phi,T)]^{3/2}-\sum_B\frac{m_B^4(\phi,T)}{64\pi^2}\ln\frac{m_B^2(\phi,T)}{A_bT^2} \\ &+ 12\frac{m_t^4(\phi)}{64\pi^2}\ln\frac{m_t^2(\phi)}{A_fT^2} \end{aligned} \tag{4.76}$$

where bosonic sum is taken over, h, $G^\pm$, G^0, Δ^{++}, Δ^+, Δ^0, $W^\pm$ and Z with corresponding degrees of freedom, g_i are $\{h, G^\pm, G^0, \Delta^{++}, \Delta^+, \Delta^0, W^\pm, Z, t\} = \{1, 2, 1, 2, 2, 2, 6, 3, 12\}$. Also Q is the renormalization scale and in $\overline{MS}$ scheme, $\{c_S, c_F, c_{GB}\} = \{3/2, 3/2, 5/6\}$.

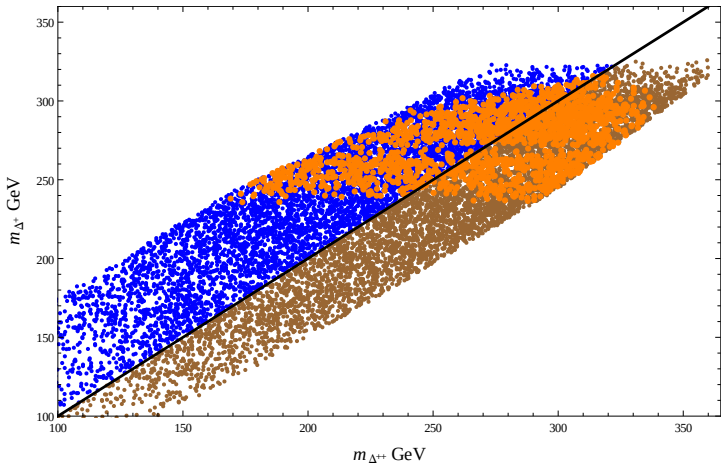

Figure 4.4: Correlation between $m_{\Delta^{++}}$ and m_{Δ^+} in the inert complex triplet model. We have scanned the parameter space: $M \in (10, 150)$ GeV, $\alpha \in (0, 3)$, $\lambda_{2,3} \in (0, 0.01)$ and $|\beta| \in (0, 2)$. Here for $\beta < 0$ (brown points) we have $m_{\Delta^0} < m_{\Delta^+} < m_{\Delta^{++}}$ and strong EWPhT region (orange points) lies for $m_{\Delta^{++}} \sim 250 - 340$ GeV. For $\beta > 0$ (blue points) the mass hierarchy is opposite and strong EWPhT region (orange points) lies for $m_{\Delta^{++}} \sim 170 - 315$ GeV. In random scan, for $\beta > 0$ and $\beta < 0$, out of initial 10^4 points, 8.54% and 8.79% points which are consistent with stability conditions and electroweak precision data (EWPD) showed strong EWPhT respectively. The straight line represents $m_{\Delta^{++}} = m_{\Delta^+}$. Taken from [144].

In the above analysis, Z_2 symmetry is retained but one can introduce the term $\mu\Phi^T\epsilon\Delta^\dagger\Phi$ which breaks Z_2 symmetry softly, which happens, for

example, in the type-II seesaw model. Such term will induce a triplet vev, $\langle\Delta^0\rangle = v_\Delta$ where $v_\Delta = \frac{\mu v^2}{\sqrt{2}M_\Delta^2}$. As indicated in [194], such term will modify the Higgs quartic coupling to $\frac{\lambda_1}{4} \to \frac{\lambda_1}{4} - \frac{\mu^2}{2M_\Delta^2}$ which in turn, will reduce the effective Higgs quartic coupling and enhance the strength of the transition. The upper bound of v_Δ set by precision measurement of ρ parameter, is $2.5 - 4.6$ GeV [195] and lower bound is 10^{-10} GeV set by the neutrino mass [197]. Now from inequality Eq.(4.59), one can see that strong 1st order EWPhT favors $M_\Delta \leq T_c \sim 100 - 120$ GeV. Therefore, μ will lie within the range $10^{-11} \leq \mu \leq 1.5$ GeV. Hence, the correction to the Higgs quartic coupling is about $O(10^{-3})$ so it is negligible and does not quantitatively change the transition which is mostly driven by large α coupling of the potential. Also correction to the mass spectrum due to non zero μ term (therefore, nonzero v_Δ) is $O(\frac{v_\Delta^2}{v^2})$ and thus very small. So EWPhT results obtained in Z_2 symmetric triplet case also holds for softly broken Z_2 symmetric model.

In [196], for like-sign dilepton final states with 100% branching ratio at 7 TeV LHC run, the lower limit on mass of the doubly charged scalar was put as 409 GeV, 398 GeV and 375 GeV for $e^\pm e^\pm$, $\mu^\pm\mu^\pm$ and $e^\pm\mu^\pm$ final states. But as pointed out in [197] the mass limit crucially depends on the value of v_Δ and the di-leptonic decay channel $\Gamma_{\Delta^{++}\to l_i l_j}$ is dominant only when $10^{-10} \leq v_\Delta \leq 10^{-5} - 10^{-4}$ GeV and when $v_\Delta = 10^{-4} - 10^{-3}$ it becomes comparable to $\Gamma_{\Delta^{++}\to W^+W^+}$. Also for mass difference $\Delta M = m_{\Delta^{++}} - m_{\Delta^+} \geq 5$ GeV and $v_\Delta \geq 10^{-4}$ GeV, cascade decay is the most dominant decay channel ($\beta < 0$). Therefore when $v_\Delta \sim 4 \times 10^{-5}$ GeV, di-leptonic branching ratio is around 11% and lower limits on $m_{\Delta^{++}}$ are 212 GeV (e^+e^+), 216 GeV ($\mu^+\mu^+$) and 190 GeV ($e^+\mu^+$)[6] which is still compatible with strong EWPhT region shown in Fig.(4.4). Moreover, for $v_\Delta \geq 10^{-4}$ the limit goes down all the way to $m_{\Delta^{++}} \geq 100$ GeV and thus again compatible with strong EWPhT region.

Quartet representation

In case of quartet representation, the thermal mass for the Higgs and Goldstone fields are

$$m_h^2(\phi, T) = -\mu^2 + 3\lambda_1\phi^2 + a_q\frac{T^2}{12} \tag{4.77}$$

$$m_{G^\pm}^2 = m_{G^0}^2 = -\mu^2 + \lambda_1\phi^2 + a_q\frac{T^2}{12} \tag{4.78}$$

[6]Table.1 of [196]

And for quartet, the thermal mass for the component fields are

$$
\begin{aligned}
m_S^2(\phi,T) &= M_Q^2+\frac{1}{2}(\alpha+\frac{1}{4}\beta-2\gamma)\phi^2+b_q\frac{T^2}{12} && (4.79)\\
m_A^2(\phi,T) &= M_Q^2+\frac{1}{2}(\alpha+\frac{1}{4}\beta+2\gamma)\phi^2+b_q\frac{T^2}{12} && (4.80)\\
m_{Q^{++}}^2(\phi,T) &= M_Q^2+\frac{1}{2}(\alpha-\frac{3}{4}\beta)\phi^2+b_q\frac{T^2}{12} && (4.81)\\
m_{Q_1^+}^2(\phi,T) &= M_Q^2+\frac{1}{2}(\alpha+\frac{1}{4}\beta-\frac{1}{2}\sqrt{\beta^2+12\gamma^2})\phi^2+b_q\frac{T^2}{12} && (4.82)\\
m_{Q_2^+}^2(\phi,T) &= M_Q^2+\frac{1}{2}(\alpha+\frac{1}{4}\beta+\frac{1}{2}\sqrt{\beta^2+12\gamma^2})\phi^2+b_q\frac{T^2}{12} && (4.83)
\end{aligned}
$$

The thermal coefficients a_q and b_q are,

$$
\begin{aligned}
a_q &= 6\lambda_1+4\alpha+\frac{9}{4}g^2+\frac{3}{4}g'^2+3y_t^2 && (4.84)\\
b_q &= 10\lambda_2+\frac{15}{2}\lambda_3+2\alpha+\frac{45}{4}g^2+\frac{3}{4}g'^2 && (4.85)
\end{aligned}
$$

Here, M_Q and λ_2 are denoting common mass term and self quartic coupling of the quartet respectively. Similarly the thermal potential is

$$
\begin{aligned}
V_{eff}(\phi,T) &= \frac{1}{2}(-\mu^2+a_q\frac{T^2}{12})\phi^2+\frac{\lambda_1}{4}\phi^4+\sum_i(\pm)g_i\frac{m_i(\phi)^4}{64\pi^2}\left[\ln\frac{m_i^2(\phi)}{Q^2}-c_i\right]\\
&- \frac{T}{12\pi}\sum_B g_B[m_B^2(\phi,T)]^{3/2}-\sum_B\frac{m_B^4(\phi,T)}{64\pi^2}\ln\frac{m_B^2(\phi,T)}{A_bT^2}\\
&+ 12\frac{m_t^4(\phi)}{64\pi^2}\ln\frac{m_t^2(\phi)}{A_fT^2} && (4.86)
\end{aligned}
$$

where bosonic sum is taken over, h, $G^\pm$, G^0, Q^{++}, Q_1^+, Q_2^+, S, A, $W^\pm$ and Z with corresponding degrees of freedom, $\{h,G^\pm,G^0,Q^{++},Q_1^+,Q_2^+,S,A,W^\pm,Z,t\}=\{1,2,1,2,2,2,1,1,6,3,12\}$.

Expansion parameter One also has to keep in mind the validity of finite temperature perturbation expansion. In case of the Standard Model, the first order phase transition is dominated by the gauge bosons but for the case of inert doublet, complex triplet or quartet, the phase transition is mainly driven by new scalar couplings to the Higgs. Therefore, we can safely neglect the gauge boson contribution. As an illustration, we can see by simplifying Eq.(4.51) and Eq.(4.53) that if the effective scalar coupling, α_S is responsible for the transition, in the region near the symmetry breaking

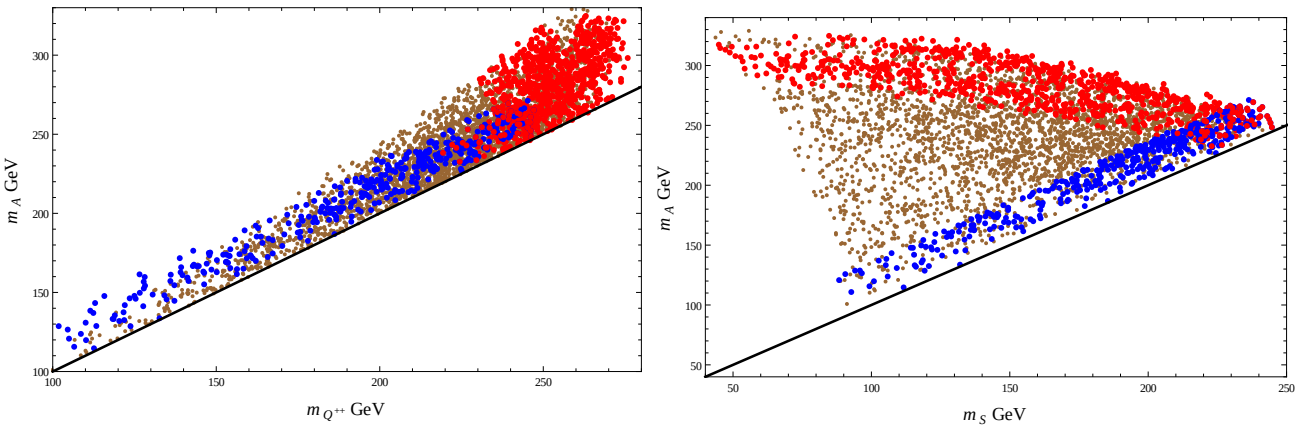

Figure 4.5: Correlation between (left fig.) $m_{Q^{++}}$ and m_A and (right fig.) m_S and m_A in the quartet model. We have scanned the parameter space: $M \in (0, 60)$ GeV, $\lambda_{2,3} \in (0, 0.01)$, $\alpha \in (0, 2)$, $|\beta| \in (0, 1.5)$ and $\gamma \in (0, 1.5)$. Out of initial 10^5 models, for $\beta > 0$ (blue points in left and right fig.), 0.43% points satisfy stability conditions + precision data and mass hierarchy when considering S to be dark matter where as for $\beta < 0$ (brown points in both fig.), 3.47% points satisfy the same bounds. In addition, for $\beta > 0$ and $\beta < 0$, strong EWPhT condition (red points in both figures) is satisfied by 0.04% points with $m_{Q^{++}} \sim 200 - 250$ GeV and $m_A \sim 230 - 270$ and 0.8% points with $m_{Q^{++}} \sim 230 - 275$ GeV and $m_A \sim 235 - 320$ respectively. The straight line in left fig. represents $m_{Q^{++}} = m_A$ and in right fig., $m_S = m_A$. Taken from [144].

minimum, $\phi/T \sim \alpha_S^{3/2}/\lambda_1$. The thermal mass of the corresponding particle is,

$$m_S^2(\phi, T) = M^2 + \frac{1}{2}\alpha_S\phi^2 + \Pi(T) \tag{4.87}$$

Additional loop containing scalar will cost a factor $\sim \alpha_S T$ and loop expansion parameter can be obtained by dividing this factor with the leading mass of the theory which in this case is the mass of the new scalar; $\beta \sim \frac{\alpha_S T}{m_S}$. Now only in the limit, $M^2 + \Pi(T) \ll \alpha_S\phi^2$, we have, $\beta \sim \sqrt{\alpha_S}\frac{T}{\phi}$ or, near the region of minimum, $\beta \sim \frac{\lambda_1}{\alpha_S} \sim \frac{m_h^2}{m_S^2}$. Therefore, perturbation makes sense only for $\lambda_1 < \alpha_S$ or $m_h < m_S$. On the other hand if $M^2 + \Pi(T)$ term is significantly larger, it will reduce the order parameter and eventually transition will cease to be first order. In the case of complex triplet, from Fig.(4.4), the 1st order EWPhT occurs for region: $m_{\Delta^{++}} \sim 170 - 340$ GeV. And for the quartet, from Fig.(4.5), first order EWPhT region is: $m_{Q^{++}} \sim 200 - 275$ GeV and $m_A \sim 230 - 320$ GeV. Therefore we can see that for both cases,

the mass regions where first order transition occurs are larger than the Higgs mass and hence, within the validity of perturbation theory.

Other uncertainties? So far, we have worked in the improved one-loop approximation for the effective potential at non-zero temperature, and so one can question its reliability at higher orders in the perturbation theory. In fact, in the MSSM, it turns out that the two-loop effects [198] help to strengthen the phase transition. Similarly, the non-perturbative lattice simulations tend to do the same over the perturbative results [199].

4.2.3 Impact of multiplets' sizes on EWPhT

Latent heat release The phase transition is characterized by the release of latent heat. If there is a latent heat release, the transition is first order in nature otherwise it is second or higher order (as in Ehrenfest's classification). The nature of cosmological phase transition is addressed in [200, 201]. In this section, we have addressed how the size of the representation affects the latent heat release during the electroweak phase transition with assumption that the transition is first order driven by large Higgs-inert scalar coupling, i.e. α. Consider a system gone through first order phase transition at temperature, T_c. The high temperature phase consists of radiation energy and false vacuum energy and energy density is denoted as ρ_+. On the other hand, although low temperature phase has equal free energy F it will have different energy density, ρ_-. The discontinuity $\Delta\rho(T_c) = \rho_+(T_c) - \rho_-(T_c)$, gives the latent heat, $L = \Delta\rho(T_c) = T_c\Delta s(T_c)$ where $\Delta s(T_c) = s_+ - s_-$ is entropy density difference and it is liberated when the region of high-T phase is converted into the low-T phase. Therefore, using $F = \rho - Ts$ with $s = -\frac{dF}{dT}$ and from expression for effective potential (equivalent to free energy), Eq.(4.44) and as for 1st order phase transition, $F_+(0, T_c) = F_-(\phi_c, T_c)$, we have the latent heat for the transition,

$$L = T\frac{dF_-}{dT}|_{(\phi_c,T_c)} - T\frac{dF_+}{dT}|_{(0,T_c)} \tag{4.88}$$

For simplicity we can again take real degenerate representation for probing the impact of dimension of large multiplet on the latent heat release. As the amount of latent heat represents the strength of first order transition, it is already clear from Fig.(4.6) that larger representation disfavors first order phase transition. In addition, in section 4.1.3 we have seen that arbitrarily large scalar multiplet makes gauge and scalar couplings non-perturbative in TeV or even at smaller scale. Therefore, larger scalar multiplet cannot simultaneously strengthen the electroweak phase transition and stay consistent

with perturbativity and unitarity of the theory. Similar conclusion can be drawn for complex even integer and half integer multiplets.

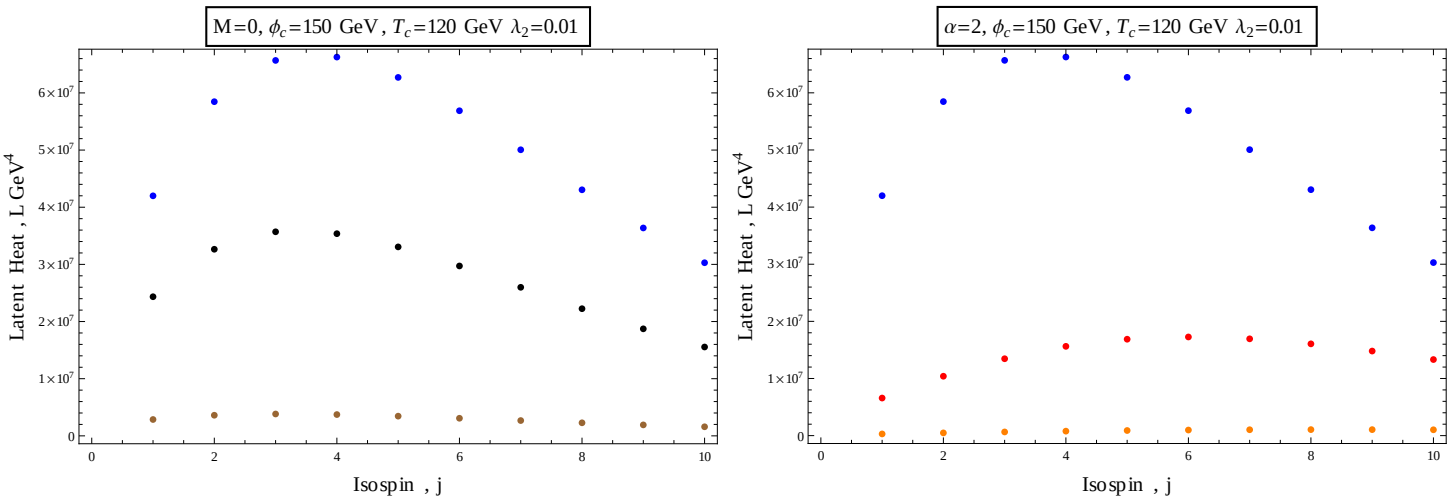

Figure 4.6: In the left graph, latent heat decreases when isospin increases; blue, black and brown dots represents α =2, 1 and 0.1 respectively. On the right, we can see again the reduction of latent heat with isospin for invariant mass term, $M = 0$ (blue), 500 (red) and 1000 (orange) GeV respectively.

Latent heat and Φ_c/T_c Though the correspondence between the latent heat and ϕ_c/T_c is not straightforward, we can use the simplified form of the effective potential to show the correlation manifestly. The potential Eq.(4.51) is re-written in the following way,

$$\tilde{V}_T(\phi, T) = \frac{a(j)}{12}(T^2 - T_0^2)\phi^2 - y\tilde{\beta}(j)T\phi^3 + \frac{1}{4}\lambda_1\phi^4 \tag{4.89}$$

where, $\tilde{\beta}(j) = \frac{2j+1}{12\pi}(\frac{\alpha}{2})^{\frac{3}{2}}$ and $T_0^2 = \frac{6\mu^2}{a(j)}$ is the second order transition temperature. y parameterizes the cubic thermal term in such a way that, when $\phi \gg K(T)$, $y \sim 1$ and when $\phi \ll K(T)$, $y \sim 0$. Now from Eq.(4.89), using the conditions for first order transition we have, $\frac{\phi_c}{T_c} = \frac{3y\tilde{\beta}(j)}{2\lambda_1}$ and Eq.(4.88) immediately gives,

$$L = T_c^4 \frac{\phi_c^2}{T_c^2}\left(\frac{a(j)}{6} - 3y\tilde{\beta}(j)\frac{\phi_c}{T_c}\right) \tag{4.90}$$

From Eq.(4.90), we can see that, latent heat becomes negative for larger multiplets but it is defined as a non-negative quantity in Eq.(4.88). Therefore,

with increasing size of the multiplet, j, the ratio, $\frac{\phi_c}{T_c}$ has to be decreasing (< 1) to keep L non-negative and thus unable to satisfy the strong EWPhT condition, $\frac{\phi_c}{T_c} \geq 1$, relevant for electroweak baryogenesis. Evaluating L using full thermal integrals will lead to results of Fig.(4.6). So we can see from this example that, latent heat measure can be a complement to ϕ_c/T_c for studying the impact of larger representations on the EWPhT.

4.3 Interplay between EWPhT and CDM constraints in the Inert Doublet

4.3.1 The inert doublet as dark matter

The neutral component of the inert doublet, S is considered as a thermal DM candidate, as in the conventional WIMP picture. The main processes governing the freeze out include annihilation into gauge bosons W, Z and to fermions via the Higgs boson exchange. It has been shown in [44] that the WMAP already puts strong constraints on the viable parameter space.

The spin independent cross section is given by,

$$\sigma_{SI} = \frac{\lambda_S^2 f^2}{4\pi} \frac{\mu^2 m_n^2}{m_h^4 m_S^2} \tag{4.91}$$

Here, $\mu = m_n m_s/(m_n + m_s)$ is the DM-nucleon reduced mass. f parameterizes the nuclear matrix element, $\sum_{u,d,s,c,b,t} \langle n|m_q \bar{q} q|n\rangle \equiv f m_n \bar{n} n$ and from recent lattice results [206], $f = 0.347131$. XENON100 with 100 days live data [207] set bound on cross section to be $\sigma_{SI} \lesssim 7 \times 10^{-45}\text{cm}^2$. From section 4.2.2, we can see that A and C are much heavier than S. So in this case, their roles in thermal freeze out and direct detection are safely negligible.

The combined limit from both relic density and direct detection experiments seen in Fig.(4.7) indicates that the DM mass lies approximately between $45-80\,\text{GeV}$ [35]. Here $m_h = 120$ GeV was used, the present value of 126 GeV does not change the results significantly as will be seen the CDM study for quartet. In the above favored DM mass window, XENON100 also put tight constraint on the interaction between DM and the Higgs boson,

$$\lambda_S \lesssim 0.1 \ . \tag{4.92}$$

A useful constraint follows from the above results. The mass spectrum in Eq.(4.9) leads to $\gamma \approx \beta/2$, when $m_A \approx m_C \gg m_S$, up to corrections of order $10\,\%$. Furthermore, the mono-chromatic gamma ray line from DM annihilation in the galaxy could also serve as a promising indirect detection

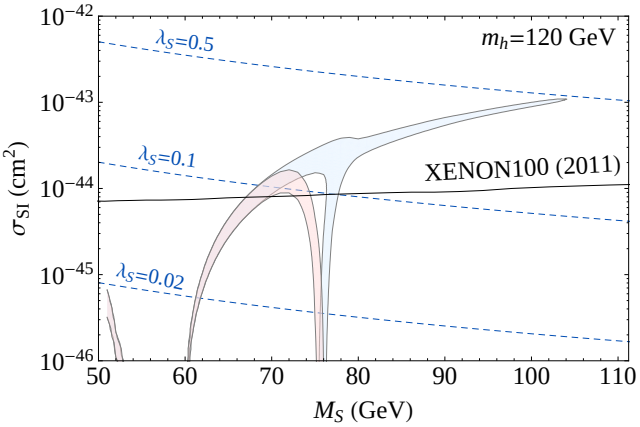

Figure 4.7: Spin-independent direct detection cross section on nucleon plotted as a function of the DM mass. Colored regions represent DM relic density favored by WMAP, $\Omega_{\rm DM}h^2 \in (0.085, 0.139)$ at 3σ, for positive (red) and negative (blue) λ_S. We have taken SM Higgs mass $m_h = 120\,\text{GeV}$. The lower limit on the direct detection cross section from XENON100 experiment is shown by the black solid line. Also shown in the figure are the dashed curves for constant $|\lambda_S|$. Taken from [27].

of DM. In this model, the flux is predicted [35] to lie only a factor of 4−5 below the current Fermi-LAT limit.

4.3.2 Interplay between EWPhT and CDM constraints

After identifying the CDM constraints on the inert doublet, we try to identify the interplay between strong EWPhT condition and DM properties of inert doublet. As pointed out in section 4.2.2, the ϕ-independent terms in the thermal masses of A and C introduce plasma screening and these had to be small enough in order not to dilute their contribution to the thermal cubic term which drives the transition. Namely, the optimal situation is realized when the following term,

$$M_D^2 + \frac{T_c^2}{12}\left[6\lambda_D + \frac{m_S^2+m_A^2+2m_C^2-4m_D^2}{\phi_c^2} + \frac{9g^2+3g'^2}{4}\right] \tag{4.93}$$

is minimized at the critical temperature. For a given mass spectrum, this means that there is a window for M_D^2 where the phase transition could be strongly first order. Since S shares the same M_D^2 contribution to the mass as its heavier partners, i.e., $M_D^2 = m_S^2 - \lambda_S v^2/2$, it in turn predicts a lower bound on the DM direct detection rate, as shown in Fig. 4.8. This is an important

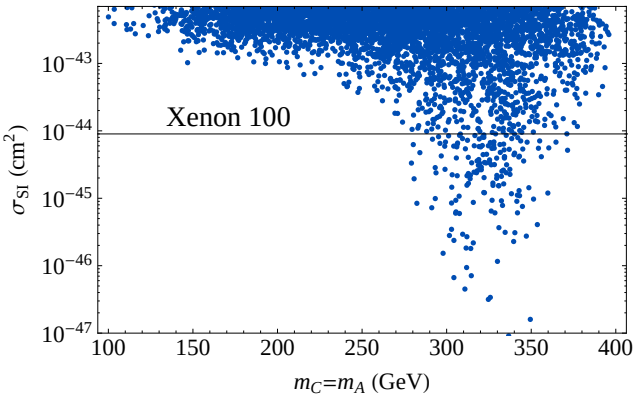

Figure 4.8: Correlation between spin-independent direct detection cross section and the mass of the charged scalar, after imposing the strong electroweak transition condition $\phi_c/T_c > 1$. We have scanned the parameter space: $m_h \in (115, 200)\,\text{GeV}$, $m_S \in (40, 80)\,\text{GeV}$, $m_A \in (100, 500)\,\text{GeV}$, $m_C \in (m_A - 10\,\text{GeV}, m_A + 10\,\text{GeV})$, $\lambda_S \in (0, 1)$ and $\lambda_D \in (0, 3)$. We veto points where the thermal mass of A or C exceeds $1.8\,T_c$, which would invalidate the high temperature expansion. Taken from [27].

result in view of the upper bound set by XENON100, which constrains the masses of A and C to lie in a window between $270-350\,\text{GeV}$.

This mass window of heavy scalar masses can be probed by the LHC. In particular, the pseudo-scalar component A can be produced in association with the DM S, and leads to dilepton final state with missing energy. Here, the preferred mass difference between A and S is larger than the sample values studied in [51], which makes it easier to be distinguished from the SM background by imposing a harder cut on the missing energy.

Why not a singlet? Before turning to higher representations, let us discuss explicitly the case of the singlet DM. After all, this is a simpler possibility with fewer couplings and thus more constrained. In fact, it fails to do the job. More precisely, while the singlet by itself can actually help the phase transition to be of the first order [17], it cannot simultaneously be the DM [210], and vice versa.

What happens is the following. In this case, there is only one coupling with the Higgs and $\lambda_A \equiv \lambda_C \equiv \lambda_S$. We survey all the points in Fig. 4.8 and find they all satisfy $\lambda_{A,C} \gtrsim 1$. On the other hand, direct detection, as shown in Eq. (4.92), constrains this coupling to be much smaller than what is needed to trigger a strong first-order phase transition. The failure of the

real singlet thus makes the choice of the inert doublet scalar the simplest one. One can further extend the real scalar singlet case to a complex one. It was shown [63] that the double job of dark matter and strong electroweak phase transition can be achieved in this case.

4.4 The Quartet/Doublet versus EW, EWPhT and CDM constraints.

In this section, we have tried to identify the region of parameter space for higher representations where one can have a light DM candidate consistent with other phenomenological constraints along with strong EWPhT. As already pointed out in section (4.1.2), the DM of complex even integer multiplet ($Y \neq 0$) is excluded by the bound from the direct detection. On the other hand, the γ term of Eq.(4.1) can split the neutral component of half integer representation and one can easily obtain a light DM component. As quartet multiplet ($j = 3/2$) is the immediate generalization of the inert doublet, we have focused on identifying DM properties in parallel with its impact on strong EWPhT.

4.4.1 Model parameters scan and constraints

The masses of quartet's component fields are determined by four free parameters $\{M_Q, \alpha, \beta, \gamma\}$, Eq.(4.13). But (co)annihilation cross sections which control the relic density of the dark matter depend on the mass splittings among the dark matter and the other components in the multiplet. Therefore we used alternative free parameter set $\{m_S, \lambda_S, m_{Q^{++}}, m_A\}$ where m_S is the DM mass and $\lambda_S = \alpha + \frac{1}{4}\beta - 2\gamma$ is the coupling between the Higgs and dark matter component. One can express $\{M_Q, \alpha, \beta, \gamma, m_{Q_1^+}, m_{Q_2^+}\}$ in terms of these four parameters using mass relations Eq.(4.13). Moreover, in the case of quartet, for S to be the lightest component of the multiplet, one needs to impose two conditions, $\gamma > 0$ and $\gamma \geq \frac{|\beta|}{2}$ which in turn sets the mass spectrum to be $m_S < m_{Q_1^+} < m_{Q^{++}} < m_{Q_2^+} < m_A$.

Collider constraints:

Direct collider searches at LEP II has put a strong bound on single charged particle which is $m_{Q_1^+} > 70 - 90$ GeV [203]. But the doubly charged scalar of the quartet which only has the cascade decay channel is not strongly constrained by collider searches. One constraint can come from W and Z boson width. In our case, setting S as DM imposes in the mass spectrum:

$m_{Q^{++}} \geq m_{Q_1^+}$, so the constraint on the single charged scalar is also translated into a bound on the doubly charged scalar for such mass spectrum. Moreover, the deviations of W and Z width from their SM values can take place through decay channels: $W^\pm \to SQ_1^\pm / AQ_1^\pm / Q^{\pm\pm}Q_1^\mp$ and $Z \to Q_1^+Q_1^- / SA / Q^{++}Q^{--}$. Therefore to avoid such deviation the following mass constraints are also imposed: $m_S + m_{Q_1^+} > m_W$, $m_A + m_{Q_1^+} > m_W$, $m_{Q^{++}} + m_{Q_1^+} > m_W$, $m_{Q_1^+} > m_Z/2$, $m_{Q^{++}} > m_Z/2$ and $m_S + m_A > m_Z$. Apart from collider constraints, one also impose constraints coming from electroweak precision observables. In our scan, we used the allowed range of T parameter, Eq.(4.39) and S parameter, Eq.(4.41).

DM relic density constraint:

The dark matter density of the universe measured by Planck collaboration is $\Omega_{DM}h^2 = 0.1196 \pm 0.0031$ (68% CL) [9]. To determine the relic density of the multiplets, we used FeynRules [205] to generate the model files for MicrOMEGAs [211]. For inert multiplets, mass splitting between components are set by both β and γ couplings. In case of doublet, one can set β and γ to produce large spitting between S component and single charged component C^+ or between S and A in such way that such splitting is compatible with electroweak precision observables. Such large splitting can lead to suppression of co-annihilation channels $SA, SC^+ \to$ SM particles. But such simple tuning of the couplings like in the doublet is not possible for quartet because of the mass relation Eq.(4.13). Therefore there is a possibility for co-annihilation channel to open up when $m_{Q_1^+}/m_S \leq 1.5$ ([204]).

Apart from co-annihilation, other dominant channels which will control the relic density of DM at the low mass region are $SS \to h^* \to b\bar{b}$ and $SS \to WW$.

Direct DM detection and invisible Higgs decay constraints:

The updated direct detection limit on the spin independent DM-nucleon cross section is set by XENON100 with 225 days live data [208] where $\sigma_{SI} \lesssim 2 \times 10^{-45}\text{cm}^2$. In addition, the future XENON1T will reach the sensitivity of $\sigma_{SI} \lesssim 2 \times 10^{-47}\text{cm}^2$ [209].

Also if the mass of the dark matter is smaller than half of the Higgs mass, it will contribute to the invisible decay of the Higgs through $h \to SS$ with branching ratio $Br_{\text{inv}} = \Gamma_{\text{inv}}/(\Gamma_{\text{SM}} + \Gamma_{\text{inv}})$, where $\Gamma_{\text{SM}} = 6.1$ MeV and,

$$\Gamma_{inv} = \frac{\lambda_S^2 v^2}{64\pi m_h}\sqrt{1 - \frac{4m_S^2}{m_h^2}} \tag{4.94}$$

Consequently, current limit on the branching ratio for Higgs invisible decay [202] will constrain the λ_S coupling. However, note that as can be seen in Fig.(4.9), the limit imposed on λ_S by XENON100 is more stringent than the limit coming from invisible Higgs decay for mass range $45 \leq m_S \leq 63$ GeV.

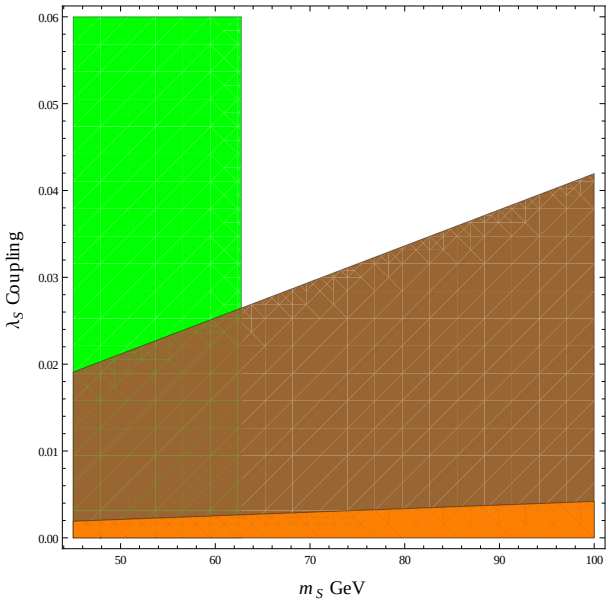

Figure 4.9: The region in $m_S - \lambda_S$ plane allowed by invisible branching ratio limit $Br_{inv} \leq 0.65$ (green region) and XENON100 limit (brown region) and XENON1T limit (orange region) respectively for DM mass range $45 \leq m_S \leq 100$ GeV. The future XENON1T will significantly reduce the allowed region down to $0.002 \lesssim \lambda_S \lesssim 0.004$ for $m_S = 45 - 100$ GeV. Taken from [144].

4.4.2 Allowed parameter regions

To determine the allowed parameter region for the quartet and compare it with the inert doublet case, we used dark matter relic density constraint at 5σ to take into account all the numerical uncertainties. For numerical scanning, we considered the following range: $m_S \in (45, 100)$ GeV, $\lambda_S \in (0.001, 0.02)$, $m_{Q^{++}} \in (100, 350)$ GeV and $m_A \in (100, 350)$ GeV for both doublet and quartet case.

At low mass region ($m_S \leq m_W$), the dominant annihilation channel is $SS \to h^* \to b\bar{b}$. When the mass becomes larger than m_W and m_Z, $SS \to W^+W^-$ and $SS \to ZZ$ open up and dominate the annihilation rate.

Therefore the relic density becomes much lower than the observed relic density. Subsequent increase of m_S will open up $SS \to hh$ and $SS \to t\bar{t}$ which will dominate along with WW and ZZ annihilation channels and eventually the relic density will be much smaller than observed value. The inert doublet has already shown such behavior [35, 44].

From scatter plot, Fig.(4.10) we can see that, unlike the doublet case, for the quartet, the parameter space allowing both light DM consistent with observed relic density and strong first order phase transition is hard to achieve. Out of initial 10^5 models, for the doublet, 20% are consistent with stability conditions + precision data+ collider constraints, 0.77% satisfy, in addition, the EWPhT condition $\phi_c/T_c \geq 1$ and 0.234% agree with the observed $\Omega_{DM}h^2$ at 5σ, DM direct detection bounds and invisible Higgs decay limits. Only 0.02% of the initial models survive all the constraints. In contrast, for the quartet, from an initial of 10^5 models only 2% satisfy stability conditions + EWPD +collider constraints, 0.13% points satisfy additional strong EWPhT condition and only 0.03% models, observed $\Omega_{DM}h^2$ at 5σ and direct detection bounds. Lastly, only 0.003% models satisfied all the conditions. Therefore, in case of providing strong EWPhT with a light dark matter, the quartet is disfavored with respect to the doublet.

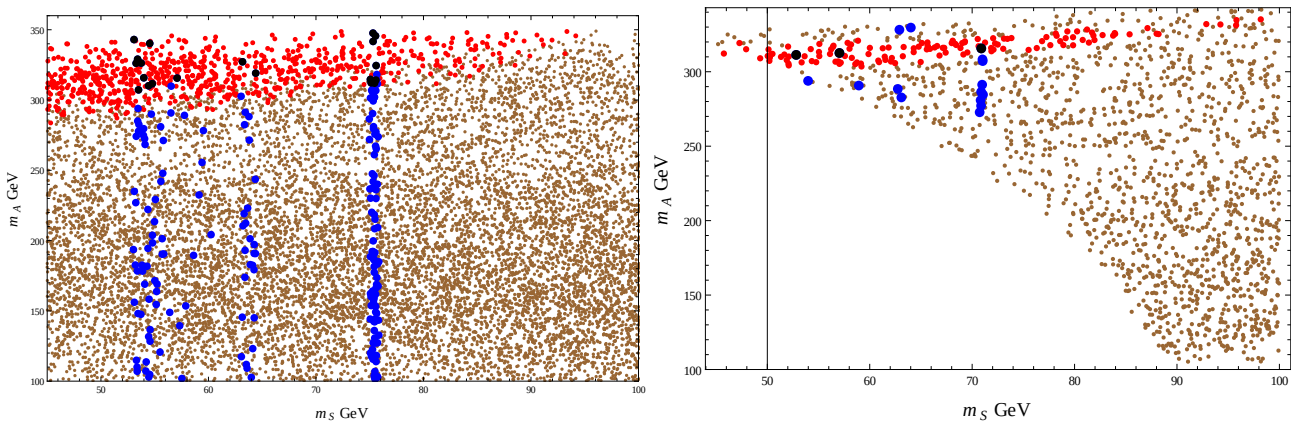

Figure 4.10: Scatter plot representing the correlation between m_S and m_A for doublet(left fig.) and quartet (right fig.). Brown points represent models satisfying stability conditions + precision bounds+collider constraints. Red points correspond to models also satisfying the EWPhT condition $\phi_c/T_c \geq 1$ and blue points correspond to models consistent only with observed relic density at 5σ and DM direct detection and invisible Higgs decay bounds. Black points are models consistent with stability conditions + EWPD + collider constraints + the EWPhT condition $\phi_c/T_c \geq 1$ + observed $\Omega_{DM}h^2$ + DM direct detection and invisible Higgs decay limits. Taken from [144].

4.5 Summary

The combination of the electroweak constraints with the results of EWPhT and dark matter properties for the inert doublet and the quartet has pointed out that the inert quartet provides much smaller region of parameter space compared to the doublet in this class of models. Therefore, the inert doublet can be a more plausible candidate for the dark matter which simultaneously provides strong first order EWPhT in the universe.

Chapter 5

Conclusions and outlook

We have considered the electroweak phase transition and dark matter phenomenology with various inert scalar representations used for extending the SM's Higgs sector. The details of the phenomenological studies are done by making random scans of parameters within the triplet and quartet context. The results from our analyses in comparing the allowed parameter regions of the above mentioned models with the inert doublet model case are summarized as follows

- As the size of an inert multiplet which can be added to the SM is not arbitrary but is rather controlled by the perturbativity of SU(2) gauge coupling at TeV scale ($\sim$ 10 TeV), which sets an upper bound on the size of the multiplet to be $j \leq 5$, that motivated us to study the EWPhT (and subsequently, the DM characteristics) for inert doublet, triplet and quartet models as representatives for allowed larger multiplets. We explicitly showed that it is possible to have strong EWPhT within the inert doublet, complex inert triplet and the inert quartet models.

  - In case of inert doublet, from Fig.(4.7), we can see that, the strong EWPhT region: $m_A \equiv m_C \sim 270 - 350$ GeV.
  - For complex triplet, from Fig.(4.4), the 1st order EWPhT occurs for region: $m_{\Delta^{++}} \sim 170 - 340$ GeV.
  - For quartet, from Fig.(4.5), first order EWPhT region is: $m_{Q^{++}} \sim 200 - 275$ GeV and $m_A \sim 230 - 320$ GeV.

- Using the expression for the latent heat measure, we have made a generic study of the impact of higher (than the doublet) scalar multiplets on the strength of electroweak phase transition. The competition between the number of scalar quasiparticles coupled to EW plasma with

large couplings and the screening of those particles resulting from scalar self quartic and gauge boson interaction, which will decouple them from the plasma, determines the strength of the transition. The rise and fall of the latent heat with large multiplet, as shown in Fig.(4.6), qualitatively shows such variation of the EWPhT strength.

- Next we require the simultaneous explanation of EWPhT and the cold DM content of the universe within the doublet and quartet frame. The triplet with $Y = 2$, unlike the half integer representations, is already excluded by the direct detection limit thus can't play any viable role of DM triggering strong EWPhT. For both doublet and quartet cases, we first identified the region of parameter space, out of the randomly scanned parameter points, which allows both strong EWPhT and a light DM candidate by imposing stability conditions, electroweak precision bounds and corresponding experimental limits. Afterwards The parameter regions for doublet and quartet that survive all constraints are compared with each other. Requiring that all the CDM content of the universe is explained by the scalar multiplet then, from the scatter plot Fig.(4.10), it can be seen that the quartet has only a very small allowed parameter space in contrast to inert doublet case. Moreover, the allowed parameter space for having DM with observed relic density and strong EWPhT in both inert doublet and quartet cases will be significantly constrained by future XENON1T experiment.

Why higher multiplets are disfavored The above results combined together point out that the higher inert representations are rather disfavored compared to the inert doublet. In the case of quartet, when masses of doubly charged scalar and pseudoscalar are set to have strong EWPhT (i.e. $m_{Q^{++}} \sim 200 - 275$ GeV and $m_A \sim 230 - 320$ GeV), bounds on electroweak precision variables, specially on T parameter that depends on the mass differences between the components of the multiplet, makes the mass of one of the single charged components comparable with the DM mass and that leads to coannihilation which in turn gives relic density much smaller than the observed value. In addition, the mass of that light charged scalar becomes smaller than the LEP II bound (~ 90 GeV) when all other constraints are combined. Larger allowed multiplets $j = 5/2, 7/2$ also have more than one single charged scalars and similar situation will arise when different constraints will be combined. Therefore it is harder to satisfy strong EWPhT condition, EWPD constraints, collider bounds, observed $\Omega_{DM}h^2$ and DM direct detection constraints simultaneously for higher representations.

The conclusion is qualitative and only valid within the set of experimental

and phenomenological constrains considered. There are however room for doing more in directions we did not consider here:

- The computational and phenomenological machineries are well within reach for making detailed quantitative analyses within Bayesian statistical framework. Using strong EWPhT condition and recent results from relic density measurement, direct and indirect detection limits and collider constraints from LHC, a comparison between the allowed parameter spaces of inert doublet and quartet can be carried out in this Bayesian framework, in a similar manner to the work done for comparing different supersymmetric models [212, 213] and for comparing a single versus multi-particle CDM universe hypotheses [214].

- Higher (than doublet) scalar multiplets have relatively more charged components that couple to the Higgs. As such, they will alter the decay rate of Higgs going to two photons relative to the SM value [215–220]. Persistence of the apparent (given the large uncertainties) excess in the $h \to \gamma\gamma$ data will severely constrain the triplet and quartet parameter regions with EWPhT driven by large positive couplings [221, 222]. This and similar studies will be interesting for establishing the inert multiplets' status and/or prospects within collider phenomenology framework.

- Successful baryogenesis requires CP violation, not only the first order phase transition. It is easy to imagine new sources of CP violation, but the problem then arises as to whether the new physics behind it affects the nature of the phase transition. In this sense, new fermions are more welcome, at least in the perturbative regime, while adding new scalars is less desirable since they may upset the first order phase transition. Of course, there is always a large parameter space where they are innocuous, since even tiny couplings with the SM particles may give enough CP violation.

- Apart from detecting new particles within the mass ranges where they trigger strong first order electroweak phase transition, one could have a more direct consequence of it in the production of gravitational waves [223–226] in the universe.

- Another possibility is the pre-existence of baryon asymmetry in the universe. In order to elucidate this possibility, let us recall the problem in the conventional picture: due to the symmetry restoration at high temperature, the unsuppressed rate of sphaleron transition erase any

original $B + L$ asymmetry unless the $B - L$ or any other conserved charge in the electroweak plasma is non-zero. This, however, is not necessarily true in the BSM physics with enlarged Higgs sector: gauge symmetry may get even more broken at high temperature [75, 79]. For this to happen, it suffices that the cross-term couplings between different scalar multiplets be negative. It may be worthwhile to investigate this possibility; however it requires improving the perturbative results for next-to-leading effects which tend to be large [227].

Appendix A

Mathematical tools

A.1 Properties of $\Gamma(s)$ and $\zeta(s)$

In the following we have collected some properties of $\Gamma(s)$ and $\zeta(s)$ that are used in evaluating thermal integrals.

$$\Gamma(s) = \int_0^\infty dx x^{s-1} e^{-x} \tag{A.1}$$

$$\Gamma(s) = \frac{\Gamma(s+1)}{s} \tag{A.2}$$

$$\begin{aligned}
\Gamma'(1) &= -\gamma_E = -0.57721... \\
\Gamma(\frac{1}{2}) &= \sqrt{\pi} \\
\Gamma'(\frac{1}{2}) &= -\sqrt{\pi}(\gamma_E + 2\ln 2) \\
\Gamma(\frac{1}{2}+\epsilon) &= \sqrt{\pi}(1 - \epsilon(\gamma_E + 2\ln 2) + O(\epsilon^2)) \\
\Gamma(-\frac{1}{2}+\epsilon) &= -2\sqrt{\pi} + O(\epsilon)
\end{aligned} \tag{A.3}$$

$$\zeta(s) = \sum_{n=1}^{\infty} \frac{1}{s^n} \tag{A.4}$$

$$\begin{aligned}
\zeta(0) &= -\frac{1}{2} \\
\zeta'(0) &= -\frac{1}{2}\ln(2\pi) \\
\zeta(s) &= 2^s \pi^{s-1} \sin(\frac{\pi s}{2}) \Gamma(1-s)\zeta(1-s)
\end{aligned} \tag{A.5}$$

For any positive even integer $2n$,

$$\zeta(2n) = \frac{(-1)^{n+1}(2\pi)^{2n}B_{2n}}{2(2n)!} \tag{A.6}$$

where, B_{2n} are the Bernoulli numbers; $B_0 = 1$, $B_2 = 1/6$, $B_4 = -1/30$,...and $B_1 = \pm\frac{1}{2}$, $B_3 = B_5 = 0$,...

$$\zeta(2) = \frac{\pi^2}{6} \; ; \; \zeta(3) = 1.202.. \; ; \; \zeta(4) = \frac{\pi^4}{90} \tag{A.7}$$

Moreover, we also have,

$$\begin{aligned}
\zeta(-1+\epsilon) &= -\frac{1}{12} + O(\epsilon) \\
\zeta(1+\epsilon) &= 2^{1+\epsilon}\pi^{\epsilon}(\sin\frac{\pi}{2}(1+\epsilon))\Gamma(-\epsilon)\zeta(-\epsilon) \\
&= -\frac{1}{\epsilon} + \gamma_E + O(\epsilon) \\
\zeta(3+\epsilon) &\sim \zeta(3) + O(\epsilon) \sim 1.202... + O(\epsilon)
\end{aligned} \tag{A.8}$$

A.2 Some useful integrals

$$I_n^{\pm} = \int_0^{\infty} dx \frac{x^n}{e^x \pm 1} \tag{A.9}$$

$$\begin{aligned}
I_n^- - I_n^+ &= \int_0^{\infty} dx x^n \frac{2}{e^{2x} - 1} \\
&= \frac{1}{2^n}\int_0^{\infty} dy \frac{y^n}{e^y - 1} \\
&= \frac{1}{2^n} I_n^-
\end{aligned}$$

$$I_n^+ = (1 - \frac{1}{2^n}) I_n^- \tag{A.10}$$

Evaluation of I_n^-

$$\begin{aligned} I_n^- &= \int_0^\infty dx \frac{x^n}{e^x - 1} \\ &= \int_0^\infty dx x^n e^{-x}(1 - e^{-x})^{-1} \\ &= \int_0^\infty dx \sum_{m=1}^\infty x^n e^{-mx} \\ &= \sum_{m=1}^\infty \frac{1}{m^{n+1}} \int_0^\infty dy y^n e^{-y} \\ &= \zeta(n+1)\Gamma(n+1) \end{aligned} \tag{A.11}$$

Evaluation by dimensional regularization We define a function $f(m, D, n)$ which is used to evaluate the integrals by dimensional regularization.

$$\begin{aligned} f(m, D, n) &= \int \frac{d^D k}{(2\pi)^D} \frac{1}{(k^2 + m^2)^n} \\ &= \frac{1}{(4\pi)^{D/2}\Gamma(D/2)} \int_0^\infty (k^2)^{\frac{D}{2}-1} \frac{1}{(k^2 + m^2)^n} \\ &= \frac{1}{(4\pi)^{D/2}} (m^2)^{\frac{D}{2}-n} \frac{\Gamma(n - \frac{D}{2})}{\Gamma(n)} \end{aligned} \tag{A.12}$$

When $D = 3 - \epsilon$, we have

$$f(m, 3-\epsilon, n) = \frac{\mu^{-\epsilon}}{(4\pi)^{\frac{3}{2}}} (\frac{4\pi\mu^2}{m^2})^{\frac{\epsilon}{2}} (m^2)^{\frac{3}{2}-n} \frac{\Gamma(n - \frac{3}{2} + \frac{\epsilon}{2})}{\Gamma(n)} \tag{A.13}$$

A.3 Frequency sum

When we deal with loop diagrams in the finite temperature field theory in the imaginary time formalism, we usually need to evaluate the summation given the following

$$\sum_{n=-\infty}^{\infty} \frac{1}{n^2 + y^2} \tag{A.14}$$

where n is even and odd respectively. First we focus on the even n.

Consider a complex function $f(z)$ with the property $|f(z)| \leq \frac{M}{|z|^p}$ where $p > 1$ and M is a constant. $\cot(\frac{\pi}{2}z)$ has poles at $z = 0, \pm 2, \pm 4, ...$ So the

residues of $f(z)\cot(\frac{\pi}{2}z)$ at $z=n$ with n even integer and provided $f(z)$ does not have poles at n,

$$\begin{aligned}\text{Res}_n &= \lim_{z\to n}(z-n)\frac{\cos(\frac{\pi}{2}z)}{\sin(\frac{\pi}{2}z)}f(z) \\ &= \frac{2}{\pi}f(n) \end{aligned} \tag{A.15}$$

If $f(z)=\frac{1}{z^2+y^2}$, the poles are $z=\pm iy$ will give residues

$$\text{Res}_{\pm iy} = -\frac{i}{y}\cot(\frac{i\pi}{2}y) \tag{A.16}$$

Consider the contour integral where the path C circulates the poles of $\cot(\frac{\pi}{2}z)$ and $f(z)$ so

$$\int_C f(z)\cot(\frac{\pi}{2}z)dz = 2\pi i\sum_i \text{Res}_i \tag{A.17}$$

But this contour can be deformed so that the integral will be zero. So we immediately get,

$$\begin{aligned}\sum_{n=-\infty,\text{even}}^{\infty}\frac{1}{n^2+y^2} &= \frac{i\pi}{2y}\cot(\frac{i\pi}{2}y) \\ &= \frac{\pi}{2y}\coth(\frac{\pi}{2}y) \end{aligned} \tag{A.18}$$

where $\coth(x)=i\cot(ix)$ is used.

On the other hand, when $n=\pm1,\pm3,...,$ $\tan(\frac{\pi}{2}n)$ has poles at those values of n. Therefore, following the same line of arguments, we can derive that

$$\sum_{n=-\infty,\text{odd}}^{\infty}\frac{1}{n^2+y^2} = \frac{\pi}{2y}\tanh(\frac{\pi}{2}y) \tag{A.19}$$

We will use the following two simplifications of $\coth(x)$ and $\tanh(x)$,

$$\coth(x) = 1+\frac{2}{e^{2x}-1} \tag{A.20}$$

$$\tanh(x) = 1-\frac{2}{e^{2x}+1} \tag{A.21}$$

Appendix B

Coleman-Weinberg potential

In this appendix, we have collected the expression for the one-loop Coleman Weinberg (CW) potential in both $\overline{MS}$ scheme and cut-off regularization scheme. Here we have presented $\overline{MS}$ renormalization scheme for zero-temperature one loop Coleman-Weinberg potential as an illustration.

B.1 $\overline{MS}$ renormalization

From Eq.(2.132), we have

$$V_{\rm CW}^{(1)} = \int \frac{d^D k}{(2\pi)^D} \frac{\sqrt{k^2+m^2}}{2} \tag{B.1}$$

Using Eq.(A.12) and Eq.(A.13) we have,

$$\begin{aligned} V_{S\rm CW}^{(1)} &= \frac{1}{2} f(m, 3-\epsilon, -1/2) \\ &= \frac{\mu^{-\epsilon} m^4}{2(4\pi)^{3/2}} (\frac{4\pi\mu^2}{m^2})^{\epsilon/2} \frac{\Gamma(-2+\frac{\epsilon}{2})}{\Gamma(-\frac{1}{2})} \end{aligned} \tag{B.2}$$

As $\Gamma(-\frac{1}{2}) = -2\sqrt{\pi}$ and $\Gamma(-2+\frac{\epsilon}{2}) = \frac{1}{\epsilon} + \frac{3}{4} - \frac{\gamma_E}{2} + O(\epsilon)$, we have from Eq.(B.2) in the limit $\epsilon \to 0$,

$$V_{S\rm CW}^{(1)} = -\frac{m^4}{64\pi^2}(\frac{2}{\epsilon} - \gamma_E + \ln 4\pi) + \frac{m^4}{64\pi^2}(\ln\frac{m^2}{\mu^2} - \frac{3}{2}) \tag{B.3}$$

So removing the first term in $\bar{M}S$ scheme, we have,

$$V_{S\rm CW}^{(1)} = \frac{m_s^4(\phi_c)}{64\pi^2}(\ln\frac{m_s^2(\phi_c)}{\mu^2} - \frac{3}{2}) \tag{B.4}$$

Similarly for fermions, we have from Eq.(2.144) by removing the divergent part in $\bar{M}S$ scheme,

$$V^{(1)}_{F\mathrm{CW}} = -2g_f \frac{m_f^4(\phi_c)}{64\pi^2}(\ln\frac{m_f^2(\phi_c)}{\mu^2} - \frac{3}{2}) \tag{B.5}$$

On the other hand for the gauge bosons we have

$$V^{(1)}_{gb\mathrm{CW}} = 3\frac{m_{gb}^4(\phi_c)}{64\pi^2}(\ln\frac{m_{gb}^2(\phi_c)}{\mu^2} - \frac{5}{6}) \tag{B.6}$$

B.2 CW effective potential in the Standard Model

Here we collect the expression for one loop CW potential for the Standard Model. The Higgs field of the Standard Model is,

$$\Phi = \begin{pmatrix} G^{\pm} \\ \dfrac{\phi_c + h + iG^0}{\sqrt{2}} \end{pmatrix} \tag{B.7}$$

where ϕ_c is the real constant background, h the Higgs field, and $G^{\pm}$ and G^0 are the three Goldstone bosons. The tree level potential reads, in terms of the background field, as

$$V_0(\phi_c) = -\frac{m^2}{2}\phi_c^2 + \frac{\lambda}{4}\phi_c^4 \tag{B.8}$$

with positive λ and m^2, and the tree level minimum corresponding to

$$v^2 = \frac{m^2}{\lambda}.$$

The field dependent masses of the scalar fields are

$$\begin{aligned} m_h^2(\phi_c) &= -m^2 + 3\lambda\phi_c^2 \\ m^2_{G^{\pm},G^0}(\phi_c) &= -m^2 + \lambda\phi_c^2 \end{aligned} \tag{B.9}$$

so that $m_h^2(v) = 2\lambda v^2 = 2m^2$ and $m^2_{G^{\pm},G^0}(v) = 0$. The gauge bosons contributing to the one-loop effective potential are $W^{\pm}$ and Z, with tree level field dependent masses,

$$\begin{aligned} m_W^2(\phi_c) &= \frac{g^2}{4}\phi_c^2 \\ m_Z^2(\phi_c) &= \frac{g^2 + g'^2}{4}\phi_c^2 \end{aligned} \tag{B.10}$$

Finally, the only fermion which can give a significant contribution to the one loop effective potential is the top quark, with a field-dependent mass

$$m_t^2(\phi_c) = \frac{y_t^2}{2}\phi_c^2 \tag{B.11}$$

where y_t is the top quark Yukawa coupling.

B.2.1 $\overline{\text{MS}}$ renormalization

In the $\overline{\text{MS}}$ renormalization scheme the finite effective potential for the SM is provided by

$$V(\phi_c) = V_0(\phi_c) + \frac{1}{64\pi^2}\sum_{i=W,Z,h,G^\pm,G^0,t} n_i m_i^4(\phi_c)\left[\log\frac{m_i^2(\phi_c)}{\mu^2} - C_i\right] \tag{B.12}$$

where C_i are constants given by,

$$\begin{aligned} C_W = C_Z &= \frac{5}{6} \\ C_h = C_{G^\pm,G^0} = C_t &= \frac{3}{2} \end{aligned} \tag{B.13}$$

and n_i are the degrees of freedom

$$n_W = 6,\ n_Z = 3,\ n_h = 1,\ n_{G^\pm,G^0} = 3,\ n_t = -12 \tag{B.14}$$

B.2.2 Cut-off regularization

A useful cut-off regularization scheme was presented in [17] where the following two conditions are imposed:

- the tree level minimum is preserved at one loop.
- At one loop, tree level value of the Higgs mass is also preserved

or in other words,

$$\begin{aligned} \left.\frac{d(V_1 + V_{ct})}{d\phi_c}\right|_{\phi_c=v} &= 0 \\ \left.\frac{d^2(V_1 + V_{ct})}{d\phi_c^2}\right|_{\phi_c=v} &= 0 \end{aligned} \tag{B.15}$$

where V_1 is the one loop effective potential and V_{ct} is the counter-term potential to remove the divergences. The final result is [17, 84],

$$V(\phi_c) = V_0(\phi_c) + \frac{1}{64\pi^2}\sum_i \left\{ m_i^4(\phi_c)\left(\log\frac{m_i^2(\phi_c)}{m_i^2(v)} - \frac{3}{2}\right) + 2m_i^2(v)m_i^2(\phi_c)\right\} \tag{B.16}$$

Appendix C

High and low temperature expansion

C.1 Limits of thermodynamic quantities

The high and low temperature limits, which is also called relativistic and non-relativistic limits follow $m_i/T \ll 1$ and $m_i \gg p, T$ respectively.

For convenience at first we present the following two results from section A.2 which are going to used for evaluating momentum integrals. The integrals are

$$I_n^{\pm} = \int_0^{\infty} dx \frac{x^n}{e^x \pm 1} \tag{C.1}$$

$$I_n^{+} = (1 - \frac{1}{2^n}) I_n^{-} \tag{C.2}$$

$$I_n^{-} = \zeta(n+1)\Gamma(n+1) \tag{C.3}$$

Now let us consider first Eq.(2.11) in the relativistic limit,

$$\begin{aligned} n_B &= \frac{1}{2\pi^2} \int_0^{\infty} p^2 dp \frac{1}{e^{p/T} - 1} \\ &= \frac{T^3}{2\pi^2} \int_0^{\infty} dx \frac{x^2}{e^x - 1} \text{ replacing } x = p/T \\ &= \frac{\zeta(3)}{\pi^2} T^3 \end{aligned} \tag{C.4}$$

Using Eq.(C.2) we have for number density for fermionic case,

$$n_F = \frac{3}{4} \frac{\zeta(3)}{\pi^2} T^3 \tag{C.5}$$

Here, $\zeta(3) = 1.202..$ is the Riemann zeta function. If the degrees of freedom for bosons and fermions are g_B and g_F respectively, we have the total number density in the relativistic limit,

$$n = (g_B + \frac{3}{4} g_F) \frac{\zeta(3)}{\pi^2} T^3 \tag{C.6}$$

For example, for photons, $g_B = 2$, for real(complex) scalar, $g_B = 1(2)$ and for Majorana(Dirac) fermion, $g_F = 4(2)$.

Now let us consider the relativistic limit for the energy density. From Eq.(2.13), we can see that there are two contributions. The first term is the zero temperature one-loop Coleman Weinberg potential and second term represents the finite temperature part. Focusing on second term, again in the relativistic limit, we have from Eq.(2.13),

$$\begin{aligned} \rho_B &= \frac{1}{2\pi^2} \int_0^\infty p^2 dp \frac{p}{e^{p/T} - 1} \\ &= \frac{T^4}{2\pi^2} \int_0^\infty dx \frac{x^3}{e^x - 1} \\ &= \frac{\pi^2}{30} T^4 \end{aligned} \tag{C.7}$$

Similarly again using Eq.(C.2), we have for fermionic case,

$$\rho_F = \frac{7}{8} \frac{\pi^2}{30} T^4 \tag{C.8}$$

So the total energy density in the relativistic limit is

$$\rho = (g_B + \frac{7}{8} g_F) \frac{\pi^2}{30} T^4 \tag{C.9}$$

Now let us consider the non-relativistic case where $m \gg p, T$. In this limit,

$$\begin{aligned} n &= \frac{1}{2\pi^2} \int_0^\infty p^2 dp e^{-\sqrt{(p^2+m^2)/T^2}} \\ &= \frac{T^3}{2\pi^2} \int_0^\infty dx x^2 e^{-\sqrt{x^2+y^2}} \ ; y = m/T \\ &= \frac{T^3}{\pi^2} \int_y^\infty dz z \sqrt{z^2 - y^2} e^{-z} \ ; x^2 = z^2 - y^2 \\ &= \frac{T^3}{\pi^2} \sqrt{2} y^{\frac{3}{2}} e^{-y} \int_0^\infty dv v^{\frac{1}{2}} e^{-v} \ ; v = z + y \\ &= \left(\frac{mT}{2\pi} \right)^{3/2} e^{-m/T} \end{aligned} \tag{C.10}$$

And the energy density in non-relativistic case is

$$\rho_B = \rho_F = mn \tag{C.11}$$

We can see that, the contribution of non-relativistic spices in the number and energy densities is very small compared to the relativistic particles.

Let us now consider the entropy and the free energy of in the relativistic limits. From Eq.(2.16), the first term has turned out to be,

$$s_{B1} = \frac{\pi^2}{30} T^3 \tag{C.12}$$

The second term of entropy in Eq.(2.16) is evaluated in the following way. In the relativistic limit, we can write it as

$$s_{B2} = \frac{1}{2\pi^2} \int_0^\infty dp\, p^2 \ln(1 - e^{-p/T}) \tag{C.13}$$

So we can have,

$$\begin{aligned} \frac{\partial s_{B2}}{\partial T} &= -\frac{1}{2\pi^2 T^2} \int_0^\infty dp \frac{p^3}{e^{p/T} - 1} \\ &= -\frac{T^2}{2\pi^2} \int_0^\infty dx \frac{x^3}{e^x - 1} \\ &= -\frac{T^2}{2\pi^2} \zeta(4)\Gamma(4) = -\frac{\pi^2}{30} T^2 \end{aligned}$$

So we have

$$s_{B2} = -\frac{\pi^2}{90} T^3 \tag{C.14}$$

By adding two pieces,

$$s_B = \frac{2\pi^2}{45} T^3 \tag{C.15}$$

In case of fermion, the entropy density is

$$s_F = \frac{2\pi^2}{45} \frac{7}{8} T^3 \tag{C.16}$$

Therefore the total entropy density of the system will be

$$s = \frac{2\pi^2}{45} T^3 (g_B + \frac{7}{8} g_F) \tag{C.17}$$

Finally let us address the free energy density in the relativistic limit. From Eq.(2.19), considering only the temperature dependent part, we have,

$$f_B = \frac{T}{2\pi^2} \int_0^\infty dp\, p^2 \ln(1 - e^{-p/T}) \tag{C.18}$$

Following the same steps for Eq.(C.13), we have

$$f_B = -\frac{\pi^2}{90}T^4 \tag{C.19}$$

So now the total free energy density and the pressure of a system with bosons and fermions is,

$$f = -p = -\frac{\pi^2}{90}T^4(g_B - \frac{7}{8}g_F) \tag{C.20}$$

C.2 High temperature expansion for the toy model

In this section we have presented the derivation of high temperature limit of scalar and fermionic contribution to scalar self energy and find out the Debye screening which occurs at finite temperature. The high temperature limit is the condition, $m_i/T \ll 1$. First we consider bosonic contribution.

$$\begin{aligned}\delta^{(B)}m_T^2 &= \frac{\lambda}{2}\int\frac{d^3k}{(2\pi)^3}\frac{1}{\omega_k}\frac{1}{e^{\omega_k/T}-1} \\ &= \frac{\lambda T^2}{4\pi^2}\int dx\frac{x^2}{\sqrt{x^2+m^2/T^2}}\frac{1}{e^{\sqrt{x^2+m^2/T^2}}-1}\end{aligned}$$

At the high temperature limit it is reduced to

$$\begin{aligned}\delta^{(B)}m_T^2 &= \frac{\lambda T^2}{4\pi^2}\int_0^\infty dx\frac{x}{e^x-1} = \frac{\lambda T^2}{4\pi^2}\zeta(2)\Gamma(2) \\ &= \frac{\lambda T^2}{24}\end{aligned} \tag{C.21}$$

Following similar steps for fermion loop, we have,

$$\begin{aligned}\delta^{(F)}m_T^2 &= \frac{2y_\phi^2T^2}{\pi^2}\int_0^\infty dx\frac{x}{e^x+1} \\ &= y_\phi^2\frac{T^2}{6}\end{aligned} \tag{C.22}$$

Therefore the Debye screening is,

$$\Pi(T) = (\frac{\lambda}{2} + 2y_\phi^2)\frac{T^2}{12} \tag{C.23}$$

C.3 High and low temperature expansion of the effective potential

The high and low temperature expansion of the finite temperature effective potential is done following [85]. Let us first consider the bosonic finite temperature effective potential.

C.3.1 Bosonic high temperature expansion

The starting expression for the bosonic effective potential is

$$\begin{aligned} V_{\rm eff}^{T}(\phi_c) &= T\sum_{n=-\infty}^{\infty}\int\frac{d^3k}{(2\pi)^3}\ln(4\pi^2n^2T^2+\vec{k}^2+m(\phi_c)^2) \\ &= T\sum_{n=-\infty}^{\infty}\int\frac{d^3k}{(2\pi)^3}\ln(4\pi^2n^2T^2+\omega^2) \end{aligned} \tag{C.24}$$

Therefore let us define,

$$J(m,T)=T\sum_{n=-\infty}^{\infty}\int\frac{d^Dk}{(2\pi)^D}\ln(4\pi^2n^2T^2+k^2+m^2) \tag{C.25}$$

And,

$$H(m,T)=T\sum_{n=-\infty}^{\infty}\int\frac{d^Dk}{(2\pi)^D}\frac{1}{4\pi^2n^2T^2+k^2+m^2} \tag{C.26}$$

From Eq.(C.25) and Eq.(C.26) we can see that,

$$H(m,T)=\frac{1}{m}\frac{d}{dm}J(m,T) \tag{C.27}$$

$$J(m,T)=\int_0^m dm'm'H(m',T) \tag{C.28}$$

Let us start from Eq.(C.26). The zero mode contribution $n=0$ to the Eq.(C.26) can be evaluated using $f(m,3-\epsilon,1)$ in the limit $\epsilon\to 0$ as follows,

$$\begin{aligned} H^{(n=0)}(m,T) &= Tf(m,3-\epsilon,1) \\ &= T\frac{m}{(4\pi)^{\frac{3}{2}}}\Gamma(-1/2)=-\frac{mT}{4\pi} \end{aligned} \tag{C.29}$$

Now we focus on the contributions of non-zero modes in the integral Eq.(C.26).

$$\begin{aligned} H^{(n\neq 0)}(m,T) &= T\sum_n \int \frac{d^Dk}{(2\pi)^D}\frac{1}{(2\pi nT)^2+k^2+m^2} \\ &= 2T\sum_{n=1}^{\infty}\int \frac{d^Dk}{(2\pi)^D}\frac{1}{(2\pi nT)^2+k^2}(1+\frac{m^2}{(2\pi nT)^2+k^2})^{-1} \\ &= 2T\sum_{n=1}^{\infty}\sum_{l=0}^{\infty}\int \frac{d^Dk}{(2\pi)^D}(-1)^l\frac{m^{2l}}{((2\pi nT)^2+k^2)^{l+1}} \\ &= \frac{2T}{(4\pi)^{D/2}}\frac{1}{(2\pi T)^{2-D}}\sum_{l=0}^{\infty}(-1)^l\frac{m^{2l}}{(2\pi T)^{2l}}\sum_{n=1}^{\infty}\frac{1}{n^{2l+1-D}} \\ &= \frac{2T}{(4\pi)^{D/2}}\frac{1}{(2\pi T)^{2-D}}\sum_{l=0}^{\infty}(-1)^l\frac{m^{2l}}{(2\pi T)^{2l}}\zeta(2l+1-D) \end{aligned} \quad (C.30)$$

Now evaluating Eq.(C.30) for $D=3-\epsilon$ gives,

$$H^{(n\neq 0)} = \frac{\mu^{-\epsilon}T^2}{\sqrt{4\pi}}(\frac{4\pi\mu^2}{4\pi^2T^2})^{\frac{\epsilon}{2}}\sum_{l=0}^{\infty}(-1)^l(\frac{m^2}{4\pi^2T^2})^l\frac{\Gamma(l-\frac{1}{2}+\epsilon)}{\Gamma(l+1)}\zeta(2l-1+\epsilon) \quad (C.31)$$

In the following we have evaluated $H^{(n\neq 0)}$ for $l=0$ and $l=1$ respectively.

$$\begin{aligned} H^{(n\neq 0)}_{l=0} &= \frac{\mu^{-\epsilon}T^2}{\sqrt{4\pi}}(\frac{4\pi\mu^2}{4\pi^2T^2})^{\frac{\epsilon}{2}}\Gamma(-\frac{1}{2}+\epsilon)\zeta(-1+\epsilon) \\ &= \frac{T^2}{2\sqrt{\pi}}\Gamma(\frac{1}{2})\zeta(-1) \\ &= \frac{T^2}{12} \end{aligned} \quad (C.32)$$

$$\begin{aligned} H^{(n\neq 0)}_{l=1} &= -\frac{\mu^{-\epsilon}T^2}{\sqrt{4\pi}}(\frac{4\pi\mu^2}{4\pi^2T^2})^{\frac{\epsilon}{2}}\frac{m^2}{4\pi^2T^2}\frac{\Gamma(\frac{1}{2}+\frac{\epsilon}{2})}{\Gamma(2)}\zeta(1+\epsilon) \\ &= -\frac{\mu^{-\epsilon}m^2}{8\pi^2}(1+\frac{\epsilon}{2}\ln\frac{4\pi\mu^2}{4\pi^2T^2})(\frac{1}{\epsilon}+\frac{\gamma_E}{2}-\frac{1}{2}\ln 4) \\ &= -\frac{m^2}{8\pi^2\epsilon}-\frac{m^2}{8\pi^2}\ln\frac{\bar{\mu}e^{\gamma_E}}{4\pi T} \quad ;(\bar{\mu}^2=4\pi\mu^2/e^{\gamma_E}) \end{aligned} \quad (C.33)$$

where we have used

$$\Gamma(\frac{1}{2}+\frac{\epsilon}{2})\zeta(1+\epsilon) = \sqrt{\pi}(\frac{1}{\epsilon}+\frac{\gamma_E}{2}-\frac{1}{2}\ln 4+O(\epsilon)) \quad (C.34)$$

Now by using dimensional regularization again, we get the zero temperature contribution to $H(m,T)$

$$\begin{aligned} H_0(m) &= \int \frac{d^Dk}{(2\pi)^D}\frac{1}{2\sqrt{k^2+m^2}} \\ &= \frac{1}{2}f(m,3-\epsilon,\frac{1}{2}) \\ &= \frac{\mu^{-\epsilon}m^2}{2(4\pi)^{\frac{3}{2}}}(\frac{4\pi\mu^2}{m^2})^{\frac{\epsilon}{2}}\frac{\Gamma(\frac{\epsilon}{2}-1)}{\Gamma(\frac{1}{2})} \\ &= \frac{\mu^{-\epsilon}m^2}{2(4\pi)^{\frac{3}{2}}}(1+\frac{\epsilon}{2}\ln\frac{4\pi\mu^2}{m^2})\frac{1}{\sqrt{\pi}}(-\frac{2}{\epsilon}+\gamma_E-1+O(\epsilon)) \\ &= -\frac{m^2}{8\pi^2\epsilon}-\frac{m^2}{8\pi^2}\ln\frac{\bar{\mu}}{m}-\frac{m^2}{16\pi^2} \end{aligned} \tag{C.35}$$

Now the bosonic thermal integral is

$$\begin{aligned} H(m,T) &= \frac{T^2}{12}-\frac{mT}{4\pi}-\frac{m^2}{8\pi^2\epsilon}-\frac{m^2}{8\pi^2}\ln\frac{e^{\gamma_E}\bar{\mu}}{4\pi T} \\ &+ \frac{T^2}{2\sqrt{\pi}}\sum_{l=2}^{\infty}(-1)^l(\frac{m^2}{4\pi^2T^2})^l\frac{\Gamma(l-\frac{1}{2})}{\Gamma(l+1)}\zeta(2l-1) \end{aligned} \tag{C.36}$$

Therefore the thermal contribution to the bosonic integral, Eq.(C.26) is

$$\begin{aligned} H_T(m,T) &= H(m,T)-H_0(m) \\ &= \frac{T^2}{12}-\frac{mT}{4\pi}-\frac{m^2}{8\pi^2\epsilon}-\frac{m^2}{8\pi^2}\ln\frac{e^{\gamma_E}\bar{\mu}}{4\pi T} \\ &+ \frac{T^2}{2\sqrt{\pi}}\sum_{l=2}^{\infty}(-1)^l(\frac{m^2}{4\pi^2T^2})^l\frac{\Gamma(l-\frac{1}{2})}{\Gamma(l+1)}\zeta(2l-1) \\ &+ \frac{m^2}{8\pi^2\epsilon}+\frac{m^2}{8\pi^2}\ln\frac{\bar{\mu}}{m}+\frac{m^2}{16\pi^2} \end{aligned} \tag{C.37}$$

Therefore we have

$$\begin{aligned} H_T(m,T) &= \frac{T^2}{12}-\frac{mT}{4\pi}-\frac{m^2}{8\pi^2}(\ln\frac{m}{4\pi e^{-\gamma_E}T}-\frac{1}{2}) \\ &+ \frac{T^2}{2\sqrt{\pi}}\sum_{l=2}^{\infty}(-1)^l(\frac{m^2}{4\pi^2T^2})^l\frac{\Gamma(l-\frac{1}{2})}{\Gamma(l+1)}\zeta(2l-1) \end{aligned} \tag{C.38}$$

From Eq.(C.38) we have,

$$\begin{aligned} J_T(m,T) &= \int_0^m dm' m' H_T(m,T) \\ &= \frac{m^2T^2}{24} - \frac{m^3T}{12\pi} - \frac{m^4}{64\pi^2}(\ln\frac{m^2}{16\pi^2 e^{-2\gamma_E}T^2} - \frac{3}{2}) \\ &+ \frac{m^2T^2}{4\sqrt{\pi}}\sum_{l=2}^{\infty}(\frac{m^2}{4\pi^2T^2})^l \frac{\Gamma(l-\frac{1}{2})}{\Gamma(l+2)}\zeta(2l-1) \end{aligned} \tag{C.39}$$

C.3.2 Fermionic high temperature expansion

Let us now focus on the high temperature expansion of the fermionic effective potential. In bosonic case, we encounter frequency sum of the following form,

$$\sigma_b(T) = T\sum_{n=-\infty}^{\infty} f(\omega_n) \tag{C.40}$$

where $f(\omega_n) = \frac{1}{\omega_n^2+\omega^2}$ with $\omega_n = 2\pi nT$ and $\omega^2 = k^2 + m^2$.

On the other hand, for fermionic cases, the frequency sum is

$$\sigma_f(T) = T\sum_{n=-\infty}^{\infty} f(\omega_n) \tag{C.41}$$

where $\omega_n = (2n+1)\pi T$. In the following we are going to recast fermionic sum in terms of bosonic sum, Eq.(C.40).

$$\begin{aligned} \sigma_f(T) &= T[... + f(-3\pi T) + f(-\pi T) + f(\pi T) + ...] \\ &= T[... + f(-3\pi T) + f(-2\pi T) + f(-\pi T) + f(0) + f(\pi T) + f(2\pi T)...] \\ &- T[... + f(-2\pi T) + f(0) + f(2\pi T) + ...] \\ &= 2\frac{T}{2}[... + f(-6\pi\frac{T}{2}) + f(-4\pi\frac{T}{2}) + f(-2\pi\frac{T}{2}) + f(0) + f(2\pi\frac{T}{2}) + f(4\pi\frac{T}{2})...] \\ &- T[... + f(-2\pi T) + f(0) + f(2\pi T) + ...] \\ &= 2\sigma_b(\frac{T}{2}) - \sigma_b(T) \end{aligned} \tag{C.42}$$

Using Eq.(C.42), the fermionic thermal integrals can be evaluated using the

results of bosonic thermal integrals.

$$\begin{aligned}\tilde{H}(m,T) &= T\sum_n \int \frac{d^3k}{(2\pi)^3}\frac{1}{(2n+1)^2\pi^2T^2+k^2+m^2} \\ &= \int \frac{d^3k}{(2\pi)^3}\sigma_f(T) \\ &= \int \frac{d^3k}{(2\pi)^3}\left[2\sigma_b(\frac{T}{2})-\sigma_b(T)\right] \\ &= 2H(m,\frac{T}{2})-H(m,T) \qquad \text{(C.43)}\end{aligned}$$

Now using Eq.(C.36), we have

$$\begin{aligned}\tilde{H}(m,T) &= -\frac{T^2}{24}-\frac{m^2}{8\pi^2\epsilon}-\frac{m^2}{8\pi^2}\ln\frac{e^{\gamma_E}\bar{\mu}}{4\pi T}-\frac{m^2}{8\pi^2}\ln 4 \\ &- \frac{T^2}{2\sqrt{\pi}}\sum_{l=2}^{\infty}(-1)^l(1-2^{2l-1})(\frac{m^2}{4\pi^2T^2})^l\frac{\Gamma(l-\frac{1}{2})}{\Gamma(l+1)}\zeta(2l-1) \qquad \text{(C.44)}\end{aligned}$$

The thermal contribution to the fermionic integral is

$$\tilde{H}_T(m,T) = \tilde{H}(m,T) - H_0(m) \qquad \text{(C.45)}$$

$$\tilde{H}_T(m,T) = -\frac{T^2}{24}-\frac{m^2}{8\pi^2}\ln\frac{e^{\gamma_E}m}{\pi T}-\frac{T^2}{2\sqrt{\pi}}\sum_{l=2}^{\infty}(-1)^l(1-2^{2l-1})(\frac{m^2}{4\pi^2T^2})^l\frac{\Gamma(l-\frac{1}{2})}{\Gamma(l+1)}\zeta(2l-1) \qquad \text{(C.46)}$$

Therefore, from Eq.(C.46), the fermionic integral is determined as follows

$$\tilde{J}_T(m,T) = \int_0^m dm' m' \tilde{H}_T(m',T) \qquad \text{(C.47)}$$

$$\begin{aligned}\tilde{J}_T(m,T) &= -\frac{m^2T^2}{48}-\frac{m^4}{64\pi^2}(\ln\frac{m^2}{\pi^2e^{-2\gamma_E}T^2}-\frac{3}{2}) \\ &- \frac{m^2T^2}{4\sqrt{\pi}}\sum_{l=2}^{\infty}(-1)^l(1-2^{2l-1})(\frac{m^2}{4\pi^2T^2})^l\frac{\Gamma(l-\frac{1}{2})}{\Gamma(l+2)}\zeta(2l-1) \qquad \text{(C.48)}\end{aligned}$$

C.3.3 Low temperature expansion

In this section we will consider the case, $m \gg T$. Denoting $y = m/T \gg 1$ we have in such limit,

$$\begin{aligned} J_T(m,T) &= \int_0^\infty dx x^2 \ln(1 - e^{-\sqrt{x^2+y^2}}) \\ &= -\int_0^\infty dx x^2 e^{-\sqrt{x^2+y^2}} + O(e^{-2y}) \\ &= \int_y^\infty dz z\sqrt{z^2-y^2} e^{-z} + O(e^{-2y}) \\ &= -e^{-y}\int_0^\infty dv (v+y)\sqrt{v^2+2vy} e^{-v} + O(e^{-2y}) \\ &= -\sqrt{2}y^{\frac{3}{2}} e^{-y}\int_0^\infty dv v^{\frac{1}{2}} e^{-v}(1+\frac{v}{y})(1+\frac{v}{4y}) + O(e^{-2y}) \\ &= -\sqrt{2}y^{\frac{3}{2}} e^{-y}\Gamma(\frac{3}{2})(1+O(\frac{1}{y}) + O(e^{-y})) \end{aligned} \tag{C.49}$$

Therefore we have,

$$V_T = -T^4(\frac{m}{2\pi T})^{\frac{3}{2}} e^{-\frac{m}{T}}(1 + O(\frac{T}{m}) + O(e^{-\frac{m}{T}}) \tag{C.50}$$

and

$$H_T(m,T) = \frac{T^3}{m}(\frac{m}{2\pi T})^{\frac{3}{2}} e^{-\frac{m}{T}}(1 + O(\frac{T}{m}) + O(e^{-\frac{m}{T}}) \tag{C.51}$$

Therefore the high temperature expansion of thermal effective potential Eq.(2.149), we have

$$\begin{aligned} V_T(\phi_c) &= \sum_B g_B \left[\frac{m_B^2(\phi_c)T^2}{12} - \frac{m_B^3(\phi_c)T}{12\pi} - \frac{m_B^4(\phi_c)}{64\pi^2}\left(\ln\frac{m_B^2(\phi_c)}{a_b T^2} - \frac{3}{2}\right)\right] \\ &+ \sum_F g_F \left[\frac{m_F^2(\phi_c)T^2}{48} + \frac{m_F^4(\phi_c)}{64\pi^2}\left(\ln\frac{m_F^2(\phi_c)}{a_f T^2} - \frac{3}{2}\right)\right] \end{aligned} \tag{C.52}$$

where, $a_b = 16\pi^2 e^{-2\gamma_E}$ and $a_f = \pi^2 e^{-2\gamma_E}$.

Appendix D

Asymptotic limits of the sphaleron field profiles

To capture the dependence of solutions on (J, Y), in this section we have included the analytical estimates of solutions for the asymptotic region $\xi \to 0$ and $\xi \to \infty$.

For the energy functional Eq.(3.48) to be finite, the profile functions should be $f(\xi) \to 0$, $f_3(\xi) \to 0$, $f_0(\xi) \to 1$ and $h(\xi) \to 0$. Therefore, at $\xi \sim 0$, the equations Eq.(3.50) are reduced into

$$\xi^2 f'' - 4f + 2f_3 + \alpha\xi^2 h^2 = 0 \tag{D.1}$$

$$\xi^2 f_3'' - 6f_3 + 4f + \beta\xi^2 h^2 = 0 \tag{D.2}$$

$$f_0'' + 2(1 - f_0) - (\frac{g'}{g})^2 \beta\xi^2 h^2 = 0 \tag{D.3}$$

$$\xi^2 h'' + 2\xi h' - \frac{8m}{3} h = 0 \tag{D.4}$$

where

$$m = \frac{\Omega^2}{v^2}(2\alpha + \beta) \tag{D.5}$$

The solution of Eq.(D.4) which leads to the finite energy of the sphaleron is

$$h(\xi) \sim A\xi^{-\frac{1}{2}(1-p)} \tag{D.6}$$

where

$$p = \sqrt{1 + \frac{32}{3}m} \tag{D.7}$$

Now at $\xi \sim 0$, $f(\xi) \sim f_3(\xi)$, so using this approximation, from Eq.(D.1) we have,

$$f(\xi) \sim B\xi^2 - \frac{4A\alpha\xi^{\frac{1}{2}(3+p)}}{(\frac{p}{2} - 1)(\frac{p}{2} + 5)} \tag{D.8}$$

On the other hand, we have considered $f(\xi)$ as a perturbation in Eq.(D.2). Therefore, we have

$$f_3(\xi) \sim C\xi^3 + B\xi^2 - K\xi^{\frac{1}{2}(3+p)} \tag{D.9}$$

Here, K is defined as follows,

$$K = \frac{k_1}{k_2} \tag{D.10}$$

$$k_1 = 3A\{3\alpha(3p - 8m + 3) + 8m\beta(4m - 9)\} \tag{D.11}$$

$$k_2 = 4m(4m - 9)(8m + 3p - 15) \tag{D.12}$$

Finally from Eq.(D.3), we have

$$f_0(\xi) \sim 1 + D\xi^2 + \frac{3A\beta n_1^2 \xi^{\frac{1}{2}(3+p)}}{3p - 8m + 3} \tag{D.13}$$

where $n_1 = g'/g$.

Here, A, B, C and D are the integration constants.

On the other hand, for asymptotic region, $\xi \sim \infty$, all the profile functions must approach unity to have finite energy of the sphaleron. So we consider the functions to be the small perturbation to unity as follows. Taking, $f(\xi) = 1 + \delta f(\xi)$, $f_3(\xi) = 1 + \delta f_3(\xi)$, $f_0(\xi) = 1 + \delta f_0(\xi)$ and $h(\xi) = 1 + \delta h(\xi)$ and keeping only the linear terms of the variation, we have

$$\delta f'' - \alpha \delta f = 0 \tag{D.14}$$

$$\delta f_3'' + \beta(\delta f_0 - \delta f_3) = 0 \tag{D.15}$$

$$\delta f_0'' - \frac{g'^2}{g^2}\beta(\delta f_0 - \delta f_3) = 0 \tag{D.16}$$

$$\xi^2 \delta h'' - 2\xi \delta h - 3\frac{\lambda v^2}{g^2\Omega^2}\xi^2 \delta h = 0 \tag{D.17}$$

The asymptotic solutions at $\xi \sim \infty$ are,

$$f(\xi) \sim 1 + Ee^{-\sqrt{\alpha}\xi} \tag{D.18}$$

$$f_3(\xi) \sim 1 + Fe^{-\sqrt{\beta}\xi} \tag{D.19}$$

$$f_0(\xi) \sim 1 + Ge^{-\sqrt{\beta}\xi} \tag{D.20}$$

$$h(\xi) \sim 1 + \frac{He^{-\frac{\sqrt{3\lambda}v}{g\Omega}\xi}}{\xi} \tag{D.21}$$

where E, F, G and H are again integration constants. The constants from A to H depend on (J, J_3) and couplings and they are determined by matching

the corresponding asymptotic solutions and their first derivatives at $\xi = 1$. Therefore after the matching, the integration constants are,

$$H = -\frac{\frac{1}{2}(p-1)e^{\frac{v}{\Omega}n}}{\frac{1}{2}(p+1)+\frac{v}{\Omega}n} \tag{D.22}$$

$$A = 1 + He^{-\frac{v}{\Omega}n} \tag{D.23}$$

where, $n = \frac{\sqrt{3\lambda}}{g}$

The constants B and E are given as,

$$E = -\frac{e^{\sqrt{\alpha}}}{\sqrt{\alpha}+2}(2 + \frac{2A\alpha(1-p)}{(\frac{p}{2}-1)(\frac{p}{2}+5)}) \tag{D.24}$$

$$B = 1 + Ee^{-\sqrt{\alpha}} + \frac{4A\alpha}{(\frac{p}{2}-1)(\frac{p}{2}+5)} \tag{D.25}$$

Again the constants C and F are in the following,

$$F = \frac{e^{\sqrt{\beta}}}{\sqrt{\beta}+3}(-3 + B - \frac{1}{2}(3-p)K) \tag{D.26}$$

$$C = 1 + Fe^{-\sqrt{\beta}} - B + K \tag{D.27}$$

And finally D and G are given as

$$G = \frac{e^{\sqrt{\beta}}}{\sqrt{\beta}+2}\frac{3A\beta n_1^2(1-p)}{2(3p+8m-3)} \tag{D.28}$$

$$D = Ge^{-\sqrt{\beta}} - \frac{3A\beta n_1^2}{3p+8m-3} \tag{D.29}$$

Appendix E

Quartet $SU(2)$ representation

E.1 $SU(2)$ generators in the quartet

The generators $R(T^a)$ in representation R of $SU(2)$ are taken in such a way that they satisfy the following relation: $Tr[R(T^a)R(T^b)] = T(R)\delta^{ab}$. Here $T(R)$ is the dynkin index for the corresponding representation. It is obtained from $T(R)D(Ad) = C(R)D(R)$ where dimension of Adjoint reps. is $D(Ad) = 3$ for $SU(2)$ and Casimir invariant is $\sum_a R(T^a)R(T^a) = j(j+1)$ and dimension of the reps. R is $D(R) = 2j+1$. For $SU(2)$ reps. $T(\frac{1}{2}) = \frac{1}{2}$ and $T(\frac{3}{2}) = 5$.

The explicit form of the generators for quartet reps are the following:

$$T^1 = \begin{pmatrix} 0 & \frac{\sqrt{3}}{2} & 0 & 0 \\ \frac{\sqrt{3}}{2} & 0 & 1 & 0 \\ 0 & 1 & 0 & \frac{\sqrt{3}}{2} \\ 0 & 0 & \frac{\sqrt{3}}{2} & 0 \end{pmatrix}, \quad T^2 = \begin{pmatrix} 0 & -\frac{\sqrt{3}i}{2} & 0 & 0 \\ \frac{\sqrt{3}i}{2} & 0 & -i & 0 \\ 0 & i & 0 & -\frac{\sqrt{3}i}{2} \\ 0 & 0 & \frac{\sqrt{3}i}{2} & 0 \end{pmatrix}, \quad T^3 = \text{diag}(\frac{3}{2}, \frac{1}{2}, -\frac{1}{2}, -\frac{3}{2}). \tag{E.1}$$

The raising and lowering operators are defined as $T^{\pm} = T^1 \pm iT^2$. The antisymmetric matrices in doublet reps is ϵ and the similar antisymmetric matrix for quartet representation, C is constructed using the relation $CT^aC^{-1} = -T^{aT}$ because the explicit form of it depends on the matrix representation of the corresponding generators:

$$\epsilon = \begin{pmatrix} 0 & 1 \\ -1 & 0 \end{pmatrix}, \quad C = \begin{pmatrix} 0 & 0 & 0 & 1 \\ 0 & 0 & -1 & 0 \\ 0 & 1 & 0 & 0 \\ -1 & 0 & 0 & 0 \end{pmatrix} \tag{E.2}$$

E.2 Gauge-scalar-scalar vertices

In this section we have collected the gauge-scalar-scalar vertices in the quartet sector needed for the electroweak precision observables. All the momenta are taken inward.

$$Q^{++}(p_1)Q_1^-(p_2)W_\mu^- \;:\; \frac{ie}{s_w}\sqrt{\frac{3}{2}}\cos\theta(p_1-p_2)_\mu \tag{E.3}$$

$$Q^{++}(p_1)Q_2^-(p_2)W_\mu^- \;:\; \frac{ie}{s_w}\sqrt{\frac{3}{2}}\sin\theta(p_1-p_2)_\mu \tag{E.4}$$

$$Q_1^+(p_1)S(p_2)W_\mu^- \;:\; \frac{ie}{2s_w}(2\cos\theta+\sqrt{3}\sin\theta)(p_1-p_2)_\mu \tag{E.5}$$

$$Q_1^+(p_1)A(p_2)W_\mu^- \;:\; \frac{e}{2s_w}(2\cos\theta-\sqrt{3}\sin\theta)(p_1-p_2)_\mu \tag{E.6}$$

$$S(p_1)Q_2^+(p_2)W_\mu^- \;:\; \frac{ie}{2s_w}(\sqrt{3}\cos\theta-2\sin\theta)(p_1-p_2)_\mu \tag{E.7}$$

$$A(p_1)Q_2^+(p_2)W_\mu^- \;:\; -\frac{e}{2s_w}(\sqrt{3}\cos\theta+2\sin\theta)(p_1-p_2)_\mu \tag{E.8}$$

$$Q^{++}(p_1)Q^{--}(p_2)Z_\mu \;:\; \frac{ie}{2s_wc_w}(3c_w^2-s_w^2)(p_1-p_2)_\mu \tag{E.9}$$

$$Q_1^+(p_1)Q_1^-(p_2)Z_\mu \;:\; \frac{ie}{2s_wc_w}(2c_w^2-\cos 2\theta)(p_1-p_2)_\mu \tag{E.10}$$

$$Q_2^+(p_1)Q_2^-(p_2)Z_\mu \;:\; \frac{ie}{2s_wc_w}(2c_w^2+\cos 2\theta)(p_1-p_2)_\mu \tag{E.11}$$

$$S(p_1)A(p_1)Z_\mu \;:\; -\frac{e}{2s_wc_w}(p_1-p_2)_\mu \tag{E.12}$$

$$Q_1^+(p_1)Q_2^-(p_2)Z_\mu \;:\; -\frac{ie}{2s_wc_w}\sin 2\theta(p_1-p_2)_\mu \tag{E.13}$$

(E.14)

$$Q^{++}(p_1)Q^{--}(p_2)A_\mu \;:\; 2ie(p_1-p_2)_\mu \tag{E.15}$$

$$Q_1^+(p_1)Q_1^-(p_2)A_\mu \;:\; ie(p_1-p_2)_\mu \tag{E.16}$$

$$Q_2^+(p_1)Q_2^-(p_2)A_\mu \;:\; ie(p_1-p_2)_\mu \tag{E.17}$$

Appendix F

Tree-Unitarity

The tree-unitarity condition presented in section 4.1.3 is derived here based on [228, 229]. The S-matrix of the give process can be decomposed in the following way,

$$S = I + iT \tag{F.1}$$

where T is the transfer matrix containing the information of the interaction. The unitarity of S-matrix implies

$$S^\dagger S = SS^\dagger = I \tag{F.2}$$

which gives,

$$\begin{aligned} T - T^\dagger &= iT^\dagger T \\ &= iTT^\dagger \end{aligned} \tag{F.3}$$

where the two equivalent relations arises due to $S^\dagger S$ and $SS^\dagger$. If the initial and final states (also considering them to be orthonormal) are denoted as $|i\rangle$ and $|f\rangle$, then we have,

$$\langle f|T|i\rangle = i(2\pi)^4\delta^4(P_f - P_i)T_{fi} \tag{F.4}$$

where P_i and P_f are the initial and final total 4-momenta respectively. So we have,

$$\begin{aligned} T_{fi} - T^*_{if} &= i(2\pi)^4 \sum_n \delta^4(P_f - P_n)T_{fn}T^*_{in} \\ &= i(2\pi)^4 \sum_n \delta^4(P_f - P_n)T^*_{nf}T_{ni} \end{aligned} \tag{F.5}$$

where n are the intermediate multiparticle states. To characterize a state, one can use the total angular momentum J , it's projection along z-component

J_z and the helicity operator $\hat{\Lambda} = \vec{J}.\hat{p}$ because they are conserved quantities therefore serve as good quantum numbers.

Consider for simplicity the elastic scattering $A + B \to A + B$ in the center of mass frame. At first the states are labeled by momentum and helicity: initial two particle state is $|i\rangle = |p_a, \lambda_a; p_b, \lambda_b\rangle$ and final two particle state is $|f\rangle = |p'_a, \lambda'_a; p'_b, \lambda'_b\rangle$. In the center of mass frame, the 3-momenta of $|i\rangle$ are $\vec{p}_a = -\vec{p}_b = \vec{p}_i$. Similarly the 3-momenta in the final state $|f\rangle$ are $\vec{p}'_a = -\vec{p}'_b = \vec{p}_f$.

As the helicity is the component of the spin along the direction of momentum, if we now consider the two particle state as a single particle with helicity Λ in $\vec{p}_i$ direction, then $\Lambda = \lambda_a - \lambda_b$. Similarly for final state, we have $\Lambda' = \lambda'_a - \lambda'_b$ along $\vec{p}_f$ direction. Now consider, $\vec{p}_i$ is along the $\hat{z}$ axis and $\vec{p}_f$ has the polar angles ϕ and θ with respect to this fixed coordinate system. The rotation matrix R_{fi}, which is the product of the rotation of angle θ about $\hat{y}$ axis and the rotation of angle ϕ about $\hat{z}$ axis, transforms $\hat{p}_i \equiv \hat{z}$ into the unit vector $\hat{p}'_a = \frac{\vec{p}'_a}{|\vec{p}'_a|}$.

For the case of $2 \to 2$ elastic scattering, only 2 particle intermediate states will contribute in the summation. Therefore the summation over these states in Eq.(F.20) will be the integration over the intermediate 3-momenta $\vec{p}_1$ and $\vec{p}_2$ and summation over the spin quantum numbers or the helicities of the two particles denoted by λ_1 and λ_2. Also in the CM frame of this system, $\vec{p}_1 = -\vec{p}_2 = \vec{p}_k$.

$$\sum_n \to \int \frac{d^3\vec{p}_1}{(2\pi)^3 2E_1} \frac{d^3\vec{p}_2}{(2\pi)^3 2E_2} \sum_{\lambda_1,\lambda_2} \tag{F.6}$$

The rotation matrix $R_{ki}(\phi', \theta', 0)$ takes $\vec{p}_i$ into $\vec{p}_k$ and $R_{kf}(\phi'', \theta'', 0)$ takes $\vec{p}_f$ into $\vec{p}_k$. Also, $R_{ki} = R_{kf} R_{fi}$. Now combining with the delta function we have

$$\sum_{\lambda_1,\lambda_2} \int \frac{d^3\vec{p}_1}{(2\pi)^3 2E_1} \frac{d^3\vec{p}_2}{(2\pi)^3 2E_2} (2\pi)^4 \delta^4(p_1 + p_2 - P_f) = \frac{1}{32\pi^2 s} \lambda^{1/2}(s, m_a^2, m_b^2) d\Omega_k \tag{F.7}$$

with $\lambda(x_1, x_2, x_3) = (x_1^2 + x_2^2 + x_3^2)^2 - 2x_1x_2 - 2x_2x_3 - 2x_3x_1$ and $d\Omega_k = \sin\theta'' d\theta'' d\phi''$.

For any two particle system $|p_1, \lambda_1; p_2, \lambda_2\rangle$, we have $\vec{p}_1 = -\vec{p}_2 = \vec{p}$ in the CM frame and helicity $\Lambda = \lambda_1 - \lambda_2$. Moreover, the rotation $R_{\theta,\phi}$ transforms $\hat{z}$ into $\hat{p}$ direction with polar angles θ and ϕ. So in this case, the state of total angular momentum J with M being it's component in $\hat{z}$ axis is given by

$$|J, M; \lambda_1, \lambda_2\rangle = \sqrt{\frac{2J+1}{4\pi}} \int d\phi \sin\theta \, d\theta \, \mathcal{D}^J_{\lambda_1 - \lambda_2, M}(R^{-1}_{\theta,\phi}) |p_1, \lambda_1; p_2, \lambda_2\rangle \tag{F.8}$$

The Wigner's D-matrix is defined as

$$\mathcal{D}^{J}_{m',m}(\alpha,\beta,\gamma) = \langle J,m'|e^{-i\alpha\hat{J}_z}e^{-i\beta\hat{J}_y}e^{-i\gamma\hat{J}_z}|J,m\rangle \tag{F.9}$$

Here, α, β and γ are the Euler angles and $\hat{J}_i$ are the generators of the rotation group. As the helicity is a conserved under rotation, using the Wigner-Eckart theorem, we have

$$\begin{aligned} T_{fi} &= \langle p'_a,\lambda'_a;p'_b,\lambda'_b|T|p_a,\lambda_a;p_b,\lambda_b\rangle \\ &= 16\pi\sum_J(2J+1)\langle\lambda'_a,\lambda'_b|T^J(s)|\lambda_a,\lambda_b\rangle\,\mathcal{D}^{J*}_{\lambda_a-\lambda_b,\lambda'_a-\lambda'_b}(\phi,\theta,0) \end{aligned} \tag{F.10}$$

Therefore, expanding the LHS of Eq.(F.5) in angular momentum states,

$$\begin{aligned} & 16\pi\sum_J(2J+1)[\langle\lambda'_a,\lambda'_b|T^J(s)|\lambda_a,\lambda_b\rangle\,\mathcal{D}^{J*}_{\lambda_a-\lambda_b,\lambda'_a-\lambda'_b}(R_{fi}) \\ - \;& \langle\lambda'_a,\lambda'_b|T^{\dagger J}(s)|\lambda_a,\lambda_b\rangle\,\mathcal{D}^{J}_{\lambda'_a-\lambda'_b,\lambda_a-\lambda_b}(R_{fi})] \\ = \;& 16\pi\sum_J(2J+1)[\langle\lambda'_a,\lambda'_b|T^J(s)|\lambda_a,\lambda_b\rangle - \langle\lambda'_a,\lambda'_b|T^{\dagger J}(s)|\lambda_a,\lambda_b\rangle]\times \\ & \mathcal{D}^{J*}_{\lambda_a-\lambda_b,\lambda'_a-\lambda'_b}(R_{fi}) \end{aligned} \tag{F.11}$$

where symmetry property, $D^{J}_{m'm}(R) = D^{J*}_{mm'}(R)$ is used. Now the RHS of Eq.(F.5) gives,

$$\begin{aligned} & i\frac{8\lambda^{1/2}(s,m_a^2,m_b^2)}{s}\sum_{J,J'}\sum_{\lambda_1,\lambda_2}(2J+1)(2J'+1)\langle\lambda'_a,\lambda'_b|T^{\dagger J}(s)|\lambda_1,\lambda_2\rangle\,\langle\lambda_1,\lambda_2|T^J(s)|\lambda_a,\lambda_b\rangle \\ \times \;& \int d\Omega_k\mathcal{D}^{J}_{\lambda_1-\lambda_2,\lambda'_a-\lambda'_b}(R_{kf})\mathcal{D}^{J'*}_{\lambda_a-\lambda_b,\lambda_1-\lambda_2}(R_{kf})\mathcal{D}^{J'*}_{\lambda_a-\lambda_b,\lambda_1-\lambda_2}(R_{fi}) \end{aligned}$$

where we have used, $D^{J}_{m'm}(R_2.R_1) = D^{J}_{m'm}(R_2)D^{J}_{m'm}(R_1)$. Now using

$$\int d\phi\,\sin\theta\,d\theta\mathcal{D}^{J*}_{m_1m_2}(R)\mathcal{D}^{J'}_{m'_1m'_2}(R) = \frac{4\pi}{2J+1}\delta_{JJ'}\delta_{m'_1m_1}\delta_{m'_2m_2} \tag{F.12}$$

we have the RHS as follows,

$$i\frac{32\pi\lambda^{1/2}(s,m_a^2,m_b^2)}{s}\sum_J(2J+1)|\langle\lambda'_a,\lambda'_b|T^J(s)|\lambda_a,\lambda_b\rangle|^2\mathcal{D}^{J*}_{\lambda_a-\lambda_b,\lambda'_a-\lambda'_b}(R_{fi}) \tag{F.13}$$

Therefore, equating both sides and picking up J-th contribution,

$$\begin{aligned} \langle\lambda'_a,\lambda'_b|T^J(s)|\lambda_a,\lambda_b\rangle \;-\; & \langle\lambda'_a,\lambda'_b|T^{\dagger J}(s)|\lambda_a,\lambda_b\rangle \\ = \;& \frac{2i\lambda^{1/2}(s,m_a^2,m_b^2)}{s}|\langle\lambda'_a,\lambda'_b|T^J(s)|\lambda_a,\lambda_b\rangle|^2 \end{aligned} \tag{F.14}$$

In the high energy limit, when the masses of the particles can be neglected, from Eq.(F.14), by taking absolute value we have,

$$|\mathrm{Im}T^J| \geq |T^J|^2 = (\mathrm{Im}T^J)^2 + (\mathrm{Re}T^J)^2 \tag{F.15}$$

where we have suppressed the helicity indices. The unitarity of S matrix implies $|T^J| \leq 1$. Therefore by re-arranging Eq.(F.15) we have,

$$(\mathrm{Re}T^J)^2 \leq |\mathrm{Im}T^J|(1 - |\mathrm{Im}T^J|) \leq \frac{1}{4} \tag{F.16}$$

which yields the bound,

$$|\mathrm{Re}T^J| \leq \frac{1}{2} \tag{F.17}$$

In case of spinless particles, $D^J_{00}(0, \theta, 0) = P_J(\cos\theta)$ and $T^J \equiv a_J$. $P_J(\cos\theta)$ is the Legendre polynomial with θ -the scattering angle. So, Eq.(F.10) reduces to

$$T_{fi}(s, \cos\theta) = 16\pi \sum_J (2J+1) a_J(s) P_J(\cos\theta) \tag{F.18}$$

Therefore using the orthogonality of the Legendre polynomial

$$\int_{-1}^{1} d(\cos\theta) P_J(\cos\theta) P_{J'}(\cos\theta) = \frac{2}{2J+1}\delta_{JJ'} \tag{F.19}$$

we have,

$$a_J(s) = \frac{1}{32\pi} \int_{-1}^{1} d(\cos\theta) P_J(\cos\theta) T_{fi}(s, \cos\theta) \tag{F.20}$$

Since a_0 is real in the Born approximation, we can put the bound Eq.(F.17) as the following,

$$\mathrm{Re}\, a_0 \leq \frac{1}{2} \tag{F.21}$$

This is the desired tree unitarity condition.

Appendix G

Renormalization group equations

Besides the standard diagrammatic methods available to calculate one loop [155] and two loop [156–158], here we are going to describe briefly a simple and straightforward algebraic method [159, 160] to determine one loop beta functions for scalar couplings from one loop effective potential.

Consider the one loop effective potential,

$$V_{\rm eff} = V_0 + V_1 \tag{G.1}$$

where for simplicity, we have considered Z_2 invariant scalar potential,

$$\begin{aligned} V_0 &= \lambda_1(\phi^\dagger\phi)^2 + \lambda_2(\chi^\dagger\chi)^2 + \alpha\phi^\dagger\phi\,\chi^\dagger\chi + \beta\phi^\dagger\tau^a\phi\,\chi^\dagger\tau^a\chi \\ &+ \gamma[(\phi^T\epsilon\tau^a\phi)^\dagger(\chi^T\epsilon\tau^a\chi) + \text{c.c}] \end{aligned} \tag{G.2}$$

where ϕ and χ are the $SU(2)$ doublets. Moreover, τ^a are the generators of $SU(2)$ and ϵ is an antisymmetric matrix in the following,

$$\epsilon = \begin{pmatrix} 0 & -1 \\ 1 & 0 \end{pmatrix} \tag{G.3}$$

The scalar potential written in the form above can be generalized to the larger scalar multiplets.

The one-loop correction is given by,

$$V_1 = \frac{1}{64\pi^2}\text{STr}M^4\ln\frac{M^2}{\mu^2} \tag{G.4}$$

where STr is the spin-weighted trace.

In the Landau gauge, the effective potential follows the following equation,

$$\left[\mu\frac{\partial}{\partial\mu}+\sum_i\beta_{\lambda_i}\frac{\partial}{\partial\lambda_i}-(\gamma_i\xi_i\frac{\partial}{\partial\xi_i}+\text{ c.c})\right]V_{\text{eff}}=0 \tag{G.5}$$

Here, $\lambda_i=\{\lambda_1,\lambda_2,\alpha,\beta,\gamma\}$ and β_{λ_i} are the associated beta functions. Also, $\xi_i=\{\phi,\chi\}$ and $\gamma_i=\{\gamma_\phi,\gamma_\chi\}$ are the anomalous dimensions.

At one loop level,

$$D^{(1)}V_0=-\mu\frac{\partial V_1}{\partial\mu}=\frac{1}{32\pi^2}\text{STr}M^4 \tag{G.6}$$

where for n-th loop order,

$$D^{(n)}=\sum_i\beta^{(n)}_{\lambda_i}\frac{\partial}{\partial\lambda_i}-(\gamma^{(n)}_i\xi_i\frac{\partial}{\partial\xi_i}+\text{ c.c}) \tag{G.7}$$

If we know anomalous dimensions γ_i, we can determine all the one loop beta functions by comparing different quartic terms in the both sides of Eq.(G.6). Therefore let us focus on calculating the mass matrices for different fields.

For the scalar fields, the squared mass matrix is given by,

$$M_S^2=\begin{pmatrix}A & B\\ C & D\end{pmatrix} \tag{G.8}$$

where

$$A=\begin{pmatrix}\frac{\partial^2V_0}{\partial\phi_i\partial\phi^{\dagger j}} & \frac{\partial^2V_0}{\partial\phi_i\partial\chi^{\dagger j}}\\ \frac{\partial^2V_0}{\partial\chi_i\partial\phi^{\dagger j}} & \frac{\partial^2V_0}{\partial\chi_i\partial\chi^{\dagger j}}\end{pmatrix} \tag{G.9}$$

$$B=\begin{pmatrix}\frac{\partial^2V_0}{\partial\phi_i\partial\phi_j} & \frac{\partial^2V_0}{\partial\phi_i\partial\chi_j}\\ \frac{\partial^2V_0}{\partial\chi_i\partial\phi_j} & \frac{\partial^2V_0}{\partial\chi_i\partial\chi_j}\end{pmatrix} \tag{G.10}$$

and

$$C=B^\dagger\ ,\ D=A^\dagger \tag{G.11}$$

For example,

$$(A_{11})^i_j=\delta^i_j(\lambda_1\phi^\dagger\phi+\alpha\chi^\dagger\chi)+\lambda_1\phi^{\dagger i}\phi_j+\frac{\beta}{2}\chi^{\dagger i}\chi_j \tag{G.12}$$

Now,

$$\text{STr}M_S^4=\text{Tr}\,A^2+2\,\text{Tr}\,(BC)+\text{Tr}\,D^2 \tag{G.13}$$

So from Eq.(G.6), we have for scalar couplings,

$$\sum_i \beta_{\lambda_i} \frac{\partial V_0}{\partial \lambda_i} = \frac{1}{32\pi^2} \mathrm{STr} M_S^4 + (\sum_{i=\phi,\chi} \gamma_i \xi_i \frac{\partial V_0}{\partial \xi_i} + \text{ c.c}) \tag{G.14}$$

At the one-loop the anomalous dimension of scalar field is zero, so the anomalous dimensions of ϕ and χ are

$$\begin{aligned} \gamma_\phi &= 3y_t^2 - \frac{9}{4}g^2 - \frac{3}{4}g'^2 && \text{(G.15)} \\ \gamma_\chi &= -\frac{9}{4}g^2 - \frac{3}{4}g'^2 && \text{(G.16)} \end{aligned}$$

Moreover, the squared mass matrix for the vector bosons is

$$M_V^2 = \begin{pmatrix} \frac{1}{4}g^2\phi^\dagger \left\{\tau^a, \tau^b\right\} \phi + (\phi \to \chi) & \frac{1}{2}gg'\phi^\dagger \tau^a \phi + (\phi \to \chi) \\ \frac{1}{2}gg'\phi^\dagger \tau^a \phi + (\phi \to \chi) & \frac{1}{2}g'^2 \phi^\dagger \phi + (\phi \to \chi) \end{pmatrix} \tag{G.17}$$

By using the following identities,

$$\begin{aligned} \left\{\tau^a, \tau^b\right\} &= \frac{1}{2}\delta^{ab} \\ (\tau^a)^i_j (\tau^b)^k_l &= \delta^i_l \delta^k_j - \frac{1}{2}\delta^i_j \delta^k_l && \text{(G.18)} \end{aligned}$$

we have,

$$\begin{aligned} \mathrm{STr} M_V^4 &= (\frac{9}{4}g^4 + \frac{3}{4}g'^4) \left((\phi^\dagger\phi)^2 + (\chi^\dagger\chi)^2\right) \\ &+ \frac{3}{2}g^2 g'^2 \left((\phi^\dagger\phi)^2 + (\chi^\dagger\chi)^2 - \phi^\dagger\phi\chi^\dagger\chi\right) && \text{(G.19)} \end{aligned}$$

Finally, squared mass matrix for fermion is

$$M_t^2 = y_t^2 \phi^\dagger \phi \tag{G.20}$$

and therefore we have

$$\mathrm{STr} M_F^4 = -12 y_t^4 (\phi^\dagger\phi)^2 \tag{G.21}$$

The LHS of Eq.(G.14) gives,

$$\begin{aligned} \beta_{\lambda_1}(\phi^\dagger\phi)^2 &+ \beta_{\lambda_2}(\chi^\dagger\chi)^2 + \beta_\alpha \phi^\dagger\phi\, \chi^\dagger\chi + \beta_\beta \phi^\dagger\tau^a\phi\, \chi^\dagger\tau^a\chi \\ &+ \beta_\gamma[(\phi^T\epsilon\tau^a\phi)^\dagger(\chi^T\epsilon\tau^a\chi) + \text{c.c}] && \text{(G.22)} \end{aligned}$$

Comparing with the RHS of Eq.(G.14) we can immediately determine the beta functions of scalar couplings.

$$\begin{aligned}
16\pi^2\beta_{\lambda_1} &= 24\lambda_1^2 + 2\alpha^2 + \frac{1}{8}\beta^2 + \gamma^2 - 9\lambda_1 g^2 - 3\lambda_1 g'^2 + \frac{9}{4}g^4 + \frac{3}{4}g'^4 + \frac{3}{2}g^2 g'^2 + 12\lambda_1 y_t^2 - 12y_t^4 \\
16\pi^2\beta_{\lambda_2} &= 24\lambda_2^2 + 2\alpha^2 + \frac{1}{8}\beta^2 + \gamma^2 - 9\lambda_2 g^2 - 3\lambda_2 g'^2 + \frac{9}{4}g^4 + \frac{3}{4}g'^4 + \frac{3}{2}g^2 g'^2 \\
16\pi^2\beta_{\alpha} &= 4\alpha^2 + 12\lambda_1\alpha + \lambda_2\alpha + \frac{3}{4}\beta^2 + 6\gamma^2 - 9\alpha g^2 - \alpha g'^2 + \frac{9}{4}g^4 + \frac{3}{4}g'^4 - \frac{3}{2}g^2 g'^2 + 12\alpha y_t^2 \\
16\pi^2\beta_{\beta} &= 4\lambda_1\beta + 4\lambda_2\beta + 8\alpha\beta + 16\gamma^2 - 9\beta g^2 - \beta g'^2 + 12\beta y_t^2 \\
16\pi^2\beta_{\gamma} &= 4\lambda_1\gamma + 4\lambda_2\gamma + 8\alpha\gamma + 4\beta\gamma - 9\gamma g^2 - \gamma g'^2 + 12\gamma y_t^2
\end{aligned} \tag{G.23}$$

Moreover, the one loop beta functions for the $SU(2)_L$, $U(1)_Y$, $SU(3)_c$ and top-yukawa couplings g, g', g_3 and y_t respectively are,

$$\begin{aligned}
16\pi^2\beta_g &= -3g^3, \;\; 16\pi^2\beta_{g'} = \frac{22}{3}g'^3, \;\; 16\pi^2\beta_{g_3} = -7g_3^3 \\
16\pi^2\beta_{y_t} &= y_t(\frac{9}{2}y_t^2 - \frac{17}{12}g'^2 - \frac{9}{4}g^2 - 8g_3^2)
\end{aligned} \tag{G.24}$$

Here we also presented triplet RG equations [171] relevant for our analysis,

$$\begin{aligned}
16\pi^2\beta_{\lambda_1} &= 24\lambda_1^2 + 6\alpha^2 + \beta^2 - 9\lambda_1 g^2 - 3\lambda_1 g'^2 + \frac{9}{2}g^4 + \frac{3}{2}g'^4 + 3g^2 g'^2 + 12\lambda_1 y_t^2 - 6y_t^4 \\
16\pi^2\beta_{\lambda_2} &= 28\lambda_2^2 + 48\lambda_2\lambda_3 + 24\lambda_3^2 + 2\alpha^2 + \beta^2 - 24\lambda_2 g^2 - 12\lambda_2 g'^2 + 6g^4 + 6g'^4 + 24g^2 g'^2 \\
16\pi^2\beta_{\lambda_3} &= 36\lambda_3^2 + 24\lambda_2\lambda_3 - \frac{1}{2}\beta^2 - 24\lambda_3 g^2 - 12\lambda_3 g'^2 + 3g^4 - 12g^2 g'^2 \\
16\pi^2\beta_{\alpha} &= 3\alpha^2 + 6\lambda_1\alpha + 16\lambda_2\alpha + 24\lambda_3\alpha - \frac{33}{2}\alpha g^2 - \frac{15}{2}\alpha g'^2 + 6g^4 + 3g'^4 + 12y_t^2\alpha \\
16\pi^2\beta_{\beta} &= 2\lambda_1\beta + 4\lambda_2\beta - 4\lambda_3\beta + 16\alpha\beta - \frac{33}{2}\beta g^2 - \frac{15}{2}\beta g'^2 + 12g^2 g'^2 - 6\beta y_t^2 \\
16\pi^2\beta_g &= -\frac{5}{2}g^3, \;\; 16\pi^2\beta_{g'} = \frac{47}{6}\sqrt{\frac{5}{3}}g'^3, \;\; 16\pi^2\beta_{g_3} = -7g_3^3 \\
16\pi^2\beta_{y_t} &= y_t(\frac{9}{2}y_t^2 - \frac{17}{12}g'^2 - \frac{9}{4}g^2 - 8g_3^2)
\end{aligned} \tag{G.25}$$

Bibliography

[1] G. Aad *et al.* [ATLAS Collaboration], *"Observation of a new particle in the search for the Standard Model Higgs boson with the ATLAS detector at the LHC,"* Phys. Lett. B **716** (2012) 1 [arXiv:1207.7214 [hep-ex]].

[2] S. Chatrchyan *et al.* [CMS Collaboration], *"Observation of a new boson at a mass of 125 GeV with the CMS experiment at the LHC,"* Phys. Lett. B **716** (2012) 30 [arXiv:1207.7235 [hep-ex]].

[3] K. G. Begeman, A. H. Broeils and R. H. Sanders, *"Extended rotation curves of spiral galaxies: Dark haloes and modified dynamics,"* Mon. Not. Roy. Astron. Soc. **249**, 523 (1991).

[4] R. A. Flores, B. Allgood, A. V. Kravtsov, J. R. Primack, D. A. Buote and J. S. Bullock, *"The Shape of galaxy cluster dark matter haloes: Systematics of its imprint on cluster gas, and comparison to observations,"* Mon. Not. Roy. Astron. Soc. **377**, 883 (2007) [astro-ph/0508226].

[5] A. Dressler, D. Lynden-Bell, D. Burstein, R. L. Davies, S. M. Faber, R. Terlevich and G. Wegner, *"Spectroscopy and photometry of elliptical galaxies. 1. A New distance estimator,"* Astrophys. J. **313**, 42 (1987).

[6] A. S. Bolton, S. Burles, L. V. E. Koopmans, T. Treu and L. A. Moustakas, *"The sloan lens acs survey. 1. a large spectroscopically selected sample of massive early-type lens galaxies,"* Astrophys. J. **638**, 703 (2006) [astro-ph/0511453].

[7] D. Clowe, M. Bradac, A. H. Gonzalez, M. Markevitch, S. W. Randall, C. Jones and D. Zaritsky, *"A direct empirical proof of the existence of dark matter,"* Astrophys. J. **648**, L109 (2006) [astro-ph/0608407].

[8] K. N. Abazajian *et al.* [SDSS Collaboration], *"The Seventh Data Release of the Sloan Digital Sky Survey,"* Astrophys. J. Suppl. **182**, 543 (2009) [arXiv:0812.0649 [astro-ph]].

[9] P. A. R. Ade *et al.* [Planck Collaboration], *"Planck 2013 results. XVI. Cosmological parameters,"* arXiv:1303.5076 [astro-ph.CO].

[10] R. J. Scherrer, M. S. Turner, *"On the Relic, Cosmic Abundance of Stable Weakly Interacting Massive Particles,"* Phys. Rev. **D33**, 1585 (1986).

[11] A. D. Sakharov, *"Violation of CP Invariance, C Asymmetry, and Baryon Asymmetry of the Universe,"* Pisma Zh. Eksp. Teor. Fiz. **5**, 32 (1967) [JETP Lett. **5**, 24 (1967)].

[12] V. A. Kuzmin, V. A. Rubakov and M. E. Shaposhnikov, *"On the Anomalous Electroweak Baryon Number Nonconservation in the Early Universe,"* Phys. Lett. B **155**, 36 (1985).

[13] N. S. Manton, *"Topology in the Weinberg-Salam Theory,"* Phys. Rev. D **28** (1983) 2019.

[14] F. R. Klinkhamer and N. S. Manton, *"A Saddle Point Solution in the Weinberg-Salam Theory,"* Phys. Rev. D **30**, 2212 (1984).

[15] P. B. Arnold and L. D. McLerran, *"Sphalerons, Small Fluctuations and Baryon Number Violation in Electroweak Theory,"* Phys. Rev. D **36**, 581 (1987).

[16] M. Dine, P. Huet and R. L. Singleton, Jr, *"Baryogenesis at the electroweak scale,"* Nucl. Phys. B **375**, 625 (1992).

[17] G. W. Anderson and L. J. Hall, *"The Electroweak phase transition and baryogenesis,"* Phys. Rev. D **45**, 2685 (1992).

[18] M. Dine, R. G. Leigh, P. Y. Huet, A. D. Linde and D. A. Linde, *"Towards the theory of the electroweak phase transition,"* Phys. Rev. D **46**, 550 (1992) [hep-ph/9203203].

[19] M. E. Shaposhnikov, *"Baryon Asymmetry of the Universe in Standard Electroweak Theory,"* Nucl. Phys. B **287**, 757 (1987).

[20] A. I. Bochkarev and M. E. Shaposhnikov, *"Electroweak Production of Baryon Asymmetry and Upper Bounds on the Higgs and Top Masses,"* Mod. Phys. Lett. A **2**, 417 (1987).

[21] M. E. Shaposhnikov, *"Structure of the High Temperature Gauge Ground State and Electroweak Production of the Baryon Asymmetry,"* Nucl. Phys. B **299**, 797 (1988).

[22] A. I. Bochkarev, S. V. Kuzmin and M. E. Shaposhnikov, *"Electroweak baryogenesis and the Higgs boson mass problem,"* Phys. Lett. B **244**, 275 (1990).

[23] K. Kajantie, M. Laine, K. Rummukainen and M. E. Shaposhnikov, *"The Electroweak phase transition: A Nonperturbative analysis,"* Nucl. Phys. B **466**, 189 (1996) [hep-lat/9510020].

[24] K. Kajantie, M. Laine, K. Rummukainen and M. E. Shaposhnikov, *"Is there a hot electroweak phase transition at m(H) larger or equal to m(W)?,"* Phys. Rev. Lett. **77**, 2887 (1996) [hep-ph/9605288].

[25] K. Kajantie, M. Laine, K. Rummukainen and M. E. Shaposhnikov, *"A Nonperturbative analysis of the finite T phase transition in SU(2) × U(1) electroweak theory,"* Nucl. Phys. B **493**, 413 (1997) [hep-lat/9612006].

[26] http://lephiggs.web.cern.ch/LEPHIGGS/papers/CERN-EP-98-046

[27] T. A. Chowdhury, M. Nemevšek, G. Senjanović and Y. Zhang, *"Dark Matter as the Trigger of Strong Electroweak Phase Transition,"* JCAP **1202**, 029 (2012) [arXiv:1110.5334 [hep-ph]].

[28] D. Borah and J. M. Cline, *"Inert Doublet Dark Matter with Strong Electroweak Phase Transition,"* Phys. Rev. D **86**, 055001 (2012) [arXiv:1204.4722 [hep-ph]].

[29] G. Gil, P. Chankowski and M. Krawczyk, *"Inert Dark Matter and Strong Electroweak Phase Transition,"* Phys. Lett. B **717**, 396 (2012) [arXiv:1207.0084 [hep-ph]].

[30] J. M. Cline and K. Kainulainen, *"Improved Electroweak Phase Transition with Subdominant Inert Doublet Dark Matter,"* Phys. Rev. D **87**, 071701 (2013) [arXiv:1302.2614 [hep-ph]].

[31] N. G. Deshpande and E. Ma, *"Pattern of Symmetry Breaking with Two Higgs Doublets,"* Phys. Rev. D **18**, 2574 (1978).

[32] E. Ma, *"Verifiable radiative seesaw mechanism of neutrino mass and dark matter,"* Phys. Rev. D **73**, 077301 (2006) [hep-ph/0601225].

[33] R. Barbieri, L. J. Hall, V. S. Rychkov, *"Improved naturalness with a heavy Higgs: An Alternative road to LHC physics,"* Phys. Rev. **D74**, 015007 (2006). [hep-ph/0603188].

[34] H. Martinez, A. Melfo, F. Nesti, G. Senjanović, *"Three Extra Mirror or Sequential Families: A Case for Heavy Higgs and Inert Doublet,"* Phys. Rev. Lett. **106**, 191802 (2011). [arXiv:1101.3796 [hep-ph]].

[35] A. Melfo, M. Nemevšek, F. Nesti, G. Senjanović, Y. Zhang, *"Inert Doublet Dark Matter and Mirror/Extra Families after Xenon100,"* Phys. Rev. **D84** (2011) 034009. [arXiv:1105.4611 [hep-ph]].

[36] M. Gell-Mann, P. Ramond, R. Slansky, *"Color Embeddings, Charge Assignments, and Proton Stability in Unified Gauge Theories,"* Rev. Mod. Phys. **50**, 721 (1978).

[37] F. Wilczek, A. Zee, *"Families from Spinors,"* Phys. Rev. **D25**, 553 (1982).

[38] G. Senjanović, F. Wilczek, A. Zee, *"Reflections On Mirror Fermions,"* Phys. Lett. **B141**, 389 (1984).

[39] J. Bagger, S. Dimopoulos, *"O(18) Revived: Splitting The Spinor,"* Nucl. Phys. **B244**, 247 (1984).

[40] T. D. Lee, C. -N. Yang, *"Question of Parity Conservation in Weak Interactions,"* Phys. Rev. **104**, 254-258 (1956).

[41] L. Lopez Honorez, E. Nezri, J. F. Oliver and M. H. G. Tytgat, *"The Inert Doublet Model: An Archetype for Dark Matter,"* JCAP **0702**, 028 (2007) [hep-ph/0612275].

[42] S. Andreas, T. Hambye and M. H. G. Tytgat, *"WIMP dark matter, Higgs exchange and DAMA,"* JCAP **0810**, 034 (2008) [arXiv:0808.0255 [hep-ph]].

[43] T. Hambye and M. H. G. Tytgat, *"Electroweak symmetry breaking induced by dark matter,"* Phys. Lett. B **659**, 651 (2008) [arXiv:0707.0633 [hep-ph]].

[44] E. M. Dolle and S. Su, *"The Inert Dark Matter,"* Phys. Rev. D **80**, 055012 (2009) [arXiv:0906.1609 [hep-ph]].

[45] L. Lopez Honorez and C. E. Yaguna, *"A new viable region of the inert doublet model,"* JCAP **1101**, 002 (2011) [arXiv:1011.1411 [hep-ph]].

[46] P. Agrawal, E. M. Dolle and C. A. Krenke, *"Signals of Inert Doublet Dark Matter in Neutrino Telescopes,"* Phys. Rev. D **79**, 015015 (2009) [arXiv:0811.1798 [hep-ph]].

[47] S. Andreas, M. H. G. Tytgat and Q. Swillens, *"Neutrinos from Inert Doublet Dark Matter,"* JCAP **0904**, 004 (2009) [arXiv:0901.1750 [hep-ph]].

[48] E. Nezri, M. H. G. Tytgat and G. Vertongen, *"e+ and anti-p from inert doublet model dark matter,"* JCAP **0904**, 014 (2009) [arXiv:0901.2556 [hep-ph]].

[49] Q. -H. Cao, E. Ma and G. Rajasekaran, *"Observing the Dark Scalar Doublet and its Impact on the Standard-Model Higgs Boson at Colliders,"* Phys. Rev. D **76**, 095011 (2007) [arXiv:0708.2939 [hep-ph]].

[50] E. Lundstrom, M. Gustafsson and J. Edsjo, *"The Inert Doublet Model and LEP II Limits,"* Phys. Rev. D **79**, 035013 (2009) [arXiv:0810.3924 [hep-ph]].

[51] E. Dolle, X. Miao, S. Su and B. Thomas, *"Dilepton Signals in the Inert Doublet Model,"* Phys. Rev. D **81**, 035003 (2010) [arXiv:0909.3094 [hep-ph]].

[52] M. Gustafsson, *"The Inert Doublet Model and Its Phenomenology,"* PoS CHARGED **2010**, 030 (2010) [arXiv:1106.1719 [hep-ph]].

[53] M. Gustafsson, S. Rydbeck, L. Lopez-Honorez and E. Lundstrom, *"Status of the Inert Doublet Model and the Role of multileptons at the LHC,"* Phys. Rev. D **86**, 075019 (2012) [arXiv:1206.6316 [hep-ph]].

[54] M. Aoki, S. Kanemura and H. Yokoya, *"Reconstruction of Inert Doublet Scalars at the International Linear Collider,"* Phys. Lett. B **725**, 302 (2013) [arXiv:1303.6191 [hep-ph]].

[55] A. Arhrib, Y. -L. S. Tsai, Q. Yuan and T. -C. Yuan, *"An Updated Analysis of Inert Higgs Doublet Model in light of XENON100, PLANCK, AMS-02 and LHC,"* arXiv:1310.0358 [hep-ph].

[56] I. F. Ginzburg, K. A. Kanishev, M. Krawczyk and D. Sokolowska, *"Evolution of Universe to the present inert phase,"* Phys. Rev. D **82**, 123533 (2010) [arXiv:1009.4593 [hep-ph]].

[57] M. Gustafsson, E. Lundstrom, L. Bergstrom and J. Edsjo, *"Significant Gamma Lines from Inert Higgs Dark Matter,"* Phys. Rev. Lett. **99**, 041301 (2007) [astro-ph/0703512 [ASTRO-PH]].

[58] S. Profumo, M. J. Ramsey-Musolf and G. Shaughnessy, *"Singlet Higgs phenomenology and the electroweak phase transition,"* JHEP **0708**, 010 (2007) [arXiv:0705.2425 [hep-ph]].

[59] A. Ahriche, *"What is the criterion for a strong first order electroweak phase transition in singlet models?,"* Phys. Rev. D **75**, 083522 (2007) [hep-ph/0701192].

[60] J. R. Espinosa, T. Konstandin, F. Riva, *"Strong Electroweak Phase Transitions in the Standard Model with a Singlet,"* Nucl. Phys. **B854** (2012) 592-630. [arXiv:1107.5441 [hep-ph]].

[61] J. M. Cline and K. Kainulainen, *"Electroweak baryogenesis and dark matter from a singlet Higgs,"* JCAP **1301**, 012 (2013) [arXiv:1210.4196 [hep-ph]].

[62] J. M. Cline, K. Kainulainen, P. Scott and C. Weniger, *"Update on scalar singlet dark matter,"* arXiv:1306.4710 [hep-ph].

[63] V. Barger, P. Langacker, M. McCaskey, M. Ramsey-Musolf and G. Shaughnessy, *"Complex Singlet Extension of the Standard Model,"* Phys. Rev. D **79**, 015018 (2009) [arXiv:0811.0393 [hep-ph]].

[64] M. Gonderinger, H. Lim and M. J. Ramsey-Musolf, *"Complex Scalar Singlet Dark Matter: Vacuum Stability and Phenomenology,"* Phys. Rev. D **86**, 043511 (2012) [arXiv:1202.1316 [hep-ph]].

[65] A. Ahriche and S. Nasri, *"Light Dark Matter, Light Higgs and the Electroweak Phase Transition,"* Phys. Rev. D **85**, 093007 (2012) [arXiv:1201.4614 [hep-ph]].

[66] S. Das, P. J. Fox, A. Kumar, N. Weiner, *"The Dark Side of the Electroweak Phase Transition,"* JHEP **1011**, 108 (2010). [arXiv:0910.1262 [hep-ph]];

[67] M. Carena, N. R. Shah and C. E. M. Wagner, *"Light Dark Matter and the Electroweak Phase Transition in the NMSSM,"* arXiv:1110.4378 [hep-ph].

[68] A. Ahriche and S. Nasri, *"Dark matter and strong electroweak phase transition in a radiative neutrino mass model,"* JCAP **1307**, 035 (2013) [arXiv:1304.2055].

[69] M. Cirelli, N. Fornengo, A. Strumia, *"Minimal dark matter,"* Nucl. Phys. **B753**, 178-194 (2006). [hep-ph/0512090].

[70] T. Hambye, F. -S. Ling, L. Lopez Honorez and J. Rocher, *"Scalar Multiplet Dark Matter,"* JHEP **0907**, 090 (2009) [Erratum-ibid. **1005**, 066 (2010)] [arXiv:0903.4010 [hep-ph]].

[71] M. S. Carena, A. Megevand, M. Quiros and C. E. M. Wagner, *"Electroweak baryogenesis and new TeV fermions,"* Nucl. Phys. B **716**, 319 (2005) [hep-ph/0410352].

[72] H. Davoudiasl, I. Lewis and E. Ponton, *"Electroweak Phase Transition, Higgs Diphoton Rate, and New Heavy Fermions,"* arXiv:1211.3449 [hep-ph].

[73] G. Senjanović, *"Phase Transitions at High Temperature,"* Lecture notes on High Temperature Field theory and Topological defects.

[74] D. A. Kirzhnits and A. D. Linde, *"Symmetry Behavior in Gauge Theories,"* Annals Phys. **101**, 195 (1976).

[75] S. Weinberg, *"Gauge and Global Symmetries at High Temperature,"* Phys. Rev. D **9**, 3357 (1974).

[76] C. W. Bernard, *"Feynman Rules for Gauge Theories at Finite Temperature,"* Phys. Rev. D **9**, 3312 (1974).

[77] L. Dolan and R. Jackiw, *"Symmetry Behavior at Finite Temperature,"* Phys. Rev. D **9**, 3320 (1974).

[78] R. N. Mohapatra and G. Senjanović, *"Soft CP Violation at High Temperature,"* Phys. Rev. Lett. **42**, 1651 (1979).

[79] R. N. Mohapatra and G. Senjanović, *"Broken Symmetries at High Temperature,"* Phys. Rev. D **20**, 3390 (1979).

[80] Ashok. Das, "Finite Temperature Field Theory," World Scientific (1997) 416 p

[81] J. I. Kapusta and C. Gale, "Finite-temperature field theory: Principles and applications," Cambridge, UK: Univ. Pr. (2006) 428 p

[82] M. Le Bellac, "Thermal Field Theory," Cambridge, UK: Univ. Pr. (2000) 272 p

[83] N. P. Landsman and C. G. van Weert, *"Real and Imaginary Time Field Theory at Finite Temperature and Density,"* Phys. Rept. **145**, 141 (1987).

[84] M. Quiros, *"Finite temperature field theory and phase transitions,"* hep-ph/9901312.

[85] M. Laine, *"Basics of Thermal Field theory- A Tutorial of Perturbative Computations,"* Lecture notes, University of Beilefeld

[86] T. Matsubara, *"A New approach to quantum statistical mechanics,"* Prog. Theor. Phys. **14**, 351 (1955).

[87] S. R. Coleman and E. J. Weinberg, *"Radiative Corrections as the Origin of Spontaneous Symmetry Breaking,"* Phys. Rev. D **7**, 1888 (1973).

[88] R. Jackiw, *"Functional evaluation of the effective potential,"* Phys. Rev. D **9**, 1686 (1974).

[89] N. Goldenfeld, "Lectures On Phase Transitions And The Renormalization Group," Frontiers in Physics, Westview Press (1992), 414 pages

[90] R. R. Parwani, *"Resummation in a hot scalar field theory,"* Phys. Rev. D **45**, 4695 (1992) [Erratum-ibid. D **48**, 5965 (1993)] [hep-ph/9204216].

[91] P. B. Arnold and O. Espinosa, *"The Effective potential and first order phase transitions: Beyond leading-order,"* Phys. Rev. D **47**, 3546 (1993) [Erratum-ibid. D **50**, 6662 (1994)] [hep-ph/9212235].

[92] J. R. Espinosa, M. Quiros and F. Zwirner, *"On the nature of the electroweak phase transition,"* Phys. Lett. B **314**, 206 (1993) [hep-ph/9212248].

[93] V. A. Rubakov and M. E. Shaposhnikov, *"Electroweak baryon number nonconservation in the early universe and in high-energy collisions,"* Usp. Fiz. Nauk **166**, 493 (1996) [Phys. Usp. **39**, 461 (1996)] [hep-ph/9603208].

[94] M. Trodden, *"Electroweak baryogenesis,"* Rev. Mod. Phys. **71**, 1463 (1999) [hep-ph/9803479].

[95] A. Riotto, *"Theories of baryogenesis,"* hep-ph/9807454.

[96] M. Dine and A. Kusenko, *"The Origin of the matter - antimatter asymmetry,"* Rev. Mod. Phys. **76**, 1 (2003) [hep-ph/0303065].

[97] J. M. Cline, *"Baryogenesis,"* hep-ph/0609145.

[98] A. Mazumdar, *"The origin of dark matter, matter-anti-matter asymmetry, and inflation,"* arXiv:1106.5408 [hep-ph].

[99] D. E. Morrissey and M. J. Ramsey-Musolf, *"Electroweak baryogenesis,"* New J. Phys. **14**, 125003 (2012) [arXiv:1206.2942 [hep-ph]].

[100] E. A. Bogomolov, N. D. Lubyanaya, V. A. Romanov, S. V. Stepanov and M. S. Shulakova, *"A Stratospheric Magnetic Spectrometer Investigation Of The Singly Charged Component Spectra And Composition Of The Primary And Secondary Cosmic Radiation. (talk),"* In *Kyoto 1979, Proceedings, 16th International Cosmic Ray Conference, Vol.1*, 330-335

[101] R. L. Golden, S. Horan, B. G. Mauger, G. D. Badhwar, J. L. Lacy, S. A. Stephens, R. R. Daniel and J. E. Zipse, *"Evidence For The Existence Of Cosmic Ray Anti-protons,"* Phys. Rev. Lett. **43** (1979) 1196.

[102] A. Buffington, S. M. Schindler and C. R. Pennypacker, *"A measurement of the cosmic-ray antiproton flux and a search for antihelium,"* Astrophys. J. **248**, 1179 (1981).

[103] S. P. Ahlen, S. Barwick, J. J. Beatty, C. R. Bower, G. Gerbier, R. M. Heinz, D. Lowder and S. Mckee *et al.*, *"New Limit on the Low-energy Anti-proton / Proton Ratio in the Galactic Cosmic Radiation,"* Phys. Rev. Lett. **61** (1988) 145.

[104] G. Steigman, *"Observational tests of antimatter cosmologies,"* Ann. Rev. Astron. Astrophys. **14** (1976) 339.

[105] J. Alcaraz *et al.* [AMS Collaboration], *"Search for anti-helium in cosmic rays,"* Phys. Lett. B **461** (1999) 387 [hep-ex/0002048].

[106] R. H. Cyburt, *"Primordial nucleosynthesis for the new cosmology: Determining uncertainties and examining concordance,"* Phys. Rev. D **70** (2004) 023505 [astro-ph/0401091].

[107] W. Hu and S. Dodelson, *"Cosmic microwave background anisotropies,"* Ann. Rev. Astron. Astrophys. **40** (2002) 171 [astro-ph/0110414].

[108] S. Sarkar, *"Measuring the baryon content of the universe: BBN versus CMB,"* astro-ph/0205116.

[109] I. Affleck and M. Dine, *"A New Mechanism for Baryogenesis,"* Nucl. Phys. B **249**, 361 (1985).

[110] K. Enqvist and A. Mazumdar, *"Cosmological consequences of MSSM flat directions,"* Phys. Rept. **380** (2003) 99 [hep-ph/0209244].

[111] R. Allahverdi and A. Mazumdar, *"A mini review on Affleck-Dine baryogenesis,"* New J. Phys. **14** (2012) 125013.

[112] K. Fujikawa, *"Path Integral Measure for Gauge Invariant Fermion Theories,"* Phys. Rev. Lett. **42**, 1195 (1979).

[113] K. Fujikawa, *"Path Integral for Gauge Theories with Fermions,"* Phys. Rev. D **21**, 2848 (1980) [Erratum-ibid. D **22**, 1499 (1980)].

[114] G. 't Hooft, *"Symmetry Breaking Through Bell-Jackiw Anomalies,"* Phys. Rev. Lett. **37** (1976) 8.

[115] G. 't Hooft, *"Computation of the Quantum Effects Due to a Four-Dimensional Pseudoparticle,"* Phys. Rev. D **14** (1976) 3432 [Erratum-ibid. D **18** (1978) 2199].

[116] R. F. Dashen, B. Hasslacher and A. Neveu, *"Nonperturbative Methods and Extended Hadron Models in Field Theory. 3. Four-Dimensional Nonabelian Models,"* Phys. Rev. D **10** (1974) 4138.

[117] V. Soni, *"Possible Classical Solutions In The Weinberg-salam Model,"* Phys. Lett. B **93** (1980) 101.

[118] S. Y. .Khlebnikov and M. E. Shaposhnikov, *"The Statistical Theory of Anomalous Fermion Number Nonconservation,"* Nucl. Phys. B **308** (1988) 885.

[119] M. Dine, O. Lechtenfeld, B. Sakita, W. Fischler and J. Polchinski, *"Baryon Number Violation at High Temperature in the Standard Model,"* Nucl. Phys. B **342** (1990) 381.

[120] T. Akiba, H. Kikuchi and T. Yanagida, *"Static Minimum Energy Path From a Vacuum to a Sphaleron in the Weinberg-Salam Model,"* Phys. Rev. D **38** (1988) 1937.

[121] T. Akiba, H. Kikuchi and T. Yanagida, *"The Free Energy of the Sphaleron in the Weinberg-Salam Model,"* Phys. Rev. D **40** (1989) 588.

[122] L. G. Yaffe, *"Static Solutions of $SU(2)$ Higgs Theory,"* Phys. Rev. D **40** (1989) 3463.

[123] P. B. Arnold and L. D. McLerran, *"The Sphaleron Strikes Back,"* Phys. Rev. D **37** (1988) 1020.

[124] L. Carson, X. Li, L. D. McLerran and R. -T. Wang, *"Exact Computation of the Small Fluctuation Determinant Around a Sphaleron,"* Phys. Rev. D **42** (1990) 2127.

[125] L. Carson and L. D. McLerran, *"Approximate Computation of the Small Fluctuation Determinant Around a Sphaleron,"* Phys. Rev. D **41** (1990) 647.

[126] F. R. Klinkhamer and R. Laterveer, *"The Sphaleron at finite mixing angle,"* Z. Phys. C **53** (1992) 247.

[127] B. Kleihaus, J. Kunz and Y. Brihaye, *"The Electroweak sphaleron at physical mixing angle,"* Phys. Lett. B **273** (1991) 100.

[128] J. Kunz, B. Kleihaus and Y. Brihaye, *"Sphalerons at finite mixing angle,"* Phys. Rev. D **46** (1992) 3587.

[129] Y. Brihaye, B. Kleihaus and J. Kunz, *"Sphalerons at finite mixing angle and singular gauges,"* Phys. Rev. D **47** (1993) 1664.

[130] S. Braibant, Y. Brihaye and J. Kunz, *"Sphalerons at finite temperature,"* Int. J. Mod. Phys. A **8** (1993) 5563 [hep-ph/9302314].

[131] Y. Brihaye and J. Kunz, *"Electroweak bubbles and sphalerons,"* Phys. Rev. D **48** (1993) 3884 [hep-ph/9304256].

[132] J. Choi, *"Sphalerons in the standard model with a real Higgs singlet,"* Phys. Lett. B **345** (1995) 253 [hep-ph/9409360].

[133] B. M. Kastening, R. D. Peccei and X. Zhang, *"Sphalerons in the two doublet Higgs model,"* Phys. Lett. B **266** (1991) 413.

[134] J. M. Moreno, D. H. Oaknin and M. Quiros, *"Sphalerons in the MSSM,"* Nucl. Phys. B **483** (1997) 267 [hep-ph/9605387].

[135] K. Funakubo, A. Kakuto, S. Tao and F. Toyoda, *"Sphalerons in the NMSSM,"* Prog. Theor. Phys. **114** (2006) 1069 [hep-ph/0506156].

[136] A. Ahriche, *"Sphalerons on Orbifolds,"* Eur. Phys. J. C **66** (2010) 333 [arXiv:0904.0700 [hep-ph]].

[137] A. Ahriche, T. A. Chowdhury and S. Nasri, *"Sphalerons and the Electroweak Phase Transition in Models with Higher Scalar Representations,"* in preparation.

[138] P. B. Arnold, D. Son and L. G. Yaffe, *"The Hot baryon violation rate is O (alpha-w**5 T**4),"* Phys. Rev. D **55** (1997) 6264 [hep-ph/9609481].

[139] D. Bodeker, *"On the effective dynamics of soft nonAbelian gauge fields at finite temperature,"* Phys. Lett. B **426**, 351 (1998) [hep-ph/9801430].

[140] P. B. Arnold, D. T. Son and L. G. Yaffe, *"Effective dynamics of hot, soft nonAbelian gauge fields. Color conductivity and log(1/alpha) effects,"* Phys. Rev. D **59**, 105020 (1999) [hep-ph/9810216].

[141] G. D. Moore, *"Sphaleron rate in the symmetric electroweak phase,"* Phys. Rev. D **62** (2000) 085011 [hep-ph/0001216].

[142] A. I. Bochkarev, S. V. Kuzmin and M. E. Shaposhnikov, *"On the Model Dependence of the Cosmological Upper Bound on the Higgs Boson and Top Quark Masses,"* Phys. Rev. D **43** (1991) 369.

[143] J. Baacke and S. Junker, *"Quantum fluctuations around the electroweak sphaleron,"* Phys. Rev. D **49** (1994) 2055 [hep-ph/9308310], *"Quantum fluctuations of the electroweak sphaleron: Erratum and addendum,"* Phys. Rev. D **50** (1994) 4227 [hep-th/9402078].

[144] S. S. AbdusSalam and T. A. Chowdhury, *"Scalar Representations in the Light of Electroweak Phase Transition and Cold Dark Matter Phenomenology,"* JCAP **1405** (2014) 026 [arXiv:1310.8152 [hep-ph]].

[145] M. Gell-Mann, M. L. Goldberger, N. M. Kroll and F. E. Low, *"Amelioration of divergence difficulties in the theory of weak interactions,"* Phys. Rev. **179** (1969) 1518.

[146] S. Weinberg, *"Physical Processes in a Convergent Theory of the Weak and Electromagnetic Interactions,"* Phys. Rev. Lett. **27** (1971) 1688.

[147] J. Schechter and Y. Ueda, *"High-energy behavior of gauge-theory tree graphs. (erratum),"* Phys. Rev. D **7** (1973) 3119 [Erratum-ibid. D **8** (1973) 3709].

[148] J. M. Cornwall, D. N. Levin and G. Tiktopoulos, *"Uniqueness of spontaneously broken gauge theories,"* Phys. Rev. Lett. **30**, 1268 (1973) [Erratum-ibid. **31**, 572 (1973)].

[149] J. M. Cornwall, D. N. Levin and G. Tiktopoulos, *"Derivation of Gauge Invariance from High-Energy Unitarity Bounds on the s Matrix,"* Phys. Rev. D **10** (1974) 1145 [Erratum-ibid. D **11** (1975) 972].

[150] D. N. Levin and G. Tiktopoulos, *"A Search for All Renormalizable Interactions,"* Phys. Rev. D **12** (1975) 415.

[151] J. S. Bell, *"High-energy Behavior Of Tree Diagrams In Gauge Theories,"* Nucl. Phys. B **60** (1973) 427.

[152] C. H. Llewellyn Smith, *"High-Energy Behavior and Gauge Symmetry,"* Phys. Lett. B **46** (1973) 233.

[153] B. W. Lee, C. Quigg and H. B. Thacker, *"Weak Interactions at Very High-Energies: The Role of the Higgs Boson Mass,"* Phys. Rev. D **16** (1977) 1519.

[154] W. J. Marciano, G. Valencia and S. Willenbrock, *"Renormalization Group Improved Unitarity Bounds on the Higgs Boson and Top Quark Masses,"* Phys. Rev. D **40** (1989) 1725.

[155] T. P. Cheng, E. Eichten and L. F. Li, *"Higgs Phenomena in Asymptotically Free Gauge Theories,"* Phys. Rev. D **9**, 2259 (1974).

[156] M. E. Machacek and M. T. Vaughn, *"Two Loop Renormalization Group Equations in a General Quantum Field Theory. 1. Wave Function Renormalization,"* Nucl. Phys. B **222**, 83 (1983).

[157] M. E. Machacek and M. T. Vaughn, *"Two Loop Renormalization Group Equations in a General Quantum Field Theory. 2. Yukawa Couplings,"* Nucl. Phys. B **236**, 221 (1984).

[158] M. E. Machacek and M. T. Vaughn, *"Two Loop Renormalization Group Equations in a General Quantum Field Theory. 3. Scalar Quartic Couplings,"* Nucl. Phys. B **249**, 70 (1985).

[159] C. Ford, I. Jack and D. R. T. Jones, *"The Standard model effective potential at two loops,"* Nucl. Phys. B **387**, 373 (1992) [Erratum-ibid. B **504**, 551 (1997)] [hep-ph/0111190].

[160] P. M. Ferreira and D. R. T. Jones, *"Bounds on scalar masses in two Higgs doublet models,"* JHEP **0908**, 069 (2009) [arXiv:0903.2856 [hep-ph]].

[161] M. Taoso, G. Bertone and A. Masiero, *"Dark Matter Candidates: A Ten-Point Test,"* JCAP **0803**, 022 (2008) [arXiv:0711.4996 [astro-ph]].

[162] T. Hambye, *"On the stability of particle dark matter,"* PoS IDM **2010**, 098 (2011) [arXiv:1012.4587 [hep-ph]].

[163] M. Gustafsson, T. Hambye and T. Scarna, *"Effective Theory of Dark Matter Decay into Monochromatic Photons and its Implications: Constraints from Associated Cosmic-Ray Emission,"* Phys. Lett. B **724**, 288 (2013) [arXiv:1303.4423 [hep-ph]].

[164] K. Kannike, *"Vacuum Stability Conditions From Copositivity Criteria,"* Eur. Phys. J. C **72**, 2093 (2012) [arXiv:1205.3781 [hep-ph]].

[165] M. Magg and C. Wetterich, *"Neutrino Mass Problem And Gauge Hierarchy,"* Phys. Lett. **B94** (1980) 61; G. Lazarides, Q. Shafi and C. Wetterich, *"Proton Lifetime and Fermion Masses in an SO(10) Model,"* Nucl. Phys. **B181** (1981) 287; R.N. Mohapatra and G. Senjanović, *"Neutrino Masses and Mixings in Gauge Models with Spontaneous Parity Violation,"* Phys. Rev. **D23** (1981) 165; T.P. Cheng and L.-F. Li, *"Neutrino Masses, Mixings and Oscillations in SU(2) x U(1) Models of Electroweak Interactions,"* Phys. Rev. **D22** (1980) 2860.

[166] D. S. Akerib *et al.* [CDMS Collaboration], *"Limits on spin-independent wimp-nucleon interactions from the two-tower run of the cryogenic dark matter search,"* Phys. Rev. Lett. **96**, 011302 (2006) [astro-ph/0509259].

[167] M. Cirelli, A. Strumia and M. Tamburini, *"Cosmology and Astrophysics of Minimal Dark Matter,"* Nucl. Phys. B **787**, 152 (2007) [arXiv:0706.4071 [hep-ph]].

[168] P. Fileviez Perez, H. H. Patel, M. .J. Ramsey-Musolf and K. Wang, *"Triplet Scalars and Dark Matter at the LHC,"* Phys. Rev. D **79**, 055024 (2009) [arXiv:0811.3957 [hep-ph]].

[169] K. Hally, H. E. Logan and T. Pilkington, *"Constraints on large scalar multiplets from perturbative unitarity,"* Phys. Rev. D **85**, 095017 (2012) [arXiv:1202.5073 [hep-ph]].

[170] K. Earl, K. Hartling, H. E. Logan and T. Pilkington, *"Constraining models with a large scalar multiplet,"* arXiv:1303.1244 [hep-ph].

[171] M. A. Schmidt, *"Renormalization group evolution in the type I+ II seesaw model,"* Phys. Rev. D **76**, 073010 (2007) [Erratum-ibid. D **85**, 099903 (2012)] [arXiv:0705.3841 [hep-ph]].

[172] D. C. Kennedy and B. W. Lynn, *"Electroweak Radiative Corrections with an Effective Lagrangian: Four Fermion Processes,"* Nucl. Phys. B **322**, 1 (1989).

[173] M. E. Peskin and T. Takeuchi, *"Estimation of oblique electroweak corrections,"* Phys. Rev. D **46**, 381 (1992).

[174] G. Passarino and M. J. G. Veltman, *"One Loop Corrections for e+ e- Annihilation Into mu+ mu- in the Weinberg Model,"* Nucl. Phys. B **160**, 151 (1979).

[175] I. Maksymyk, C. P. Burgess and D. London, *"Beyond S, T and U,"* Phys. Rev. D **50**, 529 (1994) [hep-ph/9306267].

[176] A. Pierce and J. Thaler, *"Natural Dark Matter from an Unnatural Higgs Boson and New Colored Particles at the TeV Scale,"* JHEP **0708** (2007) 026 [hep-ph/0703056 [HEP-PH]].

[177] R. Barbieri, A. Pomarol, R. Rattazzi and A. Strumia, *"Electroweak symmetry breaking after LEP-1 and LEP-2,"* Nucl. Phys. B **703**, 127 (2004) [hep-ph/0405040].

[178] J. Beringer *et al.* [Particle Data Group Collaboration], *"Review of Particle Physics (RPP),"* Phys. Rev. D **86**, 010001 (2012).

[179] P. B. Arnold, *"The Electroweak phase transition: Part 1. Review of perturbative methods,"* In *Vladimir 1994, Proceedings, Quarks '94* 71-86, and Washington U. Seattle - UW-PT-94-13 (94/10,rec.Oct.) 17 p [hep-ph/9410294].

[180] E. J. Weinberg and A. -q. Wu, *"Understanding Complex Perturbative Effective Potentials,"* Phys. Rev. D **36**, 2474 (1987).

[181] E. J. Weinberg, *"Radiative corrections as the origin of spontaneous symmetry breaking,"* hep-th/0507214.

[182] N. K. Nielsen, *"On the Gauge Dependence of Spontaneous Symmetry Breaking in Gauge Theories,"* Nucl. Phys. B **101**, 173 (1975).

[183] W. Buchmuller, Z. Fodor and A. Hebecker, *"Gauge invariant treatment of the electroweak phase transition,"* Phys. Lett. B **331**, 131 (1994) [hep-ph/9403391].

[184] D. Boyanovsky, D. Brahm, R. Holman and D. S. Lee, *"The Gauge invariant effective potential: Equilibrium and nonequilibrium aspects,"* Phys. Rev. D **54**, 1763 (1996) [hep-ph/9603337].

[185] H. H. Patel and M. J. Ramsey-Musolf, *"Baryon Washout, Electroweak Phase Transition, and Perturbation Theory,"* JHEP **1107**, 029 (2011) [arXiv:1101.4665 [hep-ph]].

[186] M. Laine, G. Nardini and K. Rummukainen, *"Lattice study of an electroweak phase transition at m_h 126 GeV,"* JCAP **1301**, 011 (2013) [arXiv:1211.7344 [hep-ph]].

[187] J. R. Espinosa and M. Quiros, *"The Electroweak phase transition with a singlet,"* Phys. Lett. B **305**, 98 (1993) [hep-ph/9301285].

[188] N. Turok and J. Zadrozny, *"Phase transitions in the two doublet model,"* Nucl. Phys. B **369**, 729 (1992).

[189] J. M. Cline, K. Kainulainen and A. P. Vischer, *"Dynamics of two Higgs doublet CP violation and baryogenesis at the electroweak phase transition,"* Phys. Rev. D **54**, 2451 (1996) [hep-ph/9506284].

[190] J. M. Cline and P. -A. Lemieux, *"Electroweak phase transition in two Higgs doublet models,"* Phys. Rev. D **55**, 3873 (1997) [hep-ph/9609240].

[191] J. M. Cline, K. Kainulainen and M. Trott, *"Electroweak Baryogenesis in Two Higgs Doublet Models and B meson anomalies,"* JHEP **1111**, 089 (2011) [arXiv:1107.3559 [hep-ph]].

[192] J. Shu and Y. Zhang, *"Impact of a CP Violating Higgs: from LHC to Baryogenesis,"* Phys. Rev. Lett. **111**, 091801 (2013) [arXiv:1304.0773 [hep-ph]].

[193] H. H. Patel and M. J. Ramsey-Musolf, *"Stepping Into Electroweak Symmetry Breaking: Phase Transitions and Higgs Phenomenology,"* arXiv:1212.5652 [hep-ph].

[194] J. Kehayias and S. Profumo, *"Semi-Analytic Calculation of the Gravitational Wave Signal From the Electroweak Phase Transition for General Quartic Scalar Effective Potentials,"* JCAP **1003**, 003 (2010) [arXiv:0911.0687 [hep-ph]].

[195] A. Arhrib, R. Benbrik, M. Chabab, G. Moultaka, M. C. Peyranere, L. Rahili and J. Ramadan, *"The Higgs Potential in the Type II Seesaw Model,"* Phys. Rev. D **84**, 095005 (2011) [arXiv:1105.1925 [hep-ph]].

[196] G. Aad *et al.* [ATLAS Collaboration], *"Search for doubly-charged Higgs bosons in like-sign dilepton final states at $\sqrt{s} = 7$ TeV with the ATLAS detector,"* Eur. Phys. J. C **72**, 2244 (2012) [arXiv:1210.5070 [hep-ex]].

[197] A. Melfo, M. Nemevsek, F. Nesti, G. Senjanović and Y. Zhang, *"Type II Seesaw at LHC: The Roadmap,"* Phys. Rev. D **85**, 055018 (2012) [arXiv:1108.4416 [hep-ph]].

[198] J. R. Espinosa, *"Dominant two loop corrections to the MSSM finite temperature effective potential,"* Nucl. Phys. B **475** (1996) 273 [hep-ph/9604320].

[199] M. Laine, *"Electroweak phase transition beyond the standard model,"* hep-ph/0010275.

[200] A. Megevand, *"First order cosmological phase transitions in the radiation dominated era,"* Phys. Rev. D **69**, 103521 (2004) [hep-ph/0312305].

[201] A. Megevand and A. D. Sanchez, *"Supercooling and phase coexistence in cosmological phase transitions,"* Phys. Rev. D **77**, 063519 (2008) [arXiv:0712.1031 [hep-ph]].

[202] ATLAS-CONF-2013-011, *"Search for invisible decays of a Higgs boson produced in association with a Z boson in ATLAS,"* CERN, March, 2013.

[203] The LEP SUSY Working Group, http://lepsusy.web.cern.ch/lepsusy/LEPSUSYWG/01-03.1

[204] K. Griest and D. Seckel, *"Three exceptions in the calculation of relic abundances,"* Phys. Rev. D **43**, 3191 (1991).

[205] N. D. Christensen and C. Duhr, *"FeynRules - Feynman rules made easy,"* Comput. Phys. Commun. **180**, 1614 (2009) [arXiv:0806.4194 [hep-ph]].

[206] J. Giedt, A. W. Thomas and R. D. Young, *"Dark matter, the CMSSM and lattice QCD,"* Phys. Rev. Lett. **103**, 201802 (2009) [arXiv:0907.4177 [hep-ph]].

[207] E. Aprile *et al.* [XENON100 Collaboration], *"Dark Matter Results from 100 Live Days of XENON100 Data,"* Phys. Rev. Lett. **107**, 131302 (2012) [arXiv:1104.2549 [astro-ph.CO]].

[208] E. Aprile *et al.* [XENON100 Collaboration], *"Dark Matter Results from 225 Live Days of XENON100 Data,"* Phys. Rev. Lett. **109**, 181301 (2012) [arXiv:1207.5988 [astro-ph.CO]].

[209] E. Aprile [XENON1T Collaboration], *"The XENON1T Dark Matter Search Experiment,"* arXiv:1206.6288 [astro-ph.IM].

[210] J. R. Espinosa, T. Konstandin, J. M. No and M. Quiros, *"Some Cosmological Implications of Hidden Sectors,"* Phys. Rev. D **78** (2008) 123528 [arXiv:0809.3215 [hep-ph]].

[211] G. Belanger, F. Boudjema, P. Brun, A. Pukhov, S. Rosier-Lees, P. Salati and A. Semenov, *"Indirect search for dark matter with micrOMEGAs2.4,"* Comput. Phys. Commun. **182**, 842 (2011) [arXiv:1004.1092 [hep-ph]].

[212] F. Feroz, B. C. Allanach, M. Hobson, S. S. AbdusSalam, R. Trotta and A. M. Weber, *"Bayesian Selection of sign(mu) within mSUGRA in Global Fits Including WMAP5 Results,"* JHEP **0810** (2008) 064 [arXiv:0807.4512 [hep-ph]].

[213] S. S. AbdusSalam, B. C. Allanach, M. J. Dolan, F. Feroz and M. P. Hobson, *"Selecting a Model of Supersymmetry Breaking Mediation,"* Phys. Rev. D **80** (2009) 035017 [arXiv:0906.0957 [hep-ph]].

[214] S. S. AbdusSalam and F. Quevedo, *"Cold Dark Matter Hypotheses in the MSSM,"* Phys. Lett. B **700** (2011) 343 [arXiv:1009.4308 [hep-ph]].

[215] J. R. Ellis, M. K. Gaillard and D. V. Nanopoulos, *"A Phenomenological Profile of the Higgs Boson,"* Nucl. Phys. B **106**, 292 (1976).

[216] M. A. Shifman, A. I. Vainshtein, M. B. Voloshin and V. I. Zakharov, *"Low-Energy Theorems for Higgs Boson Couplings to Photons,"* Sov. J. Nucl. Phys. **30**, 711 (1979) [Yad. Fiz. **30**, 1368 (1979)].

[217] M. Carena, I. Low and C. E. M. Wagner, *"Implications of a Modified Higgs to Diphoton Decay Width,"* JHEP **1208**, 060 (2012) [arXiv:1206.1082 [hep-ph]].

[218] J. Fan and M. Reece, *"Probing Charged Matter Through Higgs Diphoton Decay, Gamma Ray Lines, and EDMs,"* JHEP **1306**, 004 (2013) [arXiv:1301.2597].

[219] I. Picek and B. Radovcic, *"Enhancement of $h \to \gamma\gamma$ by seesaw-motivated exotic scalars,"* Phys. Lett. B **719** (2013) 404 [arXiv:1210.6449 [hep-ph]].

[220] V. Brdar, I. Picek and B. Radovcic, *"Radiative Neutrino Mass with Scotogenic Scalar Triplet,"* Phys. Lett. B **728** (2014) 198 [arXiv:1310.3183 [hep-ph]].

[221] D. J. H. Chung, A. J. Long and L. -T. Wang, *"The 125 GeV Higgs and Electroweak Phase Transition Model Classes,"* Phys. Rev. D **87**, 023509 (2013) [arXiv:1209.1819 [hep-ph]].

[222] W. Huang, J. Shu and Y. Zhang, *"On the Higgs Fit and Electroweak Phase Transition,"* arXiv:1210.0906 [hep-ph].

[223] M. Kamionkowski, A. Kosowsky, M. S. Turner, *"Gravitational radiation from first order phase transitions,"* Phys. Rev. **D49**, 2837-2851 (1994). [astro-ph/9310044];

[224] R. Apreda, M. Maggiore, A. Nicolis, A. Riotto, *"Gravitational waves from electroweak phase transitions,"* Nucl. Phys. **B631**, 342-368 (2002). [gr-qc/0107033];

[225] C. Grojean, G. Servant, *"Gravitational Waves from Phase Transitions at the Electroweak Scale and Beyond,"* Phys. Rev. **D75**, 043507 (2007). [hep-ph/0607107];

[226] J. M. No, *"Large Gravitational Wave Background Signals in Electroweak Baryogenesis Scenarios,"* Phys. Rev. D **84** (2011) 124025 [arXiv:1103.2159 [hep-ph]].

[227] G. Bimonte and G. Lozano, *"Symmetry nonrestoration and inverse symmetry breaking on the lattice,"* Phys. Lett. B **388** (1996) 692 [hep-th/9603201].

[228] C. Itzykson and J. B. Zuber, New York, Usa: Mcgraw-hill (1980) 705 P.(International Series In Pure and Applied Physics)

[229] V. B. Berestetskii, E. M. Lifshitz and L. P. Pitaevskii, "Quantum Electrodynamics, Vol. 4, Course of Theoretical Physics, 2nd Edition," Pergamon Press (1982), 652 p.